QUANTUM INVARIANTS AND THEIR CONNECTIONS WITH THOMPSON'S GROUPS F AND T

Louisa Margaret Liles

Plano, Texas

Bachelor of Arts, Oberlin College, 2018

A Dissertation submitted to the Graduate Faculty
of the University of Virginia in Candidacy for the Degree of
Doctor of Philosophy

Department of Mathematics

University of Virginia
May 2025

Slava Kruskhal, Chair
Israel Klich
Thomas Mark
You Qi

Quantum Invariants and their Connections with Thompson's Groups F and T

Louisa Margaret Liles

(ABSTRACT)

This thesis concerns extensions and applications of the Jones polynomial invariant of oriented links, and the closely related Witten-Reshetikhin-Turaev (WRT) 3-manifold invariants. We calculate and establish number-theoretic properties of recently developed (t, q)-series invariants of negative definite plumbed 3-manifolds, leading to the development of new invariants which may be thought of as ζ-deformed WRT invariants, for ζ any root of unity. This thesis also presents an extension of recent work by Vaughan Jones, who constructed links in the 3-sphere from Thompson's group F, to the setting of annular links and Thompson's group T. We also present a construction of (n, n)-tangles from F, and show that the oriented subgroup $\vec{F}$ of F admits the structure of a lax group action on a category of Khovanov chain complexes associated to tangles.

Acknowledgments

There are several people I would like to thank, including:

–My advisor Slava Krushkal for your mentorship and guidance over the last five years. I am honored to be your student.

–My parents, my sister, and my extended family for your unwavering support.

–Sergei Gukov for your ongoing support and mentorship.

–Julie Bergner, Slava Krushkal, Weiqiang Wang, Mikhail Ershov, and Tom Mark for your inspiring teaching during my graduate studies at the University of Virginia.

–Ken Ono, for your helpful guidance while Eleanor and I were writing our paper.

–My math Professors at Oberlin College, including Chris Marx who convinced me not to drop out of multivariable calculus and without whom I surely would not be writing this thesis, Elizabeth Wilmer whose discrete mathematics course inspired me to declare a math minor which would later become a major, Jack Calcut whose class inspired me to become a topologist, Bob Bosch, Susan Colley, Benjamin Linowitz, Kevin Woods, Jim Walsh, and Lola Thompson.

–Marcelo Vinces and Nicollette Mitchell for your mentorship and dedication to cultivating an inclusive STEM community at Oberlin.

–My stellar math teachers from the Plano Independent School District, especially Ms. Dougherty, Ms. Mikulas, Mr. Martinez, and Ms. Costello.

–Eleanor and Yangxiao, my wonderful classmates and coauthors.

–Postdocs Sarah, Ryan, and Beth for being excellent role models and mentors.

–Maggie W. and Ryan M., for bringing the community together and helping me feel at home in Charlottesville. I'm going to miss everyone more than I can say.

–Sid, for organizing the workout group that consistently put a smile on my face at 7:00am.

–Kathy Chamberlain, my childhood ballet teacher, for thirteen years of invaluable life lessons which have shaped me as a person and mathematician.

Contents

Chapter 1

Introduction

Quantum topology is a modern field of mathematics that connects topology, representation theory, and physics. The field began in the 1980s when Vaughan Jones formulated the Jones polynomial, an invariant of oriented links in 3-space [35]. In a process known as *categorification*, Khovanov provided a link homology theory, now known as Khovanov homology, whose graded Euler characteristic recovers the Jones polynomial [39]. Khovanov's categorification introduced functoriality properties, which have many applications, such as distinguishing exotic surfaces embedded in 4-space [32]. It was shown by Kronheimer and Mrowka to detect the unknot [43], whereas the question of unknot detection for the decategorified Jones polynomial remains open. Khovanov homology has inspired extensions to tangles and links in more general 3-manifolds [8, 9, 10, 40].

The Jones polynomial itself plays a key role in the definition of quantum invariants of 3-manifolds, as every 3-manifold can be realized as Dehn surgery along a framed link in S^3. The Witten-Reshetikhin-Turaev (WRT) $SU(2)$ 3-manifold invariants, originally conceptualized in physics terms, are calculated using the Jones polynomial of a link obtained from a surgery presentation for the manifold [47, 64, 67]. More recently, Jones related links in the 3-sphere to Thompson's groups F and T [36, 37], leading to the discovery that the Jones polynomial and other link invariants can be recovered from unitary representations of these groups [4, 5, 6]. This thesis presents results related to the WRT invariants of 3-manifolds, the Thompson groups, and their connections with link homology theories.

The WRT invariants are a family of 3-manifold invariants indexed by roots of unity. Pioneering work by Lawrence and Zagier led to the development of a q-series invariant that (1) defines a holomorphic function on the unit disk, and (2) encodes, via radial limits toward roots of unity, all WRT invariants of the given manifold. Currently, this series is mathematically defined only for a class of 3-manifolds called *negative definite plumbed*, due to Gukov, Pei, Putrov, and Vafa (GPPV) [31, 30]. These authors present a conceptual framework from physics, predicting that the invariant is the graded Euler characteristic of a physically defined homology theory. It is therefore expected to play a key role in the categorification of WRT invariants, which remains an open question. Recently Akhmechet, Johnson and Krushkal developed an infinite collection of (t, q)-series invariants in which the GPPV q-series invariant corresponds to a special case [7]. These new invariants come from an extension of Némethi's theory of lattice homology [58] and are studied in Chapter 3 of this thesis.

In another direction, recent work by Vaughan Jones connects the Jones polynomial to Thompson's groups F and T, which are groups of piecewise linear self-homeomorphisms of the unit interval and circle, respectively. Jones was motivated by questions in conformal field theory to construct unitary representations of these groups, which gave rise to a construction of links in S^3 from elements of F. Jones proved that, via this construction, all link types can be realized from F, motivating the Thompson group as an analogue of braid groups for producing links. Aiello, Conti, and Jones subsequently proved that the Jones polynomial defines a positive-definite function on F, and therefore, by a known correspondence in representation theory, arises from unitary representations of the group [6].

This thesis presents results on number-theoretic aspects of the recently developed (t, q)-series by [7] and extensions of Jones' construction of links from the Thompson group in relation to link homology theories. Specifically, we:

1. Calculate radial limits and establish number-theoretic properties for the (t, q)-series invariants of certain infinite families of manifolds. This is the content of Chapter 3, based on the author's work in [49] and joint work with Eleanor McSpirit in [51].

2. Provide an analogue of Jones' program for annular links and Thompson's group T, which has F as a subgroup. This is the content of Chapter 4, based on the author's work in [50].

3. Extend Jones' construction to build (n, n)-tangles from F and show that the subgroup $\vec{F} \leq F$ has the structure of a lax group action on a category of Khovanov chain complexes associated with tangles. This is the content of Chapter 5, based on joint work with Slava Krushkal and Yangxiao Luo in [44].

We now give additional context for each of the items above.

1.0.1 (t, q)-Series invariants of 3-manifolds

The development of the GPPV q-series invariant began with a celebrated series of Lawrence and Zagier that unified the WRT invariants of the Poincaré homology sphere. Remarkably, this series was also a key first example of a *quantum modular form*, a term subsequently coined by Zagier with this series in mind [68]. Zagier's seminal work has inspired an extensive and ongoing body of research on quantum modular forms; see Chapter 21 of [13] and the references listed therein. Quantum modular forms have arisen naturally in both topology and number theory. Due to a theoretical framework initialized by Cheng, Chun, Ferrari, Gukov, and Harrison [18] and further studied in [19, 20], modularity properties of these q-series invariants are expected to shed light on the conjectured *3d-3d correspondence* in physics, which predicts mathematical relationships between Vertex Operator Algebras (VOAs), modular forms, and 3-manifold invariants.

The series of Lawrence and Zagier was extended to an invariant of Brieskorn homology spheres in [33, 45], and then to an invariant of negative definite plumbed 3-manifolds equipped with spin^c structures in [31, 30]. The authors named the q-series invariant $\widehat{Z}(q)$ or $\widehat{Z}$, and it will be referred to as such from now on. In addition to introducing dependence on spin^c structures, [30] provided a conceptual framework from physics predicting that (a) $\widehat{Z}(q)$ unifies WRT invariants for all manifolds on which it is defined, and (b) $\widehat{Z}(q)$ can be defined mathematically for all 3-manifolds. Item (a) was subsequently proved by Murakami [57], whereas item (b) remains an open question of great interest.

Since the formulation of $\widehat{Z}$, several extensions have been pursued. Quantum modularity properties of $\widehat{Z}$ were established by Bringmann, Mahlburg, and Milas for infinite families of manifolds [14, 15]. Gukov and Manolescu provided a two-variable series for knot complements, which yields, for some negative definite plumbed 3-manifolds, a formula for $\widehat{Z}$ based on Dehn surgery presentations rather than plumbing graphs [29]. Gukov, Katzarkov, and Svoboda [28] gave a calculation of the $\widehat{Z}$ series for Seifert manifolds that depends only on Seifert data and illustrates modularity properties previously established in [15]. The $\widehat{Z}$ series can also be thought of as associated to the A_1 Lie algebra, and higher-rank generalizations of the invariant are given by [63, 56].

Recently, an infinite collection of two-variable (t, q)-series invariants was developed as a common refinement of $\widehat{Z}$ and lattice homology, which is related to Heegaard Floer homology [7]. These (t, q)-series invariants, denoted $P_W(t, q)$, are indexed by admissible families of functions W, which will be defined in Section 2.6. A specific choice of admissible family $W = \widehat{W}$ leads to a series $\widehat{\widehat{Z}}(t, q) := P_{\widehat{W}}(t, q)$ with $\widehat{\widehat{Z}}(1, q) = \widehat{Z}(q)$. The authors of [7] highlighted connections between the (t, q)-series and Heegaard Floer homology, which Zemke has recently shown is isomorphic to lattice homology as $\mathbb{F}[[U]]$-modules. Zemke's result lays the groundwork for possible future connections between (t, q)-series invariants

and Heegaard Floer homology.

One focus of this thesis will be this infinite collection of (t, q)-series invariants given in [7], whose modularity properties and radial limits had not yet been explored. This thesis provides calculations of the (t, q)-series invariants for two infinite families of manifolds—Seifert manifolds and Brieskorn spheres—and uses the resulting formulae to establish radial limits and modularity properties. All manifolds in this thesis are assumed to be rational homology spheres.

First, we calculate radial limits of the series associated to Brieskorn spheres when t is fixed to be a root of unity:

Theorem A ([51], Theorem 1.1)**.** *Let ζ be a jth root of unity, ξ a Kth root of unity, and Σ a Brieskorn sphere. Define $\widehat{\widehat{Z}}_\Sigma(\zeta, \xi) := \lim_{t \searrow 0} \widehat{\widehat{Z}}_\Sigma(\zeta, \xi e^{-t})$. These limits exist and can be thought of as ζ-deformed WRT invariants. When $\zeta = 1$, the WRT invariants are recovered.*

We then show that the series studied in the previous theorem is in fact a quantum modular form.

Theorem B ([51], Theorem 1.2)**.** *Let ζ be a jth root of unity and Σ a Brieskorn sphere. The q-series invariant $\widehat{\widehat{Z}}(\zeta, q)$ of Σ is, up to normalization, a quantum modular form.*

Motivated by these results and by recent extensions in [28], the author extended the modularity result to a larger family of manifolds.

Theorem C ([49], Theorem 1.2)**.** *Let M be a Seifert manifold with three exceptional fibers and let ζ be a jth root of unity. Then the q-series invariant $\widehat{\widehat{Z}}(\zeta, q)$ of M is, up to normalization, a quantum modular form.*

Remark. *It follows from the proofs of **Theorem B** and **Theorem C** that if M is a Seifert*

manifold with three exceptional fibers and ζ is a root of unity, then radial limits of the q-series $\widehat{\widehat{Z}}(\zeta, q)$ associated to M exist and may be thought of as ζ-deformed WRT invariants.

The previous theorems concern $\widehat{\widehat{Z}}$, the series obtained from a particular choice of admissible family. The following result establishes that, in fact, any admissible family will lead to modularity in the case of Seifert manifolds with three exceptional fibers.

Theorem D ([49], Theorem 1.6)**.** *Let M be a Seifert manifold with three exceptional fibers, and let ζ be a jth root of unity. Then for any choice of W except $W = \widehat{W}$, the one-variable series $P_W(\zeta, q)$ associated to M is, up to normalization, the sum of one quantum modular form and one modular form.*

Theorems A through D are stated in Chapter 3 as Theorems 3.1.1, Theorem 3.1.2, Theorem 3.1.4, and Theorem 3.1.7, respectively.

1.0.2 Annular links from Thompson's group T

Jones first constructed a Hilbert space $\mathcal{V}$ such that each $g \in F$ gave rise to a unitary transformation $\pi_g : \mathcal{V} \to \mathcal{V}$. This Hilbert space $\mathcal{V}$ is the limit of a directed system of formal linear combinations of equivalence classes of tangles. Jones found that for a particular vector $\xi \in \mathcal{V}$, the inner product $\langle \pi_g(\xi), \xi \rangle := \mathcal{L}(g)$ in $\mathcal{V}$ gives a diagram of a link in S^3, and that any link type arises as such an inner product for some $g \in F$.

However Jones subsequently provided two equivalent ways to build $\mathcal{L}(g)$ from $g \in F$ that do not involve the use of unitary representations; see Section 2.8 of this thesis. One of these methods uses $g \in F$ to construct an edge-signed graph $\Gamma(g)$, from which a link $\mathcal{L}(g)$ can be built via Tait's construction. In fact, to prove that F gives rise to all link types, Jones showed that for every Tait graph Γ, there exists some $g \in F$ such that $\mathcal{L}(g)$ is isotopic in

the 3-sphere to the link arising from Γ.

The Thompson group has since been studied in relation to positive links [2], arborescent links [3], and closures of Conway tangles [26]. This thesis presents a method for building links in the thickened annulus $\mathbb{A} \times I$ from elements of Thompson's group T, which contains F as a subgroup. This method recovers Jones' construction for the subgroup F but differs from Jones' construction of links from T given in [36]. Whereas Jones associates links in S^3 to elements of T, this thesis builds links in $\mathbb{A} \times I$, the diagrams of which, under the inclusion $\mathbb{A} \hookrightarrow \mathbb{R}^2$, become the diagrams of the links arising from Jones' method.

Given $g \in T$, one can follow the process introduced in Section 4.2 to build an annular link $\mathcal{L}_{\mathbb{A}}(g)$. On the other hand, given an edge-signed graph $\Gamma \hookrightarrow \mathbb{A}$, one can construct a diagram of an annular link $L_{\mathbb{A}}(g)$ in analogy with Tait's construction; see Section 2.7.3. The following is an analogue of Jones' result on Tait graphs and links from F.

Theorem E ([50], Theorem 1.1)**.** *Let $\Gamma \hookrightarrow \mathbb{A}$ be an edge-signed embedded graph. Then there exists some $g \in T$ such that $\mathcal{L}_{\mathbb{A}}(g)$ is isotopic in $\mathbb{A} \times I$ to $L_{\mathbb{A}}(\Gamma)$.*

This theorem appears in Chapter 4 as Theorem 4.1.1.

Jones also introduced oriented subgroups $\vec{F}$ and $\vec{T}$ from which oriented links in S^3 can be built. The algebraic properties of these groups were studied in [23, 61], and Aiello proved that $\vec{F}$ gives rise to all oriented link types [1].

From Jones' unitary representations, one can obtain not only link diagrams but also link invariants. The authors of [4, 5, 6] showed that the Kauffman bracket and Jones polynomial of links in the 3-sphere define positive definite functions on F (or $\vec{F}$) and therefore can be recovered, in the appropriate sense, from unitary representations of these groups. This paper establishes a similar result for annular links and T, which follows from the construction of links outlined in Section 4.2 and from [5, Theorems 6.2 and 7.4].

Corollary F ([50], Corollary 1.2)**.** *For certain specializations of t and h, the Jones polynomial of annular links $V_{\mathcal{L}(g)}(t,h)$ defines a function of positive type on $\vec{T}$, and therefore arises from a unitary representation of $\vec{T}$.*

The full statement of this corollary can be found in Chapter 4 as Corollary 4.1.2.

1.0.3 Thompson's group F and link homologies

Although both braid groups and the Thompson group F give rise to all link types, a feature of braid groups not yet available for the Thompson group is a set of Markov moves relating distinct group elements that produce isotopic links. However, it is known that infinitely many elements of F produce the unknot. In other words, Jones' construction of links from F is not faithful. Based on joint work with Yangxiao Luo and Slava Krushkal in [44], this thesis presents a method for producing (n,n)-tangles $T_n(g)$ (rather than links) from $g \in F$, which has the following *asymptotic faithfulness* property:

Theorem G. *[[44], Theorem 1.1] Suppose $g, h \in F$ are two distinct elements. Then for sufficiently large n, $T_n(g) \ncong T_n(h)$.*

This is stated as Theorem 5.1.7 in Chapter 5. We also show that $\vec{F}$ gives an asymptotically faithful construction of oriented (n,n)-tangles.

Using these tangles, we establish an algebraic relationship between $\vec{F}$ and a category of Khovanov's chain complexes associated to oriented tangles. To each (m,n)-tangle Khovanov associates a chain complex of (H^m, H^n)-bimodules, where H^n and H^m are graded rings Khovanov constructed from the Temperley-Lieb 2-category [40]. He showed that the homotopy category of these chain complexes admits a braid group action. Our main result below may be thought of as an analogue for the Thompson group:

Theorem H ([44], Theorem 5.20)**.** *$\vec{F}$ has the structure of a lax group action on a category related to Khovanov chain complexes associated to tangles.*

This appears as Theorem 5.3.14 in Chapter 5.

Due to the properties of the construction of links and tangles from F, our result differs from Khovanov's braid group action in two ways. First, our action is lax (see Definition 5.3.3). This structure also appeared in work of Lipshitz, Ozsváth, and Thurston [52, Theorem 15] as a *weak action* (see [52, Definition 8.4]) of mapping class groups on bimodules in bordered Floer homology. We refer to it as a lax group action because it is equivalent to a lax functor between two 2-categories (see Section 5.3). The second modification is the category itself; we define $\overline{\mathcal{K}_n^m}$ as a mild generalization of Khovanov's category $\mathcal{K}_n^m$. Our modified category allows for countable, rather than finite, direct sums of chain complexes, and the chain complexes are not required to be bounded.

Chapter 2

Background

A link $L : \coprod_{i=1}^{k} S_i^1 \hookrightarrow M^3$ is a smooth embedding of k disjoint circles into a 3-manifold M^3. When the 3-manifold is not specified, it is assumed to be the 3-sphere S^3. As is common in the literature, we will use "L" to denote the image of the map L in M^3. A link with one component is called a knot.

We consider links up to a notion of equivalence called *isotopy*. Two links L_1 and L_2 are considered isotopic if there exists an ambient isotopy of M^3 sending L_1 to L_2. An ambient isotopy is a map

$$F : M^3 \times [0, 1] \to M^3$$

such that the map F_0, given by $F_0(x) = F(x, 0)$, is the identity map and each $F_t : M \to M$ is a homeomorphism. The ambient isotopy F sends L_1 to L_2 if $F_1 \circ L_1 = L_2$. An oriented link is a link with a choice of orientation on each component. Two oriented links are isotopic if there is an ambient isotopy preserving the orientation on each component.

Figure 2.1: A diagram of a knot.

Links are typically represented with planar diagrams (see Figure 2.1). When a link is oriented we may refer to its crossings as either "positive" or "negative" according to the convention outlined in Figure 2.3.

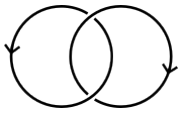

Figure 2.2: A diagram of an oriented link.

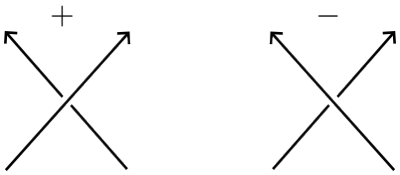

Figure 2.3: A positive crossing (left) and a negative crossing (right).

A single isotopy class of links can be represented by infinitely many diagrams. However, a classical result of Reidemeister states that two links are isotopic if and only if their diagrams can be related by a finite sequence of three moves, called Reidemeister moves (see Figure 2.4).

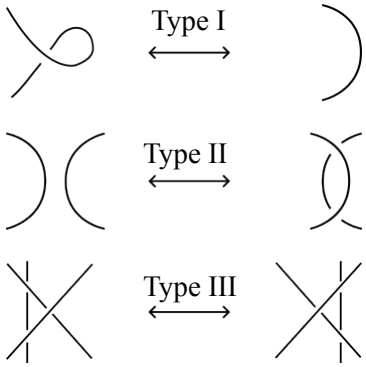

Figure 2.4: Reidemeister moves on link diagrams.

2.1 The Jones polynomial and Kauffman bracket

The Jones polynomial is an invariant of oriented links in the 3-sphere. It is often calculated via another polynomial called the Kauffman bracket, developed in [38].

The Kauffman bracket assigns to a diagram D the polynomial $\langle D \rangle \in \mathbb{Z}[A, A^{-1}]$ according

to the following rules:

1. $\langle \bigcirc \rangle = 1$.
2. $\langle D \cup \bigcirc \rangle = (-A^2 - A^{-2})\langle D \rangle$.
3. $\langle \times \rangle = A \langle \asymp \rangle + A^{-1} \langle) (\rangle$.

Rule (1) states that the Kauffman bracket polynomial of a trivial circle is equal to 1. Rule (2) states that if one takes the disjoint union of L with an unlinked trivial circle, the Kauffman bracket polynomial of the resulting diagram is equal to $(-A^2 - A^{-2})$ times the Kauffman bracket polynomial of D. Rule (3) is called a *skein relation.* In a neighborhood of a single crossing, we may change the diagram one of two ways to resolve the crossing. The resulting diagrams are depicted above as $\asymp$ and $)($, and the unchanged diagram is $\times$. The skein relation allows us to rewrite the Kauffman bracket polynomial of a diagram with k crossings as the sum of two Kauffman bracket polynomials of diagrams with $k - 1$ crossings.

In practice, by repeatedly applying the skein relation to a diagram D with k crossings, we may decompose $\langle D \rangle$ into a sum of 2^k terms, corresponding to all possible ways to resolve all crossings. The remaining diagrams contain disjoint closed circles, and can be evaluated using rules (1) and (2). One can check from the definition that $\langle D \rangle$ is invariant under Reidemeister moves of Type II and III, but not Type I.

Although the Kauffman bracket is not a link invariant, it is an invariant of *framed links*. A *framed knot* in S^3 is a knot K together with a trivialization of its normal bundle, i.e. a homeomorphism

$$\varphi : \nu K \to S^1 \times \mathbb{D}^2.$$

Equivalently a framed knot can be thought of as a knot plus an integer, which represents the linking number between K and the preimage $\varphi^{-1}(\lambda)$, where $\lambda = S^1 \times \{1\} \subset S^1 \times \mathbb{D}^2$.

A framed link is a link together with a framing of each component.

Performing a Reidemeister move of Type I on a diagram changes the framing of the link component by ± 1, whereas Reidemeister moves of Type II and III do not change the framing. Framed links arise in the study of 3-manifolds and the computation of Witten-Reshetikhin-Turaev invariants, see Section 2.2.

The Jones Polynomial

The Jones polynomial, denoted $V_L(t)$ for a link L, is an invariant of oriented links given by

$$\left((-A)^{-3w(D)}\langle D\rangle\right)|_{t^{\frac{1}{2}}=A^{-2}} \in \mathbb{Z}[t^{\frac{1}{2}}, t^{-\frac{1}{2}}],$$

where D is any diagram of L and $w(D)$ is its writhe. The writhe of a diagram is equal to the number of positive crossings, minus the number of negative crossings. One can verify that $V_L(t)$ is invariant under all three Reidemeister moves, and is therefore an invariant of oriented links.

2.2 The WRT invariants

The Witten-Reshetikhin-Turaev (WRT) invariants are a family of 3-manifold invariants indexed by roots of unity. Initially conceptualized by Witten in physics terms [67] and made mathematically precise by Reshetikhin and Turaev [64], the WRT invariants have a combinatorial formulation in terms of the Kauffman bracket, which was given by Lickorish [47].

Given a framed link L in S^3, one can construct a 3-manifold via a process known as Dehn

surgery on S^3 along L. For the details of this construction, see [48, Ch. 12]. A key result in 3-manifold topology, proven independently by Lickorish and Wallace, states that every closed, connected, orientable 3-manifold arises as Dehn surgery on S^3 along a framed link [46, 66]. A result of Kirby states that two framed links yield homeomorphic manifolds if and only if they can be related by a sequence of two moves, called Kirby moves [42].

If a manifold M can be realized as Dehn surgery along a framed link L, we say that L is a surgery presentation for M. To calculate WRT invariants using Lickorish's formulation, one fixes a surgery presentation, calculates the Kauffman bracket polynomial of a certain linear combination of framed links corresponding to L, and then evaluates the polynomial at roots of unity. The resulting value does not depend on the initial choice of surgery presentation. The details of this process are discussed in [48, Ch. 13].

2.3 Negative definite plumbed 3-manifolds

Let Γ be a finite graph with integer weights on its vertices. As in [7], we restrict to the case in which Γ is a tree. Let $m : v(\Gamma) \to \mathbb{Z}$ be the corresponding weight function and let $s = |v(\Gamma)|$. Choosing an order on $v(\Gamma)$ enables us to write a weight vector $m \in \mathbb{Z}^s$ given by $m_i = m(v_i)$ and a degree vector $\delta \in \mathbb{Z}^s$ given by $\delta_i = \delta(v_i)$. With this ordering, we can associate to Γ a symmetric $s \times s$ matrix M given by

$$M_{i,j} = \begin{cases} m_i & i = j \\ 1 & i \neq j \text{ and } v_i \text{ and } v_j \text{ are connected by an edge} \\ 0 & \text{otherwise.} \end{cases}$$

We say Γ is negative definite whenever M is negative definite.

To obtain a 3-manifold from Γ, create a framed link $\mathcal{L}(\Gamma) \subset S^3$ by associating to each vertex v_i an unknot with framing m_i and Hopf linking unknots together whenever their corresponding vertices share an edge. The linking matrix of $\mathcal{L}(\Gamma)$ is the plumbing matrix M. The 3-manifold $Y(\Gamma)$ is defined to be the result of Dehn surgery on $\mathcal{L}(\Gamma)$. Equivalently, $Y = \partial X$ where X is obtained by adding 2-handles to $\mathbb{D}^4$ along $\mathcal{L}(\Gamma)$. The second homology $H_2(X;\mathbb{Z})$ has a basis given by s spheres, corresponding to each vertex of the plumbing graph. The pairwise intersection of these spheres is given by the matrix M above, therefore M represents the intersection form on X.

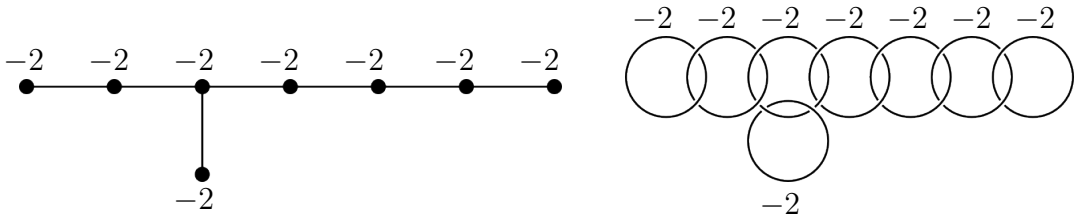

Figure 2.5: A plumbing tree and its associated link for the Poincaré homology sphere $\Sigma(2,3,5)$.

In general, we say Y is a negative definite plumbed 3-manifold if it is homeomorphic to $Y(\Gamma)$ for some negative definite plumbing graph Γ. Two distinct negative definite plumbing trees may result in homeomorphic manifolds; in fact this is the case if and only if the trees can be related by a finite sequence of Neumann moves of type (a) and (b) [59] (see Figure 2.6). Therefore an invariant of a negative definite plumbed manifold Y must be invariant under these Neumann moves on its underlying plumbing graph.

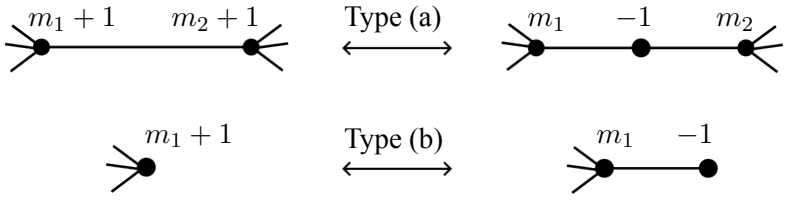

Figure 2.6: Neumann moves of Type (a) and (b).

2.3.1 Spin^c structures

Both lattice homology and the (t, q)-series invariants depend on a choice of a spin^c structure, which can be thought of as a higher-dimensional analogue of an orientation. To understand spin^c structures on a negative definite plumbed 3-manifold Y we can consider spin^c structures on the manifold X it bounds.

Since X is a 4-ball with only 2-handles attached, its fundamental group is trivial. Therefore we may apply a known fact about simply connected 4-manifolds that spin^c structures are in correspondence with elements of

$$\text{Char}(X) = \{k \in H^2(X;\mathbb{Z}) | k(x) + \langle x, x\rangle \equiv 0 \pmod 2 \text{ for all } x \in H_2(X;\mathbb{Z})\},$$

where $\langle -, -\rangle$ denotes the intersection form and $k(x)$ is the evaluation of the cohomology class k on the homology class x. The first homology $H_1(X;\mathbb{Z})$ is trivial, so by the Universal Coefficient Theorem $H^2(X;\mathbb{Z}) \cong Hom(H_2(X;\mathbb{Z}),\mathbb{Z})$. A basis for $H_2(X;\mathbb{Z})$ was previously specified, so we may consider its dual basis of $H^2(X;\mathbb{Z})$. In this framework, we identify both $H_2(X;\mathbb{Z})$ and $H^2(X;\mathbb{Z})$ with $\mathbb{Z}^s$, and $k(x) = k \cdot x$, the usual dot product.

One can check, using the basis elements above, that $\text{Char}(X) = m + 2\mathbb{Z}^s$. One can then use Poincaré duality and the long exact sequence of a pair to show that

$$\text{spin}^c(Y) \cong \frac{m + 2\mathbb{Z}^s}{2M\mathbb{Z}^s} \cong \frac{\delta + 2\mathbb{Z}^s}{2M\mathbb{Z}^s}, \tag{2.3.1}$$

where the second isomorphism is given by $[k] \mapsto [k - (m + \delta)]$ (for details see [29, Section 4.2]). Note that for $u = (1, 1, \ldots, 1)$, $(m + \delta) = Mu$. Spin^c representatives in $\frac{\delta+2\mathbb{Z}^s}{2M\mathbb{Z}^s}$ are commonly denoted $[a]$ in the literature; this thesis will follow that convention.

2.3.2 Brieskorn homology spheres

One infinite family of negative definite plumbed 3-manifolds is the set of Brieskorn homology spheres. Let (b_1, b_2, b_3) be pairwise relatively prime positive integers such that $b_1 < b_2 < b_3$. The corresponding Brieskorn sphere $\Sigma(b_1, b_2, b_3)$ is given by

$$\Sigma(b_1, b_2, b_3) = \{(z_1, z_2, z_3) \in \mathbb{C}^3 \mid z_1^{b_1} + z_2^{b_2} + z_3^{b_3} = 0\} \cap S^5 \subset \mathbb{C}^3,$$

the intersection of a singular complex surface with the unit sphere in $\mathbb{C}^3$. This intersection admits a smooth structure.

2.3.3 Seifert manifolds

Seifert manifolds are another infinite family of negative definite plumbed 3-manifolds, determined by the data

$$(b; (a_1, b_1), \ldots (a_k, b_k)),$$

for $b \in \mathbb{Z}$, $0 < a_k < b_k$, and $\gcd(a_k, b_k) = 1$. A Seifert manifold given by the data above is referred to as having "k singular fibers" or "k exceptional fibers." Brieskorn homology spheres are known to be Seifert manifolds. Given $\Sigma(c_1, c_2, c_3)$ as above, Neumann and Reymond outlined a procedure by which one can find $(b; (a_1, b_1), \ldots (a_3, b_3))$ such that $\Sigma(c_1, c_2, c_3) = M(b; (a_1, b_1), \ldots, (a_3, b_3)$ [60, Theorem 2.1].

When referring to the vertices of a Seifert manifold's plumbing graph, we will follow the convention of [28] where 1-valent vertices are called leaves, 2-valent vertices are called joints, and vertices of valence ≥ 3 are called nodes. A general Seifert manifold given by $(b; (a_1, b_1), \ldots (a_k, b_k))$ has a plumbing graph with one node of degree k and weight $-b$, k leaves, and some joints connecting the leaves to the node. The k legs of this star-shaped

graph are given by the expansions of $\frac{a_i}{b_i}, 1 \leq i \leq k$, as continued fractions (see Figure 2.7).

$$\frac{a_i}{b_i} = c_1^i - \cfrac{1}{c_2^i - \cfrac{1}{\ddots - \cfrac{1}{c_{\ell_i}^i}}}$$

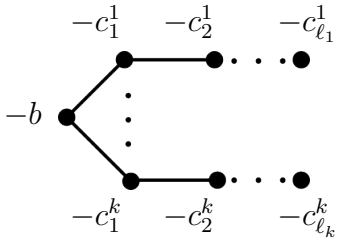

Figure 2.7: A plumbing tree for $M(b; (a_1, b_1), \ldots, (a_k, b_k))$ obtained from continued fraction decompositions of $\frac{a_i}{b_i}$.

2.4 Modular and quantum modular forms

This section provides a brief overview of modular and quantum modular forms of half-integral weight. For more details, we direct the reader to [62, 65].

Let $\mathbb{H}$ denote the upper half complex plane. Modular forms are holomorphic functions $f : \mathbb{H} \to \mathbb{C}$ that behave "nicely" with respect to the action of $\mathrm{SL}(2, \mathbb{Z})$ on $\mathbb{H}$ by linear fractional transformations. The meaning of "nicely" will be specified momentarily in Definition 2.4.1. For $\gamma = \left(\begin{smallmatrix} a & b \\ c & d \end{smallmatrix}\right) \in \mathrm{SL}(2, \mathbb{Z})$, its action on $\tau \in \mathbb{H}$ is given by

$$\gamma\tau := \frac{a\tau + b}{c\tau + d}.$$

Often functions are not modular with respect to the action of the whole group $\mathrm{SL}(2,\mathbb{Z})$, but rather with respect to that of some subgroup. Two subgroups that appear in the theory of half-integral weight modular forms are

$$\Gamma_1(N) := \left\{ \begin{pmatrix} a & b \\ c & d \end{pmatrix} \in \mathrm{SL}(2,\mathbb{Z}) : \ a \equiv d \equiv 1 \pmod{N},\ c \equiv 0 \pmod{N} \right\};$$
$$\Gamma(N) := \left\{ \begin{pmatrix} a & b \\ c & d \end{pmatrix} \in \mathrm{SL}(2,\mathbb{Z}) : \ a \equiv d \equiv 1 \pmod{N},\ b \equiv c \equiv 0 \pmod{N} \right\},$$

where N is called the *level* of the subgroup. We also define, for d odd,

$$\varepsilon_d := \begin{cases} 1 & \text{if } d \equiv 1 \pmod{4}; \\ i & \text{if } d \equiv 3 \pmod{4}, \end{cases}$$

and the Petersson slash operator of weight $k \in \frac{\mathbb{Z}}{2}$ given by

$$f|_k\gamma(\tau) := \begin{cases} (c\tau + d)^{-k} f(\gamma\tau) & \text{if } k \in \mathbb{Z}; \\ \varepsilon_d^{2k} \left(\frac{c}{d}\right) (c\tau + d)^{-k} f(\gamma\tau) & \text{if } k \in \frac{1}{2} + \mathbb{Z}, \end{cases}$$

where $(\frac{\cdot}{\cdot})$ denotes the Jacobi symbol. Throughout this thesis we let $\sqrt{z}$ be the branch of the square root with argument in $(-\pi/2, \pi/2]$. We now give a formal definition of a modular form.

Definition 2.4.1. *Let $\Gamma \leq SL(2,\mathbb{Z})$ be a subgroup of level N such that $4|N$. A holomorphic function $f : \mathbb{H} \to \mathbb{C}$ is a modular (resp. cusp) form with multiplier χ and weight $k \in \frac{\mathbb{Z}}{2}$ if*

1. *for all $\gamma \in \Gamma$, $f - \overline{\chi}(\gamma) f|_k\gamma = 0$, and*

2. *for all* $\gamma \in \mathrm{SL}(2,\mathbb{Z})$, $(c\tau+d)^{-k} f(\gamma\tau)$ *is bounded (resp. vanishes) as* $\tau \to i\infty$.

Let us now discuss quantum modular forms. These can be thought of as an analogue of modular forms, defined on $\mathbb{Q} \cup i\infty$ rather than $\mathbb{H}$. Observe that $\mathrm{SL}(2,\mathbb{Z})$ acts transitively on $\mathbb{Q} \cup i\infty$. If one were to require that a function $f : \mathbb{Q} \to \mathbb{C}$ satisfy the transformation law given in item (1) of Definition 2.4.1, the function f would be determined by a single pair $(x, f(x))$. A more interesting object $f : \mathbb{Q} \to \mathbb{C}$ is a *quantum modular form*, which admits some reasonably "nice" obstruction to modularity.

Quantum modular forms of half-integral weight are defined as follows.

Definition 2.4.2. *Let* Γ *be a subgroup of level* $4|N$. *Let* $\mathcal{Q}$ *be a denote* $\mathbb{Q}\backslash S$ *for some discrete set* S, *with* $\mathcal{Q}$ *closed under the action of* Γ. *We define a quantum modular form of weight* k *with multiplier* χ *for* Γ *to be a function* $f\colon \mathcal{Q} \to \mathbb{C}$ *such that for all* $\gamma = \left(\begin{smallmatrix} a & b \\ c & d \end{smallmatrix}\right) \in \Gamma$, *the function* $h_\gamma\colon \mathcal{Q}\backslash\{\gamma^{-1}(i\infty)\}) \to \mathbb{C}$ *given by*

$$h_\gamma(x) := f(x) - \overline{\chi}(\gamma) f|_k\gamma(x)$$

extends to some "nice" function on $\mathbb{R}$.

Remark. *The definition of quantum modularity is still under construction, and "nice" takes on different meanings in different contexts. The obstructions to modularity in Theorems 3.1.4 and 3.1.7 extend to smooth functions on* $\mathbb{R}$ *that are real-analytic on* $\mathbb{R} \setminus \gamma^{-1}(i\infty)$.

Often we use the map $\tau \mapsto q = e^{2\pi i\tau}$ to think of modular forms as functions on the interior of the unit disk in $\mathbb{C}$ rather than the upper half plane. Through this lens, quantum modular forms are defined at roots of unity. In Section 3.4, we will use the following standard lemma to renormalize powers of q:

Lemma 2.4.3. *If $\psi(\tau)$ is a quantum modular form of weight $1/2$ for $\Gamma(4pj)$ with multiplier χ, then $\psi(j\tau)$ is a quantum modular form of weight $1/2$ for $\Gamma(4pj^2)$ with the same multiplier.*

In the literature, a function F defined on the interior of the unit disk may be referred to as a quantum modular form– this is understood to mean that the radial limits as F approaches roots of unity define a quantum modular form. Quantum modular forms can also be systematically built from modular forms using the theory of Eichler integrals, which is discussed in the following section. The quantum modular forms in Chapter 3 are Eichler integrals of cusp forms.

Modularity and quantum modularity occur naturally in both number theory and topology. In fact, a key first example of quantum modularity was the q-series associated to the Poincaré homology sphere by Lawrence and Zagier [45]. Other topological invariants with connections to modular and quantum modular forms include Donaldson invariants of 4-manifolds [25] and colored Jones polynomials of framed links [22, 33, 53, 54]. Quantum modularity properties of the $\widehat{Z}$ invariant have since been established for several infinite families of manifolds by [14, 15].

2.4.1 Eichler integrals

The theory of Eichler integrals began with the work of Lawrence and Zagier [45]. Many authors have since generalized this procedure to systematically construct families of quantum modular forms from modular forms [16, 21, 24]. Below we briefly outline the procedure of [16], modified to fit the context of this thesis.

Suppose a function $F(\tau)$ for $\tau \in \mathbb{H}$ may be written as

$$F(\tau) = \sum_{n \geq 0} a(n) q^{\frac{n^2}{2M}}, \qquad (q = e^{2\pi i \tau})$$

for some integer M. If a related function f given by

$$f(t) = \sum_{n \geq 0} n \cdot a(n) q^{\frac{n^2}{2M}},$$

is a cusp form of weight $3/2$ for $\Gamma_1(N)$, then F is a quantum modular form.

To show this, Bringmann and Rolen consider the *non-holomorphic Eichler integral* of f, given by

$$F^*(\tau) := \int_{\overline{\tau}}^{i\infty} \frac{f(\omega)}{\sqrt{-i(\omega - \tau)}}\, d\omega, \qquad (\tau \in \mathbb{H}^-).$$

They show that after suitable renormalization, the functions $F(\tau)$ and $F^*(\tau)$ agree, in a precise sense, at any $x \in \mathbb{Q}$. Specifically for any x there exists a sequence $\beta(0), \beta(1), \ldots$ such that as $t \to 0^+$,

$$F\left(x + \frac{it}{2\pi}\right) \sim \sum_{r \geq 0} \beta(r) \frac{(-t)^r}{r!} \text{ and } F^*\left(x - \frac{it}{2\pi}\right) \sim \sum_{r \geq 0} \beta(r) \frac{t^r}{r!}.$$

The non-holomoprhic Eichler integral F^* above has quantum modularity properties by construction. The obstruction to modularity $h_\gamma(\tau)$ for $\tau \in \mathbb{H}^-$ and $\gamma = \left(\begin{smallmatrix} a & b \\ c & d \end{smallmatrix}\right) \in \Gamma_1(N)$, given by

$$h_\gamma(\tau) := F^*(\tau) - \left(\tfrac{-4}{d}\right) F^*|_k \gamma\,(\tau) = \int_{\gamma^{-1}(i\infty)}^{i\infty} \frac{f(\omega)}{\sqrt{-i(\omega - \tau)}}\, d\omega,$$

is "nice" in the sense that it extends to a C^∞ function on $\partial\mathbb{H}^- = \mathbb{R}$ which is real-analytic

on $\mathbb{R}\backslash\{\gamma^{-1}(i\infty)\}$. The function $F(\tau)$ inherits the quantum modularity of $F^*(\tau)$ as a consequence of their agreement at rational points.

2.5 The GPPV invariant $\widehat{Z}$

The $\widehat{Z}(q)$ series defines a holomorphic function on $|q| < 1 \subset \mathbb{C}$, and is an invariant of negative definite plumbed manifolds with spin^c structures. Throughout this section we let M denote a negative definite plumbed 3-manifold, and let $[a] \in \frac{\delta+2\mathbb{Z}^s}{2M\mathbb{Z}^s}$ denote a choice of spin^c structure.

Definition and Intuition

The $\widehat{Z}$ invariant was defined in [30] as follows:

$$\widehat{Z}_{[a]}(q) := q^{\frac{-3s-\sum_v m_v}{4}} \text{v.p.} \oint_{|z_v|=1} \prod_{v\in v(\Gamma)} \frac{dz_v}{2\pi i z_v} (z_v - z_v^{-1})^{2-\delta_v} \cdot \Theta_a^{-M}(z), \tag{2.5.1}$$

where

$$\text{v.p.} \oint_{|z_v|=1} = \text{v.p} \oint_{|z_1|=1} \text{v.p.} \oint_{|z_2|=1} \dots \text{v.p.} \oint_{|z_s|=1},$$

and

$$\Theta_a^{-M}(z) := \sum_{\ell \in a+2M\mathbb{Z}^s} q^{\frac{\ell^t M^{-1} \ell}{4}} \prod_{v\in v(\Gamma)} z_v^{\ell_v}.$$

We now discuss an interpretation, which was first given in [28], of the above formula (2.5.1). First note that $q^{\frac{-3s-\sum_v m_v}{4}}$, commonly referred to as the prefactor, is obtained from the plumbing data. The principal value, or v.p., of each integral refers to the average of two integrals over $|z_i| = 1 + \varepsilon$ and $|z_i| = 1 - \varepsilon$.

By the residue theorem, we know that

$$\oint_{|z_i|=1-\varepsilon} \frac{dz_i}{2\pi i z_i}(z_i - z_i^{-1})^{2-\delta_i}$$

identifies the constant term in the Laurent series expansion of

$$(z_i - z_i^{-1})^{2-\delta_i}$$

centered at $z_i = 0$. Similarly, the integral over $|z_i| = 1 + \varepsilon$ identifies the constant term in the expansion at $z_i = \infty$.

Definition 2.5.1. *Given a function $f(z)\colon \mathbb{C} \to \mathbb{C}$ with Laurent expansions of $\sum_k a_k z^k$ centered at $z = 0$ and $\sum_k b_k z^{-k}$ centered at $z = \infty$, define the symmetric expansion, denoted s.e., to be the formal power series given by*

$$\textit{s.e.}(f) := \frac{1}{2}(\sum_k a_k z^k + \sum_k b_k z^{-k}).$$

We can now think of

$$\text{v.p} \oint_{|z_1|=1} \text{v.p.} \oint_{|z_2=|1} \dots \text{v.p.} \oint_{|z_s|=1} \prod_{v\in v(\Gamma)} \frac{dz_v}{2\pi i z_v}(z_v - z_v^{-1})^{2-\delta_v} \tag{2.5.2}$$

as identifying the constant term in the product

$$\prod_{v\in v(\Gamma)} \text{s.e.}(z_v - z_v^{-1})^{2-\delta_v} := F_0(\vec{z}).$$

Here, note that $F_0(\vec{z})$ is a formal power series and does not necessarily converge. Fixing

some $\ell \in \mathbb{Z}^s$, let $\vec{z}^{\ell} := \prod_v z_v^{\ell_v}$. The integral

$$\oint_{|z_v|=1} \text{v.p.} \prod_{v \in v(\Gamma)} \frac{dz_v}{2\pi i z_v} (z_v - z_v^{-1})^{2-\delta_v} \vec{z}^{\ell} q^{\frac{\ell^t M^{-1} \ell}{4}}$$

returns the coefficient on $\vec{z}^{-\ell}$ in F_0, multiplied by $q^{\frac{\ell^t M^{-1} \ell}{4}}$.

The following integral can therefore be thought of us repeating the above process for each $\ell \in [a]$ and taking the sum over all ℓ:

$$\oint_{|z_v|=1} \prod_{v \in v(\Gamma)} \frac{dz_v}{2\pi i z_v} (z_v - z_v^{-1})^{2-\delta_v} \cdot \Theta_a^{-M}(z).$$

The following fact about s.e.$(z_i - z_i^{-1})^{2-\delta_i}$ will be used below and throughout this thesis.

Lemma 2.5.2. *The coefficient on z_i^{-n} is nonzero in s.e.$(z_i - z_i^{-1})^{2-\delta_i} \Rightarrow n \equiv \delta_i \pmod 2$.*

Proof. The conclusion follows from the fact that the Laurent expansion of $(z_i - z_i^{-1})^{2-\delta_i}$ on $|z_i| < 1$ is

$$(-\sum_{k \geq 0} z_i^{2k+1})^{\delta_i - 2},$$

and the expansion on $|z_k| > 1$ is

$$(\sum_{k \geq 0} z_i^{-(2k+1)})^{\delta_i - 2}.$$

□

From Lemma 2.5.2 it follows that

$$F_0 = \sum_{a \in \text{spin}^c(M)} F_{[a]},$$

where each $F_{[a]}$ consists only of terms $\vec{z}^{\ell}$ for $[\ell] = [a]$. Therefore another way to write the $\widehat{Z}$ series for the pair $(M, [a])$ is

$$\widehat{Z}_{[a]}(q) = q^{\frac{-3s-\sum_v m_v}{4}} \mathcal{L}_M(F_{[a]}(z))),$$

where $\mathcal{L}_M$ is a Laplace transform sending $\vec{z}^{\ell} \mapsto q^{\frac{\ell^t M^{-1} \ell}{4}}$.

Fixing a manifold M and summing over all its spin^c structures, one obtains a related invariant series $\widehat{Z}_0(q)$ which no longer depends on a choice of spin^c structure, given by

$$\widehat{Z}_0(q) := \sum_{[a] \in \text{spin}^c(M)} \widehat{Z}_{[a]}(q) = q^{\frac{-3s-\sum_v m_v}{4}} \mathcal{L}_M(F_0(\vec{z})).$$

Reduction Theorem of Gukov-Katzarkov-Svoboda

The authors of [28] provided a formula for the $\widehat{Z}_0$ invariant of Seifert manifolds which depends only on Seifert data. Specifically, given $M = M(b; (a_1, b_1), \ldots, (a_k, b_k))$, let $A := \prod_{1 \leq i \leq k} a_i$, $\overline{a_i} := \frac{A}{a_i}$, and $f_0(z)$ be the rational function given by

$$f_0(z) := \frac{\prod_{1 \leq i \leq k} (z^{\overline{a_i}} - z^{-\overline{a_i}})}{z^A - z^{-A}}.$$

The authors of [28] show that one can calculate $\widehat{Z}$ for a Seifert manifold by instead considering the symmetric expansion of f_0 and performing a Laplace transform $\mathcal{L}_A$ sending $z^n \mapsto q^{\frac{n^2}{4A}}$.

Theorem 2.5.3 ([28], Theorem 4.2)**.** *Let $M = M(b; (a_1, b_1), \ldots, (a_k, b_k))$ be a rational homology sphere, and let $|H| := |H_1(M; \mathbb{Z})|$. Then*

$$\widehat{Z}_0(q^{|H|}) := q^{\Lambda} \mathcal{L}_A(s.e.(f_0(z))),$$

where $\Lambda \in \mathbb{Q}$ can be obtained from the plumbing data.

Remark. *The authors of [28] also show that Λ can be expressed in terms of the Casson-Walker invariant of M and its plumbing data.*

Theorem 2.5.3 is particularly useful because it allows one to more easily see some of the modularity properties first established by [14, 15]. Its proof significantly inspired that of Theorem 3.1.3 in Chapter 3, from which new modularity properties of the (t, q)-series follow. The full result of [28, Theorem 4.2] also specifies how to decompose the $\widehat{Z}_0$ series into a sum of series associated to spin^c structures.

2.6 The (t, q)-series invariants

This section gives an overview of the (t, q)-series invariants of 3-manifolds developed by [7] as a common refinement of the $\widehat{Z}$ series and lattice cohomology. These series, denoted $P^{\infty}_{W,[k]}(t, q)$, depend on a choice of *admissible family* W of functions.

Definition 2.6.1 ([7], Definition 4.1)**.** *Fix a commutative ring $\mathcal{R}$. A family of functions $\{W_n : \mathbb{Z} \to \mathcal{R}\}_{n\in\mathbb{N}}$ is called admissible if it satisfies two axioms:*

- *$F_2(0) = 1$ and $F_2(r) = 0$ for $r \neq 0$;*
- *For $n \geq 1, r \in \mathbb{Z}, F_n(r + 1) - F_n(r - 1) = F_{n-1}(r)$.*

Fixing $\mathcal{R}$, there are infinitely many choices of admissible families giving rise to infinitely many two-variable series invariants [7, Proposition 4.4]. In this thesis $\mathcal{R} = \frac{\mathbb{Z}}{2}$. We now proceed in defining the (t, q)-series invariants.

Definitions 2.6.2 ([7]). *Fix a negative definite plumbed 3-manifold M, an admissible family W, and a spin^c representative $k \in \mathbb{Z}^s$ for $[k] \in \dfrac{m + 2\mathbb{Z}^s}{2M\mathbb{Z}^s}$. Let Γ refer to the plumbing graph of M, let $\langle -, - \rangle$ denote the bilinear form given by the plumbing matrix M, and let $(\cdot)$ denote the standard Euclidean inner product. For $x \in \mathbb{Z}^s$, we define*

$$\chi_k(x) := \frac{-k \cdot x + \langle x, x \rangle}{2} \in \mathbb{Z}$$

and

$$W_{\Gamma,k}(x) := \prod_{v_i \in v(\Gamma)} W_{\delta_i}((2Mx + k - Mu)_i).$$

We also define

$$\Theta_k := \frac{k \cdot u - \langle u, u \rangle}{2},$$

where $u = (1, 1, \ldots, 1)$ as before and

$$\varepsilon_k := -\frac{(k - Mu)^2 + 3s + \sum_v m_v}{4} + 2\chi_k(x) + \langle x, u \rangle.$$

The authors of [7] show that these functions give rise to an invariant of negative definite plumbed 3-manifolds with spin^c structures.

Theorem 2.6.3 ([7], Theorem 6.3 and Remark 6.5). *Fix an admissible family W. Given a negative definite plumbed 3-manifold M equipped with a spin^c structure $[k]$, the series*

$$P^{\infty}_{W,[k]}(M)(t, q) := \sum_{x \in \mathbb{Z}^s} W_{\Gamma,k}(x) q^{\varepsilon_k(x)} t^{\Theta_k + \langle x, u \rangle}$$

is an invariant of the pair $(M, [k])$ up to Neumann moves of Type (a) and (b).

A particular family $W = \widehat{W}$ gives rise to the series

$$\widehat{\widehat{Z}}_{[k]}(t,q) := P^{\infty}_{\widehat{W},[k]},$$

for which

$$\widehat{\widehat{Z}}_{[k]}(1,q) = \widehat{Z}_{[k-Mu]}(q).$$

The family $\widehat{W}$ was constructed in [7, Definition 7.1] so that $\widehat{W}_d(n)$ captures the coefficient on z^{-n} in the *symmetric expansion* of $(z - z^{-1})^{2-d}$ [7, Definition 7.1].

Recall that the spin^c dependence of $\widehat{Z}$ can be eliminated by instead studying the sum of the series associated to each spin^c structure, denoted $\widehat{Z}_0(q)$. Below we introduce the analogue for the two variable series.

Definition 2.6.4. *Let M be a negative definite plumbed 3-manifold. Define*

$$P^{\infty}_{W,0}(M)(t,q) := \sum_{[k]\in spin^c(M)} P^{\infty}_{W,[k]}(M)(t,q).$$

The (t,q)-series invariants were previously described as a common refinement with $\widehat{Z}$ and lattice homology; we now discuss the connection of the (t,q)-series with the latter.

The 0th lattice homology of any pair $(Y,[a])$ can be encoded by a combinatorial object called a graded root. The authors of [7] use the plumbing data and choice of admissible family to assign Laurent polynomial weights to vertices of this root, so that the new "weighted graded root" remains invariant of the manifold. The $P_W(t,q)$ series results from taking the limit, in a precise sense, of these weights. Weighted graded roots themselves are new invariants whose computation remains an open question.

2.7 Thompson's groups F and T

This section introduces Thompson's groups and Jones' construction of links in S^3 from them. For more details on Thompson's groups, see [17].

2.7.1 Thompson's group F

The Thompson group F consists of piecewise linear self-homeomorphisms of the unit interval $[0,1]$ such that all derivatives are powers of 2 and all points of non-differentiability occur at dyadic numbers, that is, numbers of the form $\frac{a}{2^b}$ for $a, b \in \mathbb{Z}$. For example:

$$g(t) = \begin{cases} \frac{1}{2}t & 0 \leq t \leq \frac{1}{2} \\ t - \frac{1}{4} & \frac{1}{2} \leq t \leq \frac{3}{4} \\ 2t - 1 & \frac{3}{4} \leq t \leq 1. \end{cases}$$

A *standard dyadic partition* is a partition of the unit interval such that all subintervals are of the form $[\frac{a}{2^b}, \frac{a+1}{2^b}]$. Any ordered pair of standard dyadic partitions with the same number of parts determines an element of F, given by the function sending the first partition to the second. For example, the function g above is given by the ordered pair

$$\{[0, \frac{1}{2}], [\frac{1}{2}, \frac{3}{4}], [\frac{3}{4}, 1]\}, \{[0, \frac{1}{4}], [\frac{1}{4}, \frac{1}{2}], [\frac{1}{2}, 1]\}).$$

Standard dyadic partitions can be represented as planar, rooted, binary trees, where each leaf represents an interval of the partition. Therefore an ordered pair of such trees (R, S) also determines an element of F. This pair of trees is often represented by taking the vertical reflection of S and attaching it to R along their leaves; see Figure 2.8.

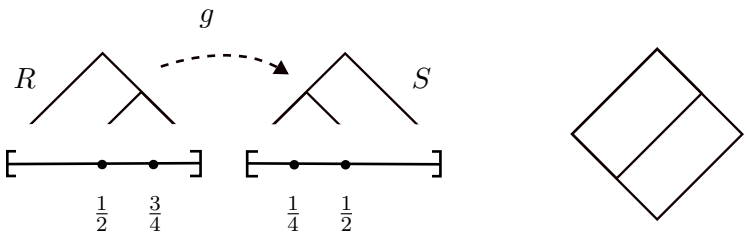

Figure 2.8: A pair of standard dyadic partitions, their corresponding trees R and S, and their associated element $g \in F$.

Conversely, for every $g \in F$ there is a standard dyadic partition J such that $g(J)$ is standard dyadic. The pair $(J, g(J))$ therefore determines g, but this pair is not unique. For any refinement J' of J which is also standard dyadic, $(J', g(J'))$ also represents g. In terms of trees, refining a pair of partitions corresponds to adding finitely many *canceling carets* to their pair of trees, as shown in Figure 2.9.

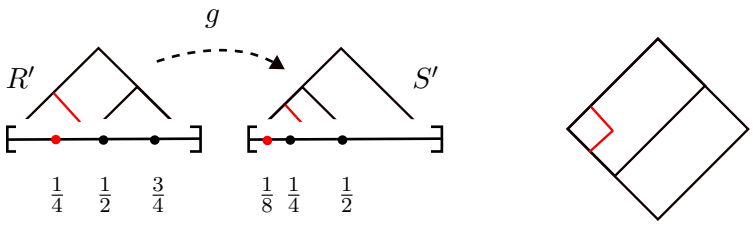

Figure 2.9: A pair-of-trees representation of the same element g from Figure 2.8, which differs from the pair in Figure 2.8 by a canceling caret.

In fact, any two pairs of trees representing the same element of F must differ by the addition or deletion of finitely many canceling carets, and a pair of trees is called *reduced* if no carets can be canceled. Reduced pairs of planar, rooted, binary trees are therefore in bijection with elements of F. From now on, an ordered pair (R, S) will refer to both a pair of standard dyadic partitions and its associated pair of trees, and elements of F will be specified by these pairs.

Pairs of trees corresponding to elements of F are part of a broader class of graphs called *strand diagrams*, introduced by Belk in [11].

Strand Diagrams

Definition 2.7.1. *An (m, n)-strand diagram Γ is a finite graph embedded in $[0, 1] \times [0, 1]$ such that:*

- *Γ has m univalent vertices on the top edge of the square, and n univalent vertices on the bottom edge of the square.*
- *Every vertex in the interior is either a merge or a split (see Figure 2.11)*
- *All edges have nonzero slope.*

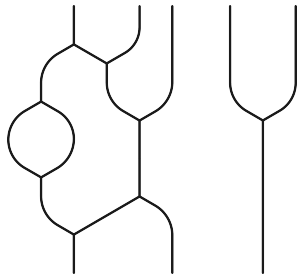

Figure 2.10: An example of a $(5, 3)$-strand diagram

Figure 2.11: A split (left) and a merge (right).

Strand diagrams are similar to braids, but instead of twists there are merges and splits, which may cause the number of points at the bottom of the square n to differ from the number of points at the top m. A pair-of-trees graph representing an element of the Thompson group can be considered a $(1, 1)$-strand diagram after (1) smoothing the 2-valent vertices that result from gluing leaves together and (2) making the roots of each tree 3-valent by adding a third edge intersecting each boundary component of $I \times I$, see Figure 2.12.

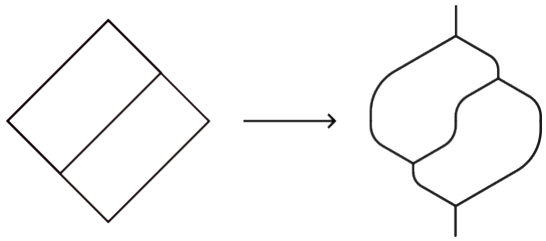

Figure 2.12: Visualizing a pair-of-trees diagram for an element of F as a $(1,1)$-strand diagram.

Isotopic strand diagrams are considered to be equal. We denote the collection of $(m,n)-$strand diagrams as $\mathcal{D}_n^m$. Strand diagrams can be reduced using two local moves, pictured in Figure 2.13. Canceling carets can be seen as Type I moves on $(1,1)$-strand diagrams.

Figure 2.13: Cancellation moves of type I (left) and Type II (right). Type I moves are applied when a split contains a merge directly below it, and the two share a pair of edges. Type II moves are applied when a merge occurs directly above a split, and the two share one edge.

Strand diagrams related by a finite sequence of these moves and their inverses are called equivalent. We let $\overline{\mathcal{D}_n^m}$ refer to the set of equivalence classes of $(m,n)-$strand diagrams. We call a strand diagram *reduced* if it is not subject to any further reductions, and we denote by $\mathcal{R}_n^m$ the set of reduced (m,n)-strand diagrams. Every (m,n)-strand diagram is equivalent to a unique reduced (m,n)-strand diagram, therefore, the reduction map $\rho\colon \overline{\mathcal{D}_n^m} \to \mathcal{R}_n^m$ is a bijection.

Given $\Gamma_1 \in \mathcal{D}_m^k$ and $\Gamma_2 \in \mathcal{D}_n^m$, we denote $\Gamma_2 \circ \Gamma_1 \in \mathcal{D}_n^k$ to be the result of placing Γ_2 below Γ_1 and joining them at their common endpoints. This vertical stacking induces a well-defined binary operation on $\overline{\mathcal{D}_n^n}$, from which we get a group structure. The identity element in $\overline{\mathcal{D}_n^n}$ is $[\mathrm{Id}_n]$, the class of the trivial (n,n)-strand diagram, which is n vertical strands. The inverse of any $[\Gamma] \in \overline{\mathcal{D}_n^n}$ is $[\Gamma^*]$, where Γ^* is the reflection of Γ over the x-axis.

Given $\Gamma_1 \in \mathcal{R}_m^k, \Gamma_2 \in \mathcal{R}_n^m$ we let $\Gamma_2 * \Gamma_1 \in \mathcal{R}_n^k$ denote the result of vertically stacking and then reducing. Observe that $\mathcal{R}_n^n$ is a group with multiplication $*$. It can also be considered as a subset of $\mathcal{D}_n^n$, but it is not a subgroup as $\mathcal{R}_n^n$ is not closed with respect to the $\circ$ operation.

Recall that elements of Thompson's group F are in bijection with reduced pairs of planar rooted binary trees, which can now be recognized as elements of $\mathcal{R}_1^1$.

Definition 2.7.2. *Let $\delta\colon F \to \mathcal{R}_1^1$ be the map sending a function in the Thompson group to its reduced pair of trees. By [12, Prop 2.5], δ is a group isomorphism.*

More generally, $F \cong \mathcal{R}_n^n$ for any $n \in \mathbb{N}$, via isomorphisms $\mathcal{R}_1^1 \to \mathcal{R}_n^n$ given by Matucci in [55]. For a $(1,1)$-reduced strand diagram Γ, this isomorphism sends Γ to $v_n * \Gamma * v_n^*$, where v_n is the "right vine" with n leaves (see Figure 2.14). This map represents conjugation by v_n, and has an inverse map which is conjugation by v_n^*. More generally, this conjugation map gives an isomorphism if we replace v_n with any element of $\mathcal{R}_n^1$.

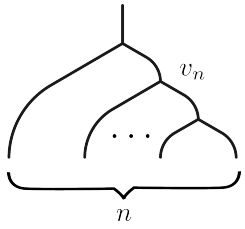

Figure 2.14: The right vine v_n

In practice, strand diagrams give us a way to compose elements of F purely diagrammatically. To compose g with f, place the pair of trees for g below that of f as in Figure 2.15 and then reduce the resulting $(1,1)$-strand diagram. This leads to the unique reduced pair-of-trees diagram representing $g \circ f$.

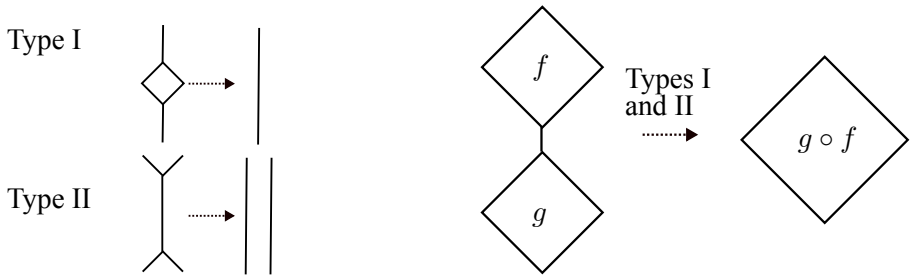

Figure 2.15: Diagrammatic composition in F as given by [11, 27].

2.7.2 Thompson's group T

T is the group of piecewise-linear self-homeomorphisms of S^1, thought of as the unit interval with its endpoints identified, such that all derivatives are powers of 2 and all points of non-differentiability occur at dyadic numbers. F is the subgroup of T whose elements send $[1] \mapsto [1]$. Elements of T are given by triples $(R, S; k)$ where (R, S) is a pair of planar, rooted, binary trees and k is a positive integer between 1 and the number of leaves of R and S. The integer k indicates that the first part of R is sent to the kth part of S, and this triple $(R, S; k)$ determines an element of T. Observe that $k = 1$ if and only if $g = (R, S; k) \in F$. To indicate the value of k in a pair-of-trees diagram, a decoration is placed on the kth leaf of S, as in Figure 2.16.

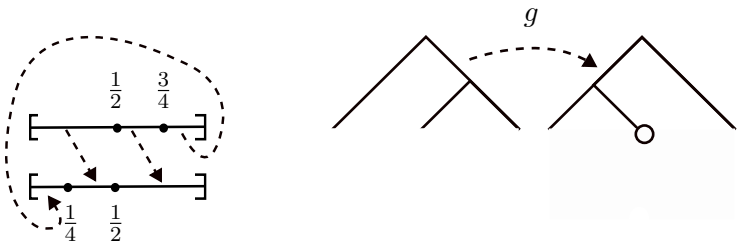

Figure 2.16: The reduced pair of trees and decorated leaf representing the element $g \in T$ which maps $[0, \frac{1}{2}] \mapsto [\frac{1}{4}, \frac{1}{2}]$, $[\frac{1}{2}, \frac{3}{4}] \mapsto [\frac{1}{2}, 1]$, and $[\frac{3}{4}, 1] \mapsto [0, \frac{1}{4}]$.

As was the case for F, one can refine the partitions R and S to produce an unreduced triple $(R', S'; k')$ which differs from $(R, S; k)$ by canceling carets; see Figure 2.17. Canceling

carets are slightly less obvious for diagrams in $T \setminus F$ due to the fact that the interval represented by the leftmost leaf of R is not mapped to the interval represented by the leftmost leaf of S.

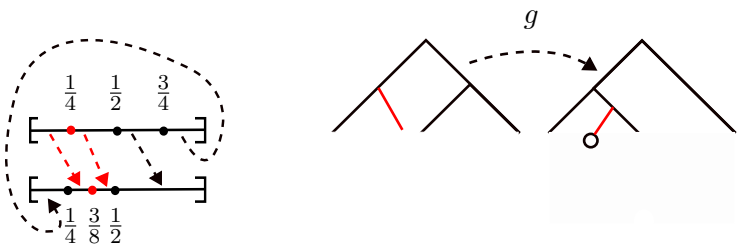

Figure 2.17: An unreduced triple representing the same element g as in Figure 2.16, which differs from the triple in Figure 2.16 by a canceling caret, shown in red.

Section 2.7.1 introduced strand diagrams as a way to visualize the group operation in F. An analogue for T was developed by Belk and Matucci [12]. Specifically, every element of T corresponds to a unique reduced *cylindrical strand diagram*, which satisfies the same conditions as a strand diagram, but is now embedded in $S^1 \times [0, 1]$ rather than the unit square. Following the definition in [12], isotopic cylindrical strand diagrams are considered equal, however isotopies are not required to fix the boundary circles. Therefore, cylindrical strand diagrams differing by Dehn twists are considered equal.

To associate a cylindrical strand diagram to an element $g = (R, S; k) \in T$, place the trees R and S in the cylinder as in Figure 2.18. Identify leaves such that the first leaf of R is sent to the kth leaf of S, and then connect the rest of the leaves in unique way for which the graph remains embedded; see Figure 2.18.

In Figure 2.18, the rightmost picture differs from the picture to its left by the smoothing of two-valent vertices given by connecting two leaves. For the rest of this paper strand

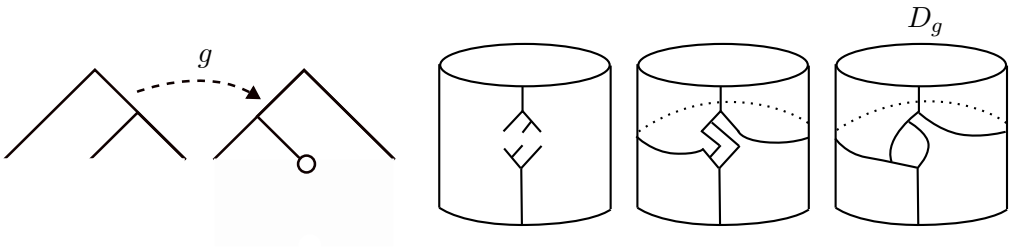

Figure 2.18: A cylindrical strand diagram D_g built from $g \in T$.

diagrams built from T will appear without this smoothing, to indicate the pair of trees from which the diagram was created.

Cylindrical strand diagrams may be reduced according to local moves of Type I and II as in Figure 2.15. As was the case for F, given cylindrical strand diagrams for $f, g \in T$, vertically stacking the cylinders and reducing using moves of Type I and II results in the reduced cylindrical strand diagram for $g \circ f$ [12]. Just as strand diagrams are used to build links from F, this paper will use cylindrical strand diagrams to construct annular links from T. Chapter 5 uses strand diagrams to relate Thompson's group F to Khovanov homology of links in 3-space based on [40, 44]; it may be possible to use cylindrical strand diagrams to give an analogue for the group T and annular link homology theories.

2.7.3 Tait graphs for links

This section introduces Tait graphs, which are a key ingredient in Jones' proof that all link types types arise from F.

A Tait graph is a planar edge-signed graph from which a link can be built. To construct a link diagram, replace vertices of the graph with disks and edges with twisted bands connecting corresponding disks. The direction of each twist is given by the sign of the corresponding edge (see Figure 2.19). Taking the boundary of the embedded surface results in a link

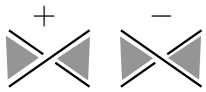

Figure 2.19: The sign convention for Tait graphs.

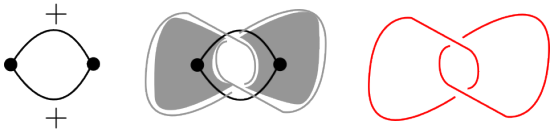

Figure 2.20: A Tait graph for the Hopf link.

diagram, see Figure 2.20.

From any link diagram, one can obtain a Tait graph by first "checkerboard coloring" the diagram so that the outermost face is unshaded, as in the middle picture of Figure 2.20. Then one assigns vertices to each shaded region, and connect vertices with edges whenever the regions are connected by a half-twist. The sign of the edge is given by the convention in Figure 2.19.

For Jones' proof that F gives rise to all link types, he introduces the concept of 2-equivalence of Tait graphs. Two edge-signed planar graphs are defined to be 2-equivalent if they are related by a finite sequence of three possible moves, which Jones refers to as 2-moves [36]. If two graphs Γ, Γ' are 2-equivalent then their associated links $L(\Gamma)$ and $L(\Gamma')$ are isotopic.

The first 2-move is the addition or deletion of a 1-valent vertex, which corresponds to a Reidemeister move of Type I. The remaining two 2-moves, each corresponding to Reidemeister moves of Type II, are shown in Figure 2.21.

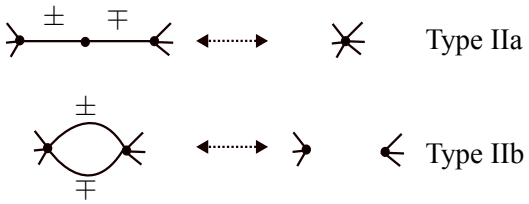

Figure 2.21: Moves of Type IIa and IIb as introduced by Jones in [36] .

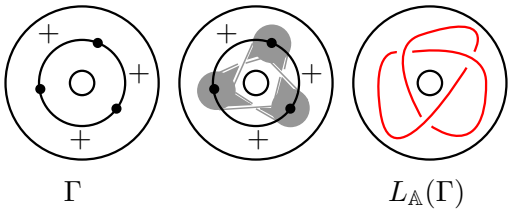

Figure 2.22: An annular link built from an edge-signed graph embedded in $\mathbb{A}$.

There is also a move on Tait graphs corresponding to Reidemeister III moves, but it is not used in Jones' proof or in this thesis.

Toward an extension of Jones' program to the annular setting, we specify an annular analogue of Tait graphs. Given an edge-signed embedded graph in the annulus $\Gamma \hookrightarrow \mathbb{A}$, replace vertices with disks and edges with twisted bands as before. Taking the boundary of the resulting embedded surface in the thickened annulus results in a diagram of an annular link $L_{\mathbb{A}}(\Gamma)$. Note that in the annulus, this process always produces a link whose checkerboard coloring leaves the faces containing boundary components of $\mathbb{A}$ unshaded. Also note that the 2-moves of Jones may be still be applied to annular Tait graphs, as long as they occur in a contractible neighborhood of the annulus.

2.8 Jones' construction of links in S^3 from F

In 2014 Jones showed how to associate links in S^3 to elements of Thompson's group F, subsequently proving that F gives rise to all link types and promoting the Thompson group as an analogue of braid groups for building links. Although F is sufficient to obtain all link types, Jones' construction of links in S^3 is also defined on $T \supset F$.

Jones' method of building links arose in the context of unitary representations of F and T. He constructed a Hilbert space $\mathcal{V}$, defined as the Hilbert completion of the limit of a

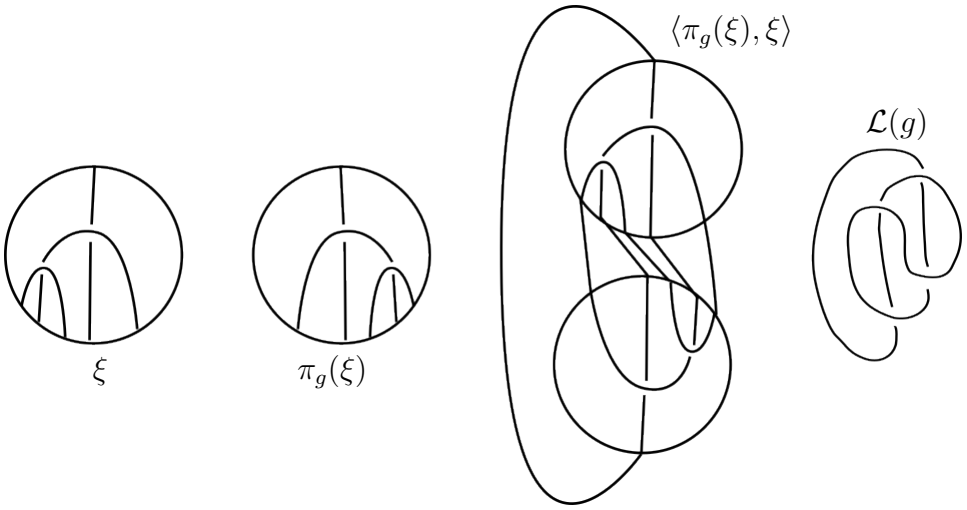

Figure 2.23: A diagram for a link $\mathcal{L}(g)$ associated to $g \in F$, given by $\langle \pi_g(\xi), \xi \rangle$

directed system of formal linear combinations of tangles, on which Thompson's groups act via unitary transformations. Each $g \in F$ (resp. T) gives a map $\pi_g : \mathcal{V} \to \mathcal{V}$, and links are constructed from the action of group elements on a distinguished vector $\xi \in \mathcal{V}$. More precisely, the inner product $\langle \pi_g(\xi), \xi \rangle$ gives a diagram for a link $\mathcal{L}_g$, see Figure 2.23.

Jones then provided two equivalent diagrammatic methods for building links from F that do not involve unitary representations [36, 37]. The first, pictured in Figure 2.24, turns a reduced pair of binary trees (R, S) into a reduced pair of ternary trees $(\phi(R), \phi(S))$ by adding a third "middle" edge to every split, connects the two roots and the leaves from left to right, and then changes 4-valent vertices to crossings.

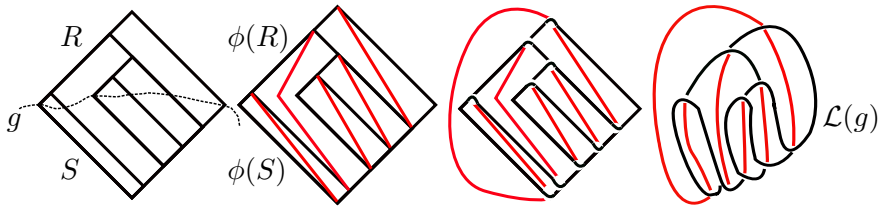

Figure 2.24: A Hopf link created from an element of F via the construction introduced by Jones [36].

The second method, pictured in Figure 2.25, builds the Tait graph $\Gamma(g)$ of $\mathcal{L}(g)$. From

$g = (R, S)$, one constructs two graphs $\Gamma(R)$ and $\Gamma(S)$ with the same number of vertices. The graph $\Gamma(R)$ has one vertex for each leaf of R, which is placed to immediately to the left of the leaf. The vertices for $\Gamma(S)$ are created in the same way. For every edge e in R (resp. S) that slopes up and to the right, $\Gamma(R)$ (resp. $\Gamma(S)$) will have one edge which transversely intersects e once and no other edges. $\Gamma(g)$ is then built by reflecting $\Gamma(S)$ over the x-axis and identifying its leaves with those of $\Gamma(R)$. Edges of $\Gamma(g)$ originating from $\Gamma(R)$ are given a positive sign and edges originating from $\Gamma(S)$ are given a negative sign.

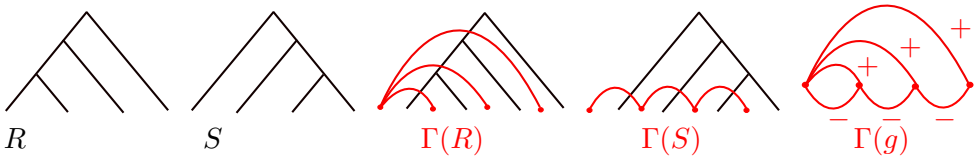

Figure 2.25: $\Gamma(g)$, the Tait graph for $\mathcal{L}(g)$, where g is specified by (R, S).

2.8.1 The Thompson badness of Tait graphs

To detect whether a general edge-signed planar graph Γ is equal to $\Gamma(g)$ for some $g \in F$, Jones introduced *Thompson Badness*, a quantity which is zero exactly when $\Gamma = \Gamma(g)$. To calculate Thompson Badness, first embed $\Gamma \hookrightarrow \mathbb{R}^2$ such that all vertices are on the x axis, the leftmost vertex is at the origin, and for each edge e, its interior, denoted $\text{int}(e)$, is either entirely above or entirely below the x axis. Consider each edge to be oriented from left to right, so that its rightmost vertex is considered the *terminal vertex*. The formula for Thompson Badness, which will be given momentarily, depends on the cardinality of the

following sets:

$$\begin{aligned}
e_v^{in} &:= \{e \in e(\Gamma) : v \text{ is the terminal vertex of } e\} \\
e^{up} &:= \{e \in e(\Gamma) : \text{int}(e) \text{ is in the upper half-plane}\} \\
e^{down} &:= \{e \in e(\Gamma) : \text{int}(e) \text{ is in the lower half-plane}\} \\
e_-^{up} &:= \{e \in e(\Gamma) : \text{int}(e) \text{ is in the upper half-plane and } e \text{ has sign } -\} \\
e_+^{down} &:= \{e \in e(\Gamma) : \text{int}(e) \text{ is in the lower half-plane and } e \text{ has sign } +\}.
\end{aligned}$$

Jones defines Thompson Badness as

$$TB(\Gamma) = \sum_{v \in V(\Gamma)\setminus\{(0,0)\}} (|1 - |e_v^{in} \cap e^{up}|| + |1 - |e_v^{in} \cap e^{down}||) + |e_-^{up}| + |e_+^{down}|.$$

In other words each vertex, other than the leftmost, must have one exactly one edge coming into it from above, and one edge coming into it from below. The edge coming from above must have a positive sign, and the edge coming from below must have a negative sign. Jones shows that $TB(\Gamma) = 0$ if and only if $\Gamma = \Gamma(g)$ for some $g \in F$ [36, Sections 4 and 5].

Thompson Badness allows Jones to prove that all link types arise from F:

Theorem 2.8.1 ([**Jones14**], Lemma 5.3.3)**.** *For all Tait graphs Γ, there exists some Γ' such that $L(\Gamma)$ is isotopic in S^3 to $L(\Gamma')$, and $TB(\Gamma') < TB(\Gamma)$.*

Jones' proof is constructive– in practice, given a link $\mathcal{L} \hookrightarrow S^3$, one can find an associated Tait graph Γ and then apply Theorem 2.8.1 several times to obtain some Γ' with $TB(\Gamma') = 0$ as above.

2.8.2 Oriented subgroups $\vec{F}$ and $\vec{T}$

Jones defined $\vec{F}$ as the set of elements $g \in F$ whose link diagram $\mathcal{L}(g)$, when given the checkerboard shading, results in an orientable surface, i.e. a Seifert surface for $\mathcal{L}(g)$. Equivalently, this can be expressed in terms of the chromatic polynomial $Chr_{\Gamma(g)}(Q)$:

$$\vec{F} = \{g \in F | Chr_{\Gamma(g)}(2) = 2\}.$$

After its introduction by Jones, the subgroup $\vec{F}$ was further studied by Golan and Sapir in [23].

If one follows the convention that the leftmost face of the checkerboard surface is always positively oriented, each $g \in \vec{F}$ yields a link $\mathcal{L}(g)$ with a natural orientation, namely that induced by the orientation of the surface it bounds 2.26. It was shown in [1] that every oriented link can be built from this subgroup, giving an analogue of the Alexander Theorem for oriented links and $\vec{F}$.

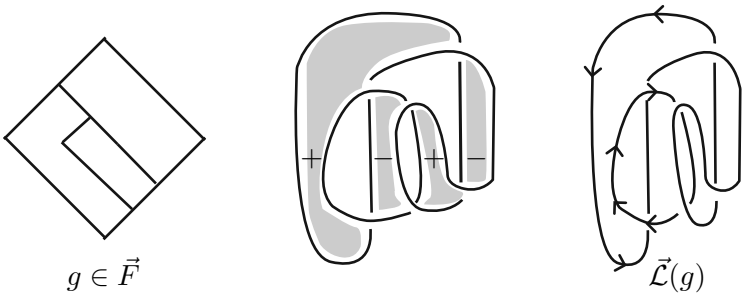

Figure 2.26: An oriented link $\vec{\mathcal{L}}(g)$ built from $g \in \vec{F}$.

From the definitions it may not be immediately clear to the reader how $\vec{F}$ is a subgroup, rather than just a subset, of F. Below we present a notion of oriented strand diagrams, which give rise to groups isomorphic to $\vec{F}$. Oriented strand diagrams may be thought of as an extension of the oriented forests introduced in [6], and will be used later in Chapter 5 to

build oriented (n, n)-tangles from $\vec{F}$ for certain values of n.

Definition 2.8.2. *An orientation on an (m, n)-strand diagram Γ is an assignment of $+$ or $-$ to each component of the complement of Γ, except for the rightmost region, such that the signs around each trivalent vertex correspond to one of the four cases shown in Figure 2.27. The region on the right of the crossing in each case appears to be unlabeled; however in fact it has a sign determined near its right boundary. An exception is the rightmost region which does not have a sign. Γ is said to be orientable if it admits an orientation.*

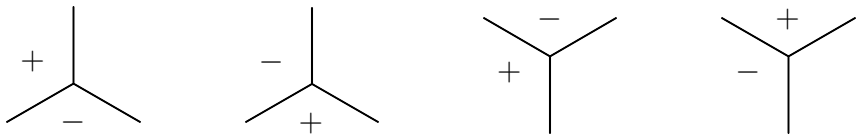

Figure 2.27: (A) A positive split. (B) A negative split. (C) A positive merge. (D) A negative merge.

Definition 2.8.3. *An n-sign is a sequence of n $+$'s or $-$'s. We will follow the convention in the literature [6] that the first two signs in the sequence are $+, -$. If the sequence has length 1, it is $+$.*

Note that an oriented (m, n)-strand diagram $\vec{\Gamma}$ induces a sequence of m signs on the top side of the square, and a sequence of n signs on the bottom side. If both of them start with $+, -$, let μ denote the top m-sign and ν the bottom n-sign ν; in this case we say that $\vec{\Gamma}$ is an oriented strand diagram from μ to ν, or $\vec{\Gamma}$ is a (μ, ν)-strand diagram. We denote the collection of (μ, ν)-strand diagrams by $\mathcal{D}^{\mu}_{\nu}$. From a (μ, ν)-strand diagram, we may obtain a (m, n)-strand diagram by forgetting orientations. Therefore we can consider $\mathcal{D}^{\mu}_{\nu}$ as a subset of $\mathcal{D}^{m}_{n}$.

Given a (μ, ν)-strand diagram $\vec{\Gamma}$, we define $(\vec{\Gamma})^*$ to be the (ν, μ)-strand diagram obtained by reflecting $\vec{\Gamma}$ over the x-axis. Given a (μ, ν)-strand diagram $\vec{\Gamma}_1$ and a (ν, ρ)-strand diagram

$\vec{\Gamma}_2$, we define $\vec{\Gamma}_2 \circ \vec{\Gamma}_1$ to be the (μ, ρ)-strand diagram obtained by concatenating strand diagrams and signed regions. The following definition extends the notion of a reduced strand diagrams to the oriented case.

Definition 2.8.4. *A reduction of an oriented strand diagram is a sequence of moves shown in Figure 2.28.*

An oriented strand diagram is said to be reduced if it is not subject to any reductions. The collection of reduced (μ, ν)-strand diagrams, which we denote $\mathcal{R}^\mu_\nu$, may be regarded as a subset of $\mathcal{D}^\mu_\nu$.

Given a reduced (μ, ν)-strand diagram $\vec{\Gamma}_1$ and a reduced (ν, ρ)-strand diagram $\vec{\Gamma}_2$, we define $\vec{\Gamma}_2 * \vec{\Gamma}_1$ to be the reduced (μ, ρ)-strand diagram obtained by fully reducing $\vec{\Gamma}_2 \circ \vec{\Gamma}_1$. Similarly to the case of reduced unoriented strand diagrams, $\mathcal{R}^\mu_\mu$ is a group with multiplication $*$.

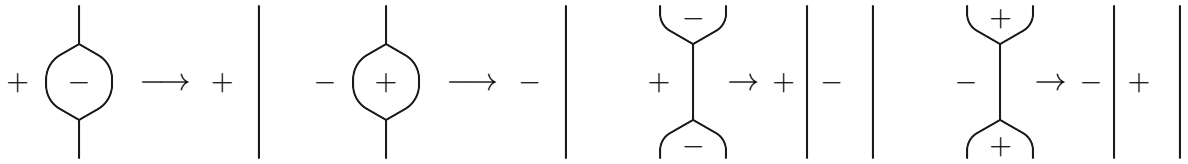

Figure 2.28: (A) A positve Type I move. (B) A negative Type I move. (C) A positive Type II move. (D) A negative Type II move.

Forgetting orientations, we may consider $\mathcal{R}^\mu_\nu$ as a subset of $\mathcal{R}^m_n$. In particular, $\mathcal{R}^\mu_\mu$ can be regarded as a subgroup of $\mathcal{R}^m_m$. In Section 2.7.1 we established an isomorphism between F and $\mathcal{R}^m_m$, for each m.

We now discuss isomorphisms between $\vec{F}$ and groups of oriented strand diagrams. Starting with the previously discussed isomorphism $\delta : F \to \mathcal{R}^1_1$, observe that for $g \in \vec{F}$ each region of the complement of $\delta(g)$ corresponds to a unique shaded region of the checkerboard surface resulting from g. This can be used to produce an orientation on $\delta(g)$, by letting regions

of the complement of $\delta(g)$ inherit the signs of their associated regions of the checkerboard surface. Due to the convention that the leftmost region is always assigned $+$, the orientation on $\delta(g)$ results in an element of $\mathcal{R}_+^+$. Here $\mathcal{R}_+^+$ stands for $\mathcal{R}_\mu^\mu$ where μ is the 1-sign $+$. We now show that this restriction $\vec{\delta} := \delta|_{\vec{F}} \colon \vec{F} \to \mathcal{R}_+^+$ is surjective, and therefore an isomorphism.

Proposition 2.8.5. *The map $\vec{\delta} \colon \vec{F} \to \mathcal{R}_+^+$ is an isomorphism.*

Proof. For any $\vec{\Gamma} \in \mathcal{R}_+^+$, we can decompose $\vec{\Gamma}$ into a tree $\vec{s}$ and an inverse tree $(\vec{t})^*$ satisfying $\sigma_s = \sigma_t$. Here, given an oriented tree $\vec{s}$ with n leaves, σ_s denotes the n-sign induced by the orientation of $\vec{s}$. Let g be the element in F corresponding to the tree diagram (s, t). Then $g \in \vec{F}$ and $\vec{\Gamma} = \vec{\delta}(g)$. □

Jones also defined the oriented subgroup $\vec{T} \leq T$ as the group of elements whose link diagrams, when given the checkerboard shading, produce orientable surfaces. Equivalently,

$$\vec{T} := \{g \in T | Chr_{\Gamma(g)}(2) = 2\}.$$

Again we follow the convention that the leftmost region of this surface has a positive orientation. Each link in S^3 built from $\vec{T}$ admits a natural orientation induced by the surface it bounds. The algebraic properties of $\vec{T}$ were further studied by Nikkel and Ren in [61].

2.8.3 Link invariants and representations of Thompson's groups

Since Jones' original construction of links from Thompson's groups, several authors have shown that various link invariants can be reconstructed from unitary representations of F and T.

A general fact from representation theory is that given a unitary representation

$$\pi : G \to \mathcal{U}(\mathcal{K})$$

of a group G for a complex Hilbert space $\mathcal{K}$, one can fix a vector $\varepsilon \in \mathcal{K}$ and consider the function $G \to \mathbb{C}$ given by

$$g \mapsto \langle \pi_g(\varepsilon), \varepsilon \rangle.$$

This function always satisfies a certain positivity condition, and is therefore called *positive definite*, or a *function of positive type*. On the other hand, given a positive definite function $f : G \mapsto \mathbb{C}$, one can always construct a Hilbert space $\mathcal{K}$ and a unitary representation such that $f(g) = \langle \pi_g(\varepsilon), \varepsilon \rangle$ for some ε.

Therefore, to show that a link invariant (or a suitable renormalization) arises from a unitary representation of F (or its oriented subgroup $\vec{F}$), one can show that it defines a positive definite function on $\mathbb{C}$. For example, one can fix $t \in \mathbb{C}$ and consider the function given by sending g to $V_{\mathcal{L}(g)}(t)$, the Jones polynomial of $\mathcal{L}(g)$ evaluated at t. Several invariants of unoriented links [4] and oriented links [5, 6] have been shown to define positive definite functions on F and T (or their oriented subgroups). In particular, a suitable renormalization of the HOMFLYPT polynomial (and therefore the Jones polynomial) evaluated at certain roots of unity defines positive definite functions on both $\vec{F}$ and $\vec{T}$ [6].

2.9 Khovanov chain complexes associated to tangles

Khovanov constructed chain complexes that are invariants, up to chain homotopy, of tangles in the 3-ball [40]. These are chain complexes of (H^n, H^m)-bimodules, where H^n is a graded ring defined in [40].

2.9.1 The ring H^n

Here we introduce Khovanov's graded ring H^n. We follow the conventions of [40] and direct the reader there for more details.

Let $\mathcal{A}$ be a free abelian group of rank 2 spanned by the elements $\mathbf{1}$ and x (where $\mathbf{1} \in \mathcal{A}$ is distinct from $1 \in \mathbb{Z}$). We say $\mathbf{1}$ has degree -1 and x has degree 1. Using $\mathcal{A}$, we will describe a $(1+1)$-dimensional topological quantum field theory (TQFT) assigning graded abelian groups to oriented closed 1-manifolds and group homomorphisms to oriented surface cobordisms between them. To a collection C of k circles in the plane, we may assign a graded ring

$$\mathcal{F}(C) := \mathcal{A}^{\otimes k}.$$

We now consider oriented surface cobordisms between collections of circles in the plane. In order to do this, we must orient each collection of circles. We follow the convention in [40] that all circles are oriented counterclockwise, and let S be an oriented surface cobordism between two collections of circles C_1 and C_2. The surface S induces a map

$$\mathcal{F}(S) : \mathcal{F}(C_1) \to \mathcal{F}(C_2),$$

which is given by appropriately composing maps corresponding to each of the elementary cobordisms pictured in Figure 2.29. One can use the maps $\varepsilon, \iota, \Delta$, and m, to verify that the homomorphisms induced by surface cobordisms depend only on the isotopy class of the surface. For example, in Figure 2.30 both S_1 and S_2 induce the identity map on $\mathcal{A}$.

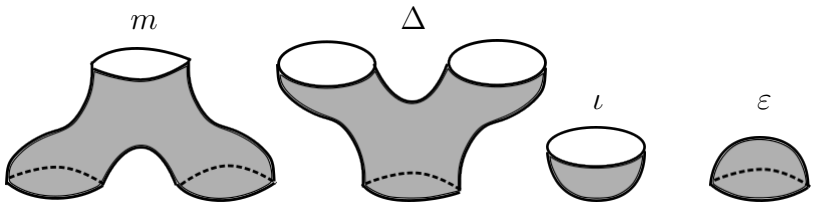

Figure 2.29: Elementary cobordisms inducing the maps $m : \mathcal{A} \otimes \mathcal{A} \to \mathcal{A}$, $\Delta : \mathcal{A} \to \mathcal{A} \otimes \mathcal{A}$, $\iota : \mathbb{Z} \to \mathcal{A}$, and $\varepsilon : \mathcal{A} \to \mathbb{Z}$.

The maps are given by

$$\begin{aligned} \iota : \mathbb{Z} &\to \mathcal{A} \\ 1 &\mapsto \mathbf{1} \end{aligned} \qquad \begin{aligned} \varepsilon : \mathcal{A} &\to \mathbb{Z} \\ \mathbf{1} &\mapsto 0 \\ x &\mapsto 1 \end{aligned}$$

$$\begin{aligned} m : \mathcal{A} \otimes \mathcal{A} &\to \mathcal{A} \\ \mathbf{1} \otimes \mathbf{1} &\mapsto \mathbf{1} \\ \mathbf{1} \otimes x &\mapsto x \\ x \otimes \mathbf{1} &\mapsto x \\ x \otimes x &\mapsto 0 \end{aligned} \qquad \begin{aligned} \Delta : \mathcal{A} &\to \mathcal{A} \otimes \mathcal{A} \\ \mathbf{1} &\mapsto \mathbf{1} \otimes x + x \otimes \mathbf{1} \\ x &\mapsto x \otimes x. \end{aligned}$$

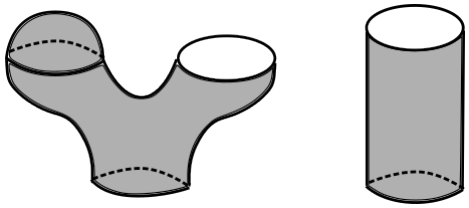

Figure 2.30: Two isotopic surfaces inducing the same map. The surface on the left is a saddle corresponding to $\Delta : \mathcal{A} \to \mathcal{A} \otimes \mathcal{A}$, followed by a cap in the first factor given by $\varepsilon \otimes \mathrm{id}$. One can check that this is equal to the identity map on $\mathcal{A}$ induced by the second (product) surface.

We now introduce more notation necessary to define Khovanov's ring H^n.

Definition 2.9.1. *Let B_n^m denote the set of isotopy classes of embeddings of $m+n$ disjoint arcs in $\mathbb{R}\times[0,1]$ whose $2(m+n)$ endpoints meet $\mathbb{R}\times\{1\}$ transversely at $2m$ points, and $\mathbb{R}\times\{0\}$ at $2n$ points.*

Definition 2.9.2. *Let $\hat{B}_n^m$ denote the set of isotopy classes of (crossingless) tangles in $\mathbb{R}\times[0,1]$, whose endpoints meet $\mathbb{R}\times\{0\}$ transversely at $2n$ points, and $\mathbb{R}\times\{1\}$ at $2m$ points. The key difference between $\hat{B}_n^m$ and B_n^m is that $\hat{B}_n^m$ may have additional closed circles in the plane, whereas B_n^m must consist only of $m+n$ arcs.*

Figure 2.31: An element of B_1^2 (left) and an element of $\hat{B}_1^2$ (right).

Definition 2.9.3. *Given $a\in B_n^m$, its reflection over the x axis is denoted $W(a)\in B_m^n$.*

Definition 2.9.4. *Given $a,b\in B_0^n$, one can stack a below $W(b)$ and rescale in the second factor to obtain a collection of circles in $\mathbb{R}\times[0,1]$. This is denoted $W(b)a\in\hat{B}_0^0$.*

Definition 2.9.5. *Given a,b as above, one can also stack b below $W(a)$ and rescale in the second factor to obtain an element $aW(b)\in B_n^n$.*

We may now define the ring H^n as follows:

$$H^n := \bigoplus_{a,b} {}_a(H^n)_b,$$

where $a,b\in B_0^n$ and

$${}_a(H^n)_b := \mathcal{F}(W(b)a)\{n\}.$$

The notation $\{n\}$ means that the grading has been shifted upward by n. In other words, if an element y has grading k, then $y\{n\}$ has grading $k+n$.

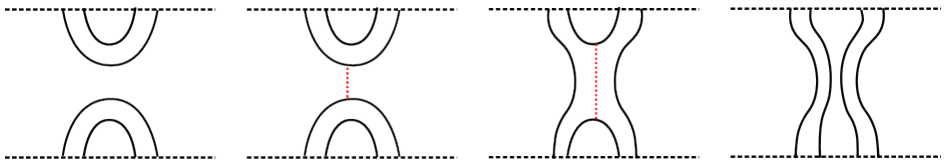

Figure 2.32: The simplest possible cobordism between $bW(b)$ and Vert_4. Dotted red arcs denote saddles.

We now define the multiplication operation in the ring, given by maps

$$ {}_d(H^n)_c \otimes {}_b(H^n)_a \to {}_d(H^n)_a.$$

If $c \neq b \in B_0^n$, then multiplication is defined to be the zero map. If $b = c$, the multiplication map will be given by the surface cobordism specified below.

First note that $W(d)b$ and $W(b)a$ are disjoint collections of circles in the plane, so we have an isomorphism

$$\mathcal{F}(W(d)b) \otimes \mathcal{F}(W(b)a) \cong \mathcal{F}(W(d)bW(b)a).$$

There is a well-defined surface cobordism S_b from $bW(b)$ to Vert_{2n}, the set of n vertical strands, given by performing the "simplest possible" series of saddle moves ([40, Section 2.4]). This surface will have n saddle points and no other critical points; an example of such a cobordism is pictured in Figure 2.32. Extending this surface by the identity on $W(d)$ and a, we get a surface cobordism $\overline{S}_b$ from $W(d)bW(b)a$ to $W(d)\text{Vert}_{2n}b$ inducing the map

$$\mathcal{F}(\overline{S}_b) : \mathcal{F}(W(d)bW(b)a) \to \mathcal{F}(W(d)\text{Vert}_{2n}a) \cong \mathcal{F}(W(d)a).$$

This map $\mathcal{F}(\overline{S}_b)$ defines multiplication in H^n.

2.9.2 Chain complexes of (H^m, H^n)-bimodules associated to (m, n)-tangles

We first introduce (H^m, H^n)-bimodules associated to elements of $\hat{B}_n^m$. Given $t \in \hat{B}_n^m$, one can construct a (H^m, H^n)-bimodule $\mathcal{F}(t)$ as follows:

$$\mathcal{F}(t) := \bigoplus_{a,b} \mathcal{F}(W(b)ta)\{n\},$$

where $a \in B_0^n$ and $b \in B_0^m$. In other words, we take the direct sum over all possible ways to "close up" t with elements of B_0^n and B_0^m. The multiplication maps in H^n and H^m give $\mathcal{F}(t)$ the structure of an (H^m, H^n)-bimodule.

Now we consider an oriented tangle T in $[0,1] \times [0,1] \times [0,1]$. Projecting onto one factor of $[0,1]$ results in a diagram D in $[0,1] \times [0,1]$ which may have crossings. From D, we will build a cube of resolutions which will not depend on the orientations of the components of D. Orientations will come into play once a chain complex is built from the cube, and their effect on the complex will be an overall shift in grading (see [40, Sections 3.2 and 3.4] for details).

Returning to D, each crossing can be resolved using either the 0-resolution or the 1-resolution as in Figure 2.33. In total there are 2^k ways to resolve the k crossings of D, and each yields an element of $\hat{B}_n^m$. The cube of resolutions is a k-dimensional cube whose 2^k vertices are in bijective correspondence with subsets I of the set of crossings K. For example, the empty subset corresponds to $(0, 0, \ldots, 0)$ and the subset K corresponds to $(1, 1, \ldots, 1)$. Edges connect vertices whenever their associated subsets I_1 and I_2 of K are such that $I_1 \subset I_2$ and

$|I_1| + 1 = |I_2|$. To each vertex, we associate the bimodule

$$\mathcal{F}(D(I))\{-|I|\},$$

where $D(I)$ is the element of $\hat{B}_n^m$ given by performing the 1-resolution at crossings in I and the 0-resolution elsewhere (see Figure 2.33.) Whenever vertices corresponding to subsets

Figure 2.33: A type 0 resolution (left) and a type 1 resolution (right).

I_1 and I_2 are connected by an edge, we have a map

$$\mathcal{F}(D(I_1)) \to \mathcal{F}(D(I_2))$$

induced by a surface cobordism which is the identity everywhere except for in a neighborhood of the unique crossing in $I_2 \setminus I_1$. In this neighborhood the cobordism has a single saddle which changes the resolution from type 0 to type 1. An example of a 2-cube of resolutions is given in Figure 2.35.

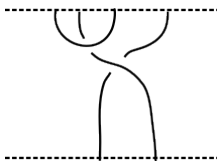

Figure 2.34: A tangle diagram D.

Tensoring this cube with an appropriate anticommutative cube E_I as in [40, Section 3.3] and shifting gradings according to the signs of the oriented crossings as in [40, Section 3.4] results in a chain complex $\mathcal{F}(D)$ of (H^m, H^n)-bimodules associated to the diagram D. The homological degree of a bimodule in this complex is determined by the number of type 1-resolutions in its corresponding element of $\hat{B}_n^m$, and the differentials are given by sums of

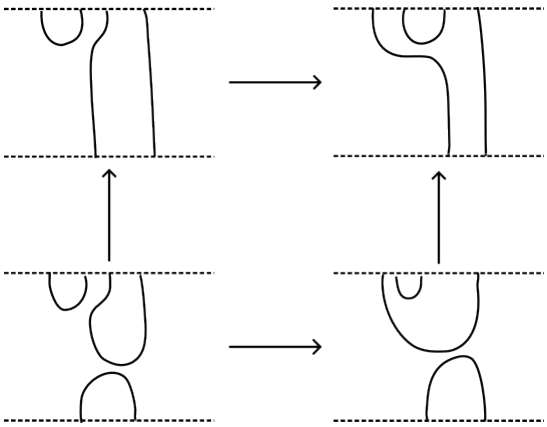

Figure 2.35: The cube of resolutions associated to the tangle diagram D. Each vertex of the cube corresponds to an element of $\hat{B}_1^2$, and the arrows correspond to saddle maps.

maps along edges of the cube. Tensoring with the anticommutative cube E_I is necessary to ensure that the differential map composed with itself is zero; we direct the reader to [40] for more details.

Theorem 2.9.6 ([40], Theorem 2)**.** *If D_1 and D_2 are diagrams of the same oriented tangle, their associated chain complexes $\mathcal{F}(D_1)$ and $\mathcal{F}(D_2)$ are chain homotopy equivalent.*

2.9.3 Bicategories

In [40] Khovanov constructed a braid group action on a bicategory of (H^m, H^n)-chain complexes associated to tangles. In Chapter 5 we will define and construct a *lax group action* of the oriented Thompson group $\vec{F}$ on a generalization of Khovanov's bicategory.

We now discuss necessary background information on bicategories, following the notation of Johnson and Yau's textbook [34]. We assume the reader is familiar with the definitions of a category ([34, Definition 1.1.4]), a functor ([34, Definition 1.1.5]), a natural transformation, and a natural isomorphism ([34, Definition 1.1.7]).

A bicategory can be thought of as a category with the added structure of morphisms between

morphisms. For any two objects X, Y in a bicategory B, the set of morphisms between them is its own category, $B(X, Y)$. The morphisms between objects of $B(X, Y)$ often referred to as 2-morphisms in B. A bicategory has, for any $X, Y, Z \in B$, functors

$$c_{XYZ} : B(Y, Z) \times B(X, Y) \to B(X, Z)$$

which describe the composition of both 1-and 2-morphisms in B. A bicategory also has associator functors, which are natural isomorphisms

$$a_{WXYZ} : c_{WXZ}(c_{XYZ} \times \mathrm{Id}_{B(W,X)}) \to c_{WYZ}(\mathrm{Id}_{B(Y,Z)} \times c_{WXY}),$$

for each tuple of objects $W, X, Y, Z \in B$. Essentially these natural isomorphisms guarantee that composition of morphisms is associative in the appropriate sense; the functor on the left describes composing morphisms in $B(Y, Z) \times B(X, Y)$, and then composing the resulting morphism with that in $B(W, X)$. On the other hand, the functor on the right describes composing the morphisms in $B(X, Y) \times B(W, X)$ first.

A bicategory also has left and right unitors, which are natural transformations

$$c_{XYY}(1_Y \times \mathrm{Id}_{B(X,y)}) \xrightarrow{\ell_{XY}} \mathrm{Id}_{B(X,Y)} \xleftarrow{r_{XY}} c_{XXY}(\mathrm{Id}_{B(X,Y)} \times 1_X),$$

for each pair of objects X, Y in B.

The definition of a bicategory requires that the associators, unitors, and identity maps in $B(X, X)$ for all objects X satisfy certain compatibility conditions. For the full definition of a bicategory, see [34, Definition 2.1.3].

Chapter 3

Infinite Families of Quantum Modular 3-Manifold Invariants

3.1 Overview of results

Results discussed in this chapter are from [49] and [51], the latter of which is joint work with Eleanor McSpirit. Relevant background information is discussed in Chapter 2, specifically Sections 2.2 through 2.6.

This project began in [51] with an investigation of the $\widehat{\widehat{Z}}$ invariant of Brieskorn spheres. In particular, we found explicit formulae for the coefficients $\varphi(n;t)$ of $\widehat{\widehat{Z}}$ as a series in q with Laurent polynomial coefficients in t. For each Brieskorn sphere Σ, its invariant series takes the form:

$$\widehat{\widehat{Z}}_{\Sigma}(t,q) = q^{\Delta}\Big(C - \sum_{n\geq 0}\varphi(n;t)q^{\frac{n^2}{4p}}\Big), \tag{3.1.1}$$

where $\Delta \in \mathbb{Q}$, $p \in \mathbb{Z}$, and C is zero unless Σ is the Poincaré homology sphere, in which case it equals $q^{1/120}(t+t^{-1})$; see Section 3.2 for full definitions.

A priori, $\widehat{\widehat{Z}}_{\Sigma}(t,q)$ is convergent as a two-variable series for $t \in \mathbb{C}$ and $|q|<1$. By leveraging the arithmetic properties of the coefficients $\varphi(n;t)$ when t is a root of unity, we are able to show the following:

Theorem 3.1.1 ([51], Theorem 1.1)**.** *Let ζ be a jth root of unity, ξ a Kth root of unity, and Σ a Brieskorn sphere. Define $\widehat{\widehat{Z}}_\Sigma(\zeta,\xi) := \lim_{t\searrow 0} \widehat{\widehat{Z}}_\Sigma(\zeta,\xi e^{-t})$. This limit exists and we have*

$$\widehat{\widehat{Z}}_\Sigma(\zeta,\xi) = \xi^{\Delta}\left(D + \sum_{n=1}^{2pjK}\left(\frac{n}{2pjK} - \frac{1}{2}\right)\varphi(n;\zeta)\xi^{\frac{n^2}{4p}}\right),$$

where $D = \xi^{1/120}2Re(\zeta)$ when Σ is the Poincaré homology sphere and equals zero otherwise.

In general, these limit calculations give a family of "ζ-deformed" WRT invariants whose topological interpretation is an open question. Using the above results we prove that for t a fixed root of unity, $\widehat{\widehat{Z}}_\Sigma(t,q)$ is, up to normalization, a quantum modular form:

Theorem 3.1.2 ([51], Theorem 1.2)**.** *Let $q = e^{2\pi i\tau}$. If ζ is a jth root of unity and Σ is a Brieskorn sphere, then*

$$\widehat{\widehat{Z}}_\Sigma(\zeta,q) = q^{\Delta}\left(C - A_\zeta(\tau)\right),$$

where $A_\zeta(\tau)$ is a quantum modular form of weight $1/2$ with respect to $\Gamma(4pj^2)$.

Remark. We further have that $A_\zeta(\tau)$ is a "strong" quantum modular form in the sense of [68].

Remark. Experts in the classical theory of theta functions may recall that forms of weight $1/2$ can be related to forms of weight $3/2$ via differentiation of the Jacobi Theta function. Indeed, differentiating the above with respect to the t variable yields a second infinite family of invariants [51, Theorem 1.3]. However, rather than forms of weight $3/2$, the resulting invariants are linear combinations of forms of $1/2$ and $3/2$, and their quantum set is notably smaller.

Now we turn our attention to a more general family of manifolds, Seifert manifolds. Recall

the Reduction Theorem for the $\widehat{Z}$ series of Seifert manifolds given in Section 2.5. The following theorem extends this to the $\widehat{\widehat{Z}}$ series.

Theorem 3.1.3 ([49], Theorem 1.1)**.** *Let $M(b;(a_1,b_1),\dots,(a_k,b_k))$ be a Seifert manifold, and let $|H| = |H_1(M;z)|$. Then:*

$$\widehat{\widehat{Z}}_0(M)(t^2,q^{|H|}) = q^{\Lambda}\mathcal{L}_A(s.e.(f_0(t,z))).$$

Definitions of Λ, $f_0(t,z)$, and $\mathcal{L}_A$ can be found in Section 3.5, and a more detailed version of this result is stated as Theorem 3.5.5. From the calculation in Theorem 3.1.3, modularity properties can be established for Seifert manifolds with three exceptional fibers. Note that not all such manifolds are Brieskorn spheres, as Brieskorn spheres are integer homology spheres but not all Seifert manifolds with 3 exceptional fibers are.

Theorem 3.1.4 ([49], Theorem 1.2)**.** *Let $M = M(b;(a_1,b_1),(a_2,b_2),(a_3,b_3))$ and fix ω to be $2j$th a root of unity. Then $\mathcal{L}_A(s.e.(f_0(\omega,z)))$ is, up to normalization, a quantum modular form of weight $\frac{1}{2}$ with respect to the subgroup $\Gamma(4a_1a_2a_3j^2) \subset SL(2,\mathbb{Z})$.*

Remark. *From the proofs of the above and from Theorem 3.1.1, it follows that radial limits of $\widehat{\widehat{Z}}$ toward roots of unity also exist for Seifert manifolds with 3-exceptional fibers, and can be thought of as ζ-deformed WRT invariants of these manifolds.*

As discussed in Section 2.6, The $\widehat{\widehat{Z}}(t,q)$ invariant is one instance in an infinite collection of two-variable series invariants developed in [7]. This collection, which will be denoted $P_W^{\infty}(t,q)$, is indexed by *admissible families* of functions $\{W_n : \mathbb{Z} \to \frac{\mathbb{Z}}{2}\}_{n\in\mathbb{N}}$ [7, Section 4]. For Seifert manifolds with three exceptional fibers, the role of W is articulated by the following definition and theorem.

Definition 3.1.5. *Given a function $f(z)\colon \mathbb{C} \to \mathbb{C}$ with Laurent expansions of $\sum_k a_k z^k$ centered at $z = 0$ and $\sum_k b_k z^{-k}$ centered at $z = \infty$, fix $y \in \mathbb{R}$ and define the asymmetric expansion, denoted a.e., to be the formal power series given by*

$$a.e._y(f) := (1-y)\sum_k a_k z^k + y\sum_k b_k z^{-k}.$$

When $y = \frac{1}{2}$, this becomes the symmetric expansion used in [28].

Theorem 3.1.6 ([49], Theorem 5.2)**.** *Fix an admissible family W and a 3-manifold $M(b; (a_1, b_1), (a_2, b_2), (a_3, b_3))$. Let $H = |H_1(M; \mathbb{Z})|$. Then*

$$P^{\infty}_{W,[0]}(M)(t^2, q^{|H|}) = q^{\Lambda}(\mathcal{L}_A(a.e._{W_3(1)}(f_0(t, z))). \tag{3.1.2}$$

Remark. *The rational power Λ of q in Theorems 3.1.3 and 3.1.6 is equal to that of the Reduction Theorem in [28].*

From the calculation in Theorem 3.1.6 we obtain a mixed modularity result when t is any root of unity:

Theorem 3.1.7 ([49], Theorem 1.6)**.** *Fix a 3-manifold $M(b; (a_1, b_1), (a_2, b_2), (a_3, b_3))$, a $2j$th root of unity ω and an admissible family W. The one-variable series $\mathcal{L}_A(a.e._{W_3(1)}(f_0(\omega, z))$ is, up to normalization, a sum of quantum-modular and modular forms of weight $\frac{1}{2}$ with respect to $\Gamma(4a_1a_2a_3j^2) \subset SL(2, \mathbb{Z})$. Specifically,*

$$\mathcal{L}_A(a.e._{W_3(1)}(f_0(\omega, z))) = p(q) + \theta_f + (\frac{1}{2} - W_3(1))\Theta_f,$$

where $p(q)$ is a polynomial, θ_f is a quantum modular form, and Θ_f is a modular form.

Remark. *When $W_3(1) = \frac{1}{2}$, the result of Theorem 3.1.4 is recovered. The novelty of Theorem 3.1.7 is that any choice of admissible family W yields modularity properties but quan-*

tum modularity, on its own, is only achieved with the $\widehat{\widehat{Z}}$ invariant. In Section 3.5.5, the admissible family W is shown to play a similar role in "asymmetrizing" the two-variable series associated to H-shaped plumbing graphs, and plumbing graphs with one node and four leaves. Explicit formulae are shown in Examples 3.5.16 and 3.5.17. However the modularity properties of these series are not presently known by the author. Modularity properties of the one-variable $\widehat{Z}$ invariant for these families are established in [14, 15].

3.2 $\widehat{\widehat{Z}}$ invariants of Brieskorn spheres

This section focuses on the $\widehat{\widehat{Z}}$ invariants associated with Brieskorn spheres $\Sigma(b_1, b_2, b_3)$. Toward the proofs of Theorems 3.1.1 and 3.1.2, we develop an explicit formula, which depends only on b_1, b_2, and b_3, for the coefficients $\varphi(n; t)$ of $\widehat{\widehat{Z}}$ as a series in q. The arithmetic properties of these coefficients will allow us to take limits toward roots of unity and establish quantum modularity properties in Sections 3.3 and 3.4. For a general negative definite plumbed 3-manifold Y, one can use a program created by Peter Johnson[1] to calculate the first N coefficients of $\widehat{\widehat{Z}}_Y(t, q)$.

Let k be a spin^c representative for the unique spin^c structure $[k]$ of Σ, and set $a = k - Mu$. For $x \in \mathbb{Z}^s$ we let $\ell := a + 2Mx$. Using the fact established in [7] that

$$\frac{\ell^T M \ell}{4} = \frac{a^2}{4} - 2\chi_k(x) - \langle x, u \rangle,$$

we write

$$\widehat{\widehat{Z}}_\Sigma(t, q) = q^{-\frac{3s+\sum_v m_v}{4}} \sum_{x \in \mathbb{Z}^s} \prod_{v_i \in v(\Gamma)} \widehat{F}_{\delta_i}(\ell_i) q^{-\frac{\ell^T M^{-1} \ell}{4}} t^{\Theta_k + \langle x, u \rangle}.$$

[1] Available at https://github.com/peterkj1/plum

Order the vertices v_1 through v_s so that v_1 through v_3 are the leaves, v_4 is the node, and the rest of the vertices are the joints. The only $x \in \mathbb{Z}^s$ for which $\prod_{v_i} \widehat{F}_{\delta_i}(\ell_i) \neq 0$ are those of the form $\ell = (\varepsilon_1, \varepsilon_2, \varepsilon_3, m, 0, \dots)$ for $\varepsilon_i \in \{\pm 1\}$ and m odd. In this case, we have that $\widehat{F}_1(\varepsilon_i) = -\varepsilon_i$ and $\widehat{F}_3(m) = \frac{1}{2}\text{sign}(m)$, so

$$\prod_{v_i \in v(\Gamma)} \widehat{F}_{\delta_i}(\ell_i) = -\frac{1}{2}\varepsilon_1\varepsilon_2\varepsilon_3\text{sign}(m).$$

Since Brieskorn spheres have unimodular plumbing matrices M, every possible combination $(\varepsilon_1, \varepsilon_2, \varepsilon_3, m, 0, \dots)$ is in $a + 2M\mathbb{Z}^s$. Therefore we can write

$$\widehat{\widehat{Z}}_\Sigma(t,q) = \frac{-q^{-\frac{3s+\sum_v m_v}{4}}}{2} \sum_{\varepsilon_i \in \{\pm 1\}} \sum_{m \text{ odd}} \varepsilon_1\varepsilon_2\varepsilon_3\text{sign}(m) q^{-\frac{\ell^T M^{-1}\ell}{4}} t^{\Theta_k + \langle x,u\rangle}.$$

One can check that $\langle u, x\rangle = \frac{\varepsilon_1+\varepsilon_2+\varepsilon_3+m-a^Tu}{2}$. Moreover, since $\widehat{\widehat{Z}}$ does not depend on a choice of spin^c representative, we make the convenient choice of $a = (1,1,1,1,0,\dots) \in \delta + 2M\mathbb{Z}^s$. In this case, $\Theta_k = 2$ and the exponent on t becomes $(\varepsilon_1 + \varepsilon_2 + \varepsilon_3 + m)/2$.

Remark. In [29, Section 4.6] the authors show how to rewrite

$$\frac{-\ell^t M^{-1}\ell}{4} = \frac{b_1b_2b_3}{4}\left(m + \sum_i \frac{\varepsilon_i}{b_i}\right)^2 - \frac{b_1b_2b_3}{4}\sum \frac{1}{b_i^2} + \frac{\sum_i h_i}{4},$$

where h_i refers to the cardinality of $H_1(\Sigma')$ for the plumbed manifold Σ' that results from removing the ith vertex of the plumbing graph for Σ. Setting

$$\Delta = \frac{1}{4}\left(\sum_i h_i - 3s - \sum_v m_v - \frac{b_2b_3}{b_1} - \frac{b_1b_3}{b_2} - \frac{b_1b_2}{b_3}\right)$$

and $\varepsilon := \varepsilon_1 + \varepsilon_2 + \varepsilon_3$, we now have

$$\hat{\hat{Z}}_\Sigma(t,q) = \frac{-q^\Delta}{2} \sum_{m \text{ odd}} \sum_{\varepsilon_i \in \{\pm 1\}} \varepsilon_1\varepsilon_2\varepsilon_3 \text{sign}(m) q^{\frac{b_1b_2b_3}{4}(m+\sum_i \frac{\varepsilon_i}{b_i})^2} t^{\frac{\varepsilon+m}{2}}. \tag{3.2.1}$$

Now, set $p := b_1b_2b_3$ and

$$\begin{aligned}
\alpha_1 &:= b_1b_2b_3 - b_1b_2 - b_1b_3 - b_2b_3;\\
\alpha_2 &:= b_1b_2b_3 + b_1b_2 - b_1b_3 - b_2b_3;\\
\alpha_3 &:= b_1b_2b_3 - b_1b_2 + b_1b_3 - b_2b_3;\\
\alpha_4 &:= b_1b_2b_3 + b_1b_2 + b_1b_3 - b_2b_3.
\end{aligned}$$

Note that unless $(b_1, b_2, b_3) = (2, 3, 5)$, we always have $0 < \alpha_i < 2p$. In the case of the Poincaré homology sphere we have

α_1	α_2	α_3	α_4
-1	11	19	31

Sometimes the fact that $\alpha_1 < 0$ will require the Poincaré homology sphere to be treated separately in calculations, as is the case below.

Theorem 3.2.1 ([51], Theorem 3.1)**.** *Let $\Sigma(b_1, b_2, b_3)$ be a Brieskorn sphere. Then*

$$\hat{\hat{Z}}_\Sigma(t,q) = q^\Delta \left(C - \sum_{n \geq 1} \varphi(n;t) q^{\frac{n^2}{4p}} \right),$$

where C is nonzero and equals $q^{\frac{1}{120}}(t+t^{-1})$ only when $(b_1,b_2,b_3)=(2,3,5)$ and

$$\varphi(n;t)=\begin{cases}\mp\frac{1}{2}(t^{\frac{\mp n+(\alpha_1+2p)}{2p}}+t^{\frac{\pm n-(\alpha_1+2p)}{2p}}) & n\equiv\pm\alpha_1 \pmod{2p},\\ \pm\frac{1}{2}(t^{\frac{\mp n+\alpha_k}{2p}}+t^{\frac{\pm n-\alpha_k}{2p}}) & n\equiv\pm\alpha_k \pmod{2p},\ k=2,3\\ \mp\frac{1}{2}(t^{\frac{\mp n+(\alpha_4-2p)}{2p}}+t^{\frac{\pm n-(\alpha_4-2p)}{2p}}) & n\equiv\pm\alpha_4 \pmod{2p},\\ 0 & otherwise.\end{cases}$$

Remark. Note that when $t=1$, this recovers the calculation of the $\widehat{Z}$ invariant in [29]. Fixing $\Sigma=\Sigma(2,3,5)$, the function $\varphi(n;1)$ is equal to $\chi_+(n)$ as defined in [45].

Proof. Begin with the calculation given by (3.2.1). Using the fact that $(\varepsilon_1)(\varepsilon_2)(\varepsilon_3)(\text{sign}(m))=(-\varepsilon_1)(-\varepsilon_2)(-\varepsilon_3)(\text{sign}(-m))$, replacing m odd with $2n+1$, and setting $\varepsilon':=\frac{\varepsilon+2n+1}{2}$, we write

$$\hat{\widehat{Z}}_\Sigma(t,q)=\frac{-q^\Delta}{2}\sum_{\varepsilon_i\in\{\pm1\}}\sum_{n\geq0}\varepsilon_1\varepsilon_2\varepsilon_3 q^{p(n^2+n+\frac{1}{4}+(n+\frac{1}{2})\sum_i\frac{\varepsilon_i}{b_i}+\frac{1}{4}(\sum_i\frac{\varepsilon_i}{b_i})^2)}(t^{\varepsilon'}+t^{-\varepsilon'}).$$

Following [29], fix ε_2 and ε_3 and split into two cases based on the value of ε_1. If $\varepsilon_1=-1$, observe that $b_1b_2b_3(1+\sum_i\frac{\varepsilon_i}{b_i})=\alpha_k$ for some $k\in\{1,2,3,4\}$. The corresponding summation over n for this triple of ε_i's is

$$-\varepsilon_2\varepsilon_3\sum_{n\geq0}q^{pn^2+\alpha_kn+\frac{\alpha_k^2}{4p}}(t^{\frac{\varepsilon_2+\varepsilon_3+2n}{2}}+t^{\frac{-(\varepsilon_2+\varepsilon_3+2n)}{2}}). \tag{3.2.2}$$

On the other hand, when $\varepsilon_1=1$, we can replace n with $n-1$ in the corresponding sum to get

$$\varepsilon_2\varepsilon_3\sum_{n\geq1}q^{pn^2-\alpha_jn+\frac{\alpha_j^2}{4p}}(t^{\frac{\varepsilon_2+\varepsilon_3+2n}{2}}+t^{\frac{-(\varepsilon_2+\varepsilon_3+2n)}{2}}), \tag{3.2.3}$$

where for each k the corresponding j is given by

k	1	2	3	4
j	4	3	2	1.

Remark. In [29], it is incorrectly claimed that $j = k$ for each k. This fact does not change the outcome of their calculations, but it does affect ours.

Summing over all four possible values of $(\varepsilon_2, \varepsilon_3)$ gives eight sums, each of which has exponent on q of the form $pn^2 \pm \alpha_k n + \frac{n^2}{4p}$ as in (3.2.2) and (3.2.3). The sums involving $+\alpha_k n$ begin at $n = 0$ and the sums involving $-\alpha_k n$ begin at $n = 1$. The four values of $(\varepsilon_1, \varepsilon_2, \varepsilon_3)$ for which $\varepsilon_2 = -\varepsilon_3$ contribute

$$\sum_{n\geq 0} q^{pn^2+\alpha_2 n+\frac{\alpha_2^2}{4p}}(t^n + t^{-n}) - \sum_{n\geq 1} q^{pn^2-\alpha_2 n+\frac{\alpha_2^2}{4p}}(t^n + t^{-n});$$

$$\sum_{n\geq 0} q^{pn^2+\alpha_3 n+\frac{\alpha_3^2}{4p}}(t^n + t^{-n}) - \sum_{n\geq 1} q^{pn^2-\alpha_3 n+\frac{\alpha_3^2}{4p}}(t^n + t^{-n}), \tag{3.2.4}$$

whereas when $\varepsilon_2 = \varepsilon_3$ we have

$$-\sum_{n\geq 0} q^{pn^2+\alpha_4 n+\frac{\alpha_4^2}{4p}}(t^{n+1} + t^{-(n+1)}) + \sum_{n\geq 1} q^{pn^2-\alpha_4 n+\frac{\alpha_4^2}{4p}}(t^{n-1} + t^{-(n-1)});$$

$$-\sum_{n\geq 0} q^{pn^2+\alpha_1 n+\frac{\alpha_1^2}{4p}}(t^{n-1} + t^{-(n-1)}) + \sum_{n\geq 1} q^{pn^2-\alpha_1 n+\frac{\alpha_1^2}{4p}}(t^{n+1} + t^{-(n+1)}). \tag{3.2.5}$$

For $t = 1$ and $\alpha_k \geq 0$, each of the above collapse to the false theta functions $\tilde{\Psi}_p^{(\alpha_k)}$ into which $\widehat{Z}$ is decomposed in [29]. The only case in which $\alpha_k < 0$ for some k is $\Sigma(2, 3, 5)$, for which $\alpha_1 = -1$. We momentarily postpone this case and take $(b_1, b_2, b_3) \neq (2, 3, 5)$. Working with (3.2.4), we write $pn^2 \pm n\alpha_3 + \frac{\alpha_3^2}{4p} = p(n \pm \frac{\alpha_3}{2p})^2$ and perform the changes of

variables $m = 2pn \pm \alpha_3$. This gives

$$\sum_{\substack{m\geq 0\\ m\equiv\alpha_3\ (2p)}} q^{\frac{m^2}{4p}}(t^{\frac{m-\alpha_3}{2p}} + t^{-\frac{m-\alpha_3}{2p}}) - \sum_{\substack{m\geq 0\\ m\equiv-\alpha_3\ (2p)}} q^{\frac{m^2}{4p}}(t^{\frac{m+\alpha_3}{2p}} + t^{-\frac{m+\alpha_3}{2p}}).$$

The calculation is the same when α_3 is replaced with α_2. When $\varepsilon_1 = \varepsilon_3 = 1$, we get the sums

$$-\sum_{\substack{m\geq 0\\ m\equiv\alpha_4\ (2p)}} q^{\frac{m^2}{4p}}(t^{\frac{m-\alpha_4}{2p}+1} + t^{-(\frac{m-\alpha_4}{2p}+1)}) + \sum_{\substack{m\geq 0\\ m\equiv-\alpha_4\ (2p)}} q^{\frac{m^2}{4p}}(t^{\frac{m+\alpha_4}{2p}-1} + t^{-(\frac{m+\alpha_4}{2p}-1)}),$$

and when $\varepsilon_2 = \varepsilon_3 = -1$ we get

$$-\sum_{\substack{m\geq 0\\ m\equiv\alpha_1\ (2p)}} q^{\frac{m^2}{4p}}(t^{\frac{m-\alpha_1}{2p}-1} + t^{-(\frac{m-\alpha_1}{2p}-1)}) + \sum_{\substack{m\geq 0\\ m\equiv-\alpha_1\ (2p)}} q^{\frac{m^2}{4p}}(t^{\frac{m+\alpha_1}{2p}+1} + t^{-(\frac{m+\alpha_1}{2p}+1)}).$$

If $(b_1, b_2, b_3) \neq (2, 3, 5)$ we are done. We conclude with the special case of the Poincaré homology sphere. The argument is the same up through the calculation of (3.2.5). In this case, we have that

$$\begin{aligned}
&-\sum_{n\geq 1} q^{30n^2-n+\frac{1}{120}}(t^{n-1} + t^{-(n-1)}) + \sum_{n\geq 0} q^{30n^2+n+\frac{1}{120}}(t^{n+1} + t^{-(n+1)}) \\
&= -\sum_{\substack{m\geq 0\\ m\equiv-1\ (60)}} q^{\frac{m^2}{120}}(t^{\frac{m-59}{60}} + t^{-(\frac{m-59}{60})}) + \sum_{\substack{m\geq 0\\ m\equiv 1\ (60)}} q^{\frac{m^2}{120}}(t^{\frac{m+59}{60}} + t^{-(\frac{m+59}{60})}),
\end{aligned}$$

and the bounds on the sums on the left hand side do not agree with those in (3.2.5). The solution is to subtract $2q^{\frac{1}{120}}(t + t^{-1})$ from (3.2.5), as they only disagree in the sign of their constant term. □

3.2.1 Example calculations

Here we calculate $\widehat{\widehat{Z}}_\Sigma(q,\zeta)$ for two Brieskorn spheres and four possible roots of unity ζ.

For ζ a root of unity, let $\Re(\zeta) = \frac{1}{2}(\zeta + \zeta^{-1})$ denote the real part of ζ. Using the formula from Theorem 3.2.1, one can rewrite $\varphi(n;\zeta)$ for any Brieskorn sphere as follows:

n	$\alpha_1 + 2pk$	$2pk - \alpha_1$	$\alpha_i + 2pk$	$2pk - \alpha_i$	$\alpha_4 + 2pk$	$2pk - \alpha_4$
$\varphi(n;\zeta)$	$-\Re(\zeta^{k-1})$	$\Re(\zeta^{k+1})$	$\Re(\zeta^k)$	$-\Re(\zeta^k)$	$-\Re(\zeta^{k+1})$	$\Re(\zeta^{k-1})$

where $i \in \{2,3\}$.

Plugging in the specific values of α_i for the Poincaré homology sphere, the function is

n	$60k+1$	$60k+11$	$60k+19$	$60k-31$	$60k+31$	$60k-19$	$60k-11$	$60k-1$
$\varphi(n;\zeta)$	$\Re(\zeta^{k+1})$	$\Re(\zeta^k)$	$\Re(\zeta^k)$	$-\Re(\zeta^{k+1})$	$\Re(\zeta^{k-1})$	$-\Re(\zeta^k)$	$-\Re(\zeta^k)$	$-\Re(\zeta^{k-1})$

Note the values are ordered left to right in order of congruence class modulo 60.

Instead plugging in the values for $\Sigma(2,3,7)$, we get:

n	$84k+1$	$84k+13$	$84k+29$	$84k+41$	$84k-41$	$84k-29$	$84k-13$	$84k-1$
$\varphi(n;\zeta)$	$-\Re(\zeta^{k-1})$	$\Re(\zeta^k)$	$\Re(\zeta^k)$	$-\Re(\zeta^{k+1})$	$\Re(\zeta^{k+1})$	$-\Re(\zeta^k)$	$-\Re(\zeta^k)$	$\Re(\zeta^{k+1})$

ζ	$\widehat{\widehat{Z}}_\Sigma(\zeta,q)$
1	$2q^{-3/2} - q^{-3/2}(1 + q + q^3 + q^7 - q^8 - q^{14} - q^{20} - q^{29} + q^{31} + q^{42} + q^{52} + \ldots)$
-1	$-2q^{-3/2} - q^{-3/2}(-1 + q + q^3 + q^7 + q^8 + q^{14} + q^{20} - q^{29} + q^{31} - q^{42} + \ldots)$
$e^{\frac{2\pi i}{3}}$	$-q^{-3/2} - q^{-3/2}(-\frac{1}{2} + q + q^3 + q^7 + \frac{1}{2}q^8 + \frac{1}{2}q^{14} + \frac{1}{2}q^{20} - q^{29} - \frac{1}{2}q^{31} + \ldots)$
i	$-q^{-3/2}(q + q^3 + q^7 - q^{29} - q^{31} + q^{69} + q^{85} + q^{99} - q^{143} - q^{161} - q^{185} + \ldots)$

Table 1: Examples of $\widehat{\widehat{Z}}_\Sigma(\zeta, q)$ for $\Sigma(2,3,5)$.

ζ	$\widehat{\widehat{Z}}_\Sigma(\zeta, q)$
1	$-q^{5/2}(-q^4+q^9+q^{17}-q^{26}+q^{87}-q^{106}-q^{130}+q^{153}-q^{275}+q^{308}+\dots)$
-1	$-q^{5/2}(q^4+q^9+q^{17}+q^{26}+q^{87}+q^{106}+q^{130}+q^{153}-q^{275}-q^{308}+\dots)$
$e^{\frac{2\pi i}{3}}$	$-q^{5/2}(\frac{1}{2}q^4+q^9+q^{17}+\frac{1}{2}q^{26}+\frac{1}{2}q^{30}-\frac{1}{2}q^{153}-q^{275}-\frac{1}{2}q^{308}-\frac{1}{2}q^{348}+\dots)$
i	$-q^{5/2}(q^9+q^{17}+q^{87}-q^{153}-q^{275}+q^{385}+q^{615}+q^{671}-q^{1027}-q^{1099}+\dots)$

Table 2: Examples of $\widehat{\widehat{Z}}_\Sigma(\zeta, q)$ for $\Sigma(2,7,15)$.

In the above examples, we factor out a rational power of q so that all other powers are integral. This can be done in general, and is explicitly realized for Brieskorn spheres in the following lemma:

Lemma 3.2.2. *Let α_k, $1 \leq k \leq 4$, be as above. Then $\alpha_1^2 \equiv \alpha_2^2 \equiv \alpha_3^2 \equiv \alpha_4^2 \pmod{4p}$.*

One can prove this by writing each α_i in terms of b_1, b_2, and b_3 ,e.g.

$$\alpha_1 = b_1b_2b_3 + b_1b_2 - b_1b_3 - b_2b_3,$$

and then squaring each expression.

3.3 Radial limits toward roots of unity

In this section, we analyze the arithmetic properties of the coefficients $\varphi(n;t)$ which will ultimately allow for the calculation of radial limits at roots of unity in terms of particular

L-functions. We first check that the coefficients of $\varphi(n;t)$ have the necessary properties for our method of calculation.

Lemma 3.3.1. *If ζ is a jth root of unity, then $\varphi(n;\zeta)$ is $2pj$-periodic and has mean value zero.*

Proof. First, we prove periodicity. If $n \not\equiv \pm\alpha_i \pmod{2p}$ for any i, then $\varphi(n;\zeta) = 0$ and $\varphi(n+2pj;\zeta) = 0$. If $\varphi(n;\zeta) \neq 0$ then $n \equiv \pm\alpha_i$ for some $1 \leq i \leq 4$. We now prove periodicity for $n \equiv +\alpha_i \pmod{2p}$; a similar argument may be applied to the other seven cases. If $n \equiv +\alpha_1 \pmod{2p}$ then $n = \alpha_i + 2pk$ for some $k \in \mathbb{Z}$.

Then

$$\varphi(n;\zeta) = -\frac{1}{2}\left(\zeta^{\frac{-2pk-\alpha_1+alpha_1+2p}{2p}} + \zeta^{\frac{2pk+\alpha_1-\alpha_1-2p}{2p}}\right) = -\frac{1}{2}\left(\zeta^{-(k-1)} + \zeta^{k-1}\right).$$

A similar calculation shows that

$$\varphi(n+2pj;\zeta) = -\frac{1}{2}\left(\zeta^{-(k+j-1)} + \zeta^{k+j-1}\right) = -\frac{1}{2}\left(\zeta^{-(k-1)} + \zeta^{k-1}\right).$$

The same strategy works for all other congruence classes of n for which $\varphi(n;\zeta) \neq 0$. From $2pj$-periodicity and the formula for $\varphi(n;t)$, it follows that

$$\varphi(n;\zeta) = -\varphi(2pj - n;\zeta).$$

Since the period of $\varphi(n;\zeta)$ is even, this implies that $\varphi(n;\zeta)$ has mean value zero. □

In order to calculate radial limits, we make use of the following general proposition.

Proposition 3.3.2. *Let $C\colon \mathbb{Z} \to \mathbb{C}$ be a periodic function with mean value zero. Then the associated L-series $L(s,C) := \sum_{n\geq 1} \frac{C(n)}{n^s}$, $\Re(s) > 1$, extends holomorphically to all of $\mathbb{C}$*

and the function $\sum_{n\geq 1} C(n)e^{-n^2t},\ t>0$*, has the asymptotic expansion*

$$\sum_{n\geq 1} C(n)e^{-n^2t} \sim \sum_{r\geq 0} L(-2r,C)\frac{(-t)^r}{r!}$$

as $t \searrow 0$*. Then numbers* $L(-r,C)$ *are given explicitly by*

$$L(-r,C) = -\frac{M^r}{r+1}\sum_{n=1}^{M} C(n)B_{r+1}\left(\frac{n}{M}\right), \quad (r=0,1,\dots), \tag{3.3.1}$$

where $B_k(x)$ *is the* k*th Bernoulli polynomial and* M *is any period of the function* $C(n)$*.*

For details, see e.g. [45] p. 98.

Note the slight abuse of notation where C may refer to either an arithmetic function or the extra term C which appears in (3.1.1) in the case were the 3-manifold in question is the Poincaré homology sphere. We will specify when unclear from context.

Proof of Theorem 3.1.1

Let ξ be a root of unity and set $C(n) := \varphi(n;\zeta)\xi^{\frac{n^2}{4p}}$. If K is a period of ξ, a straightforward calculation shows that $\xi^{\frac{(n+2pjK)^2}{4p}} = \xi^{\frac{(2pjK-n)^2}{4p}} = \xi^{\frac{n^2}{4p}}$. It follows that $C(n)$ is $2pjK$-periodic with mean value zero, and $C(2pjK-n) = -C(n)$. Let

$$A_\zeta(q) := \sum_{n\geq 0} \varphi(n;\zeta)q^{\frac{n^2}{4p}}, \tag{3.3.2}$$

and observe that

$$A_\zeta(\xi e^{-t}) = \sum_{n=1}^{\infty} C(n)e^{-n^2(t/4p)}.$$

By the previous proposition, the above has asymptotic expansion

$$\sum_{r=0}^{\infty} L(-2r, C)\frac{(-t/4p)^r}{r!}$$

as $t \searrow 0$.

Moreover, taking the limit of this L-series as $t \searrow 0$, all terms for $r > 0$ term vanish and we are left with

$$\lim_{t\searrow 0} L(0, C)\frac{(-t/4p)^0}{0!} = L(0, C).$$

Using the formula for $L(0, C)$ given in (3.3.1) and the fact that the 0th Bernoulli polynomial $B_0(x) = x - \frac{1}{2}$, we arrive at

$$L(0, C) = -\sum_{n=1}^{M}(\frac{n}{M} - \frac{1}{2})C(n) = -\sum_{n=1}^{2pjK}(\frac{n}{2pjK} - \frac{1}{2})\varphi(n; \zeta)\xi^{\frac{n^2}{4p}}$$

Evaluating both q^{Δ} and the extra term $C = q^{\frac{1}{120}}(t + t^{-1})$ (which appears only when Σ is the Poincaré homology sphere) at (ζ, ξ) gives the desired formula. □

3.3.1 Understanding ζ-deformations for $q \nearrow 1$

Radial limits toward roots of unity give a novel family of invariants which may be thought of as ζ-deformed WRT invariants. Toward a topological and physical understanding of these deformations, the author has computed the limits as $q \nearrow 1$ of $\widehat{\widehat{Z}}(\zeta, q)$ for Brieskorn homology spheres, where ζ is a general root of unity.

Proposition 3.3.3. *Fix a root of unity ζ and let $\Sigma = \Sigma(b_1, b_2, b_3)$ be a Brieskorn homology*

sphere. Then for its associated (t,q)*-series invariant* $\widehat{\widehat{Z}}$*,*

$$\lim_{q\to 1}\widehat{\widehat{Z}}(\zeta,q) := \lim_{t\searrow 0}(\zeta,e^{-t}) = \zeta+\zeta^{-1}-2.$$

Observe that this limit coincides with the value of

$$\prod_v(\zeta-\zeta^{-1})^{2-\delta_v} = \frac{(\zeta-\zeta^{-1})^3}{(\zeta-\zeta^{-1})}. \tag{3.3.3}$$

This expression is also equal to $f_0(\zeta,1)$, where $f_0(t,z)$ is a rational function associated to each Seifert manifold and defined later in Section 3.5.1.

It will follow from the definition of $f_0(t,z)$ that all Seifert manifolds have

$$f_0(\zeta,1) = \zeta+\zeta^{-1}-2,$$

which motivates the following conjecture.

Conjecture 3.3.4. *Fix a root of unity* ζ *and let* M *be a Seifert manifold. Then*

$$\widehat{\widehat{Z}}(\zeta,1) = \lim_{t\searrow 0}\widehat{\widehat{Z}}(\zeta,e^{-t}) = f_0(\zeta,1) = \zeta+\zeta^{-1}-2.$$

We now return to the proof of Proposition 3.3.3.

Proof. By Theorem 3.1.1, we know that

$$\widehat{\widehat{Z}}_\Sigma(\zeta,1) = D + \sum_{n=1}^{2pjK}\left(\frac{n}{2pjK}-\frac{1}{2}\right)\varphi(n;\zeta)\xi^{\frac{n^2}{4p}},$$

where $D = 2\Re(\zeta)$ if $\Sigma=\Sigma(2,3,5)$ and 0 otherwise.

First suppose $(b_1, b_2, b_3) \neq (2, 3, 5)$. Then we will have $0 < \alpha_i < 2p$ for all α_i and we may rewrite

$$\sum_{i=1}^{2pj}(\frac{n}{2pj} - \frac{1}{2})\varphi(n;\zeta) = -\sum_{k=0}^{j=1}(\frac{\alpha_1 + 2pk}{2pj} - \frac{1}{2})\Re(\zeta^{k-1}) + \sum_{k=0}^{j-1}(\frac{2pk + 2p - \alpha_1}{2pj} - \frac{1}{2})\Re(\zeta^{k+2}) \tag{3.3.4}$$

$$+ \sum_{k=0}^{j-1}(\frac{\alpha_2 + 2pk}{2pj} - \frac{1}{2})\Re(\zeta^{k}) - \sum_{k=0}^{j-1}(\frac{2pk + 2p - \alpha_2}{2pj} - \frac{1}{2})\Re(\zeta^{k+1}) \tag{3.3.5}$$

$$+ \sum_{k=0}^{j-1}(\frac{\alpha_3 + 2pk}{2pj} - \frac{1}{2})\Re(\zeta^{k}) - \sum_{k=0}^{j-1}(\frac{2pk + 2p - \alpha_3}{2pj} - \frac{1}{2})\Re(\zeta^{k+1}) \tag{3.3.6}$$

$$+ - \sum_{k=0}^{j-1}(\frac{\alpha_4 + 2pk}{2pj} - \frac{1}{2})\Re(\zeta^{k+1}) + \sum_{k=0}^{j-1}(\frac{2pk + 2p - \alpha_4}{2pj} - \frac{1}{2})\Re(\zeta^{k}) \tag{3.3.7}$$

Note that if $(b_1, b_2, b_3) = (2, 3, 5)$ then $\alpha_1 = -1$ and the bounds on the first two sums will change. The first sum will range from $k = 1$ to $k = j$ and the second sum will range from $k = -1$ to $k = j - 2$. We will revisit this case later. Returning for now to the case of $(b_1, b_2, b_3) \neq (2, 3, 5)$, we may combine the sums in which $\Re(\zeta^k)$ appears to obtain

$$\sum_{k=0}^{j=1}\left[\frac{6pk + 2p + \alpha_2 + \alpha_3 - \alpha_4}{2pj} - \frac{3}{2}\right]\Re(\zeta^k).$$

Using the fact that $\alpha_1 - \alpha_2 - \alpha_3 + \alpha_4 = 0$, we rewrite the above as

$$\sum_{k=0}^{j-1}\left[\frac{6pk + 2p + \alpha_1}{2pj} - \frac{3}{2}\right]\Re(\zeta^k).$$

Applying the same process to the three sums containing $\Re(\zeta^{k+1})$, we get

$$-\left(\sum_{k=0}^{j=1}\left[\frac{6pk+4p-\alpha_1}{2pj}-\frac{3}{2}\right]\right)\Re(\zeta^{k+1}.$$

Now we may rewrite the radial limit entirely in terms of α_1 :

$$\sum_{i=1}^{2pj}(\frac{n}{2pj}-\frac{1}{2})\varphi(n;\zeta)=-\sum_{k=0}^{j-1}\left[\frac{\alpha_1+2pk}{2pj}-\frac{1}{2}\right]\Re(\zeta^{k-1})+\sum_{k=0}^{j-1}\left[\frac{6pk+2p+\alpha_1}{2pj}-\frac{3}{2}\right]\Re(\zeta^{k}) \tag{3.3.8}$$

$$-\sum_{k=0}^{j-1}\left[\frac{6pk+4p-\alpha_1}{2pj}-\frac{3}{2}\right]\Re(\zeta^{k+1})+\sum_{k=0}^{j=1}\left[\frac{2pk+2p-\alpha_1}{2pj}-\frac{1}{2}\right]\Re(\zeta^{k+2}). \tag{3.3.9}$$

Next we expand (3.3.8):

$$\begin{aligned}(3.3.8)=&-\left[\frac{\alpha_1}{2pj}-\frac{1}{2}\right]\Re(\zeta^{-1})-\sum_{k=1}^{j-1}\left[\frac{\alpha_1+2pk}{2pj}-\frac{1}{2}\right]\Re(\zeta^{k-1})\\&+\sum_{k=0}^{j-2}\left[\frac{6pk+2p+\alpha_1}{2pj}-\frac{3}{2}\right]\Re(\zeta^{k})+\left[\frac{6pj-4p+\alpha_1}{2pj}-\frac{3}{2}\right]\Re(\zeta^{j-1}).\end{aligned}$$

We have separated the $k=0$ term of the first sum and the $k=j-1$ term of the second sum so that the remaining sums can be re-indexed and combined. This yields yet another expression for (3.3.8) which is

$$\left[2-\frac{4p}{2pj}\right]\Re(\zeta)+\sum_{k=1}^{j-1}\left[\frac{4pk-4p}{2pj}-1\right]\Re(\zeta^{k-1}). \tag{3.3.10}$$

We repeat the process with (3.3.9) which results in

$$\left[2-\frac{4p}{2pj}\right]\Re(\zeta)+\sum_{k=1}^{j-1}\left[\frac{-4pk-4p}{2pj}+1\right]\Re(\zeta^{k+1}). \tag{3.3.11}$$

Now we have that

$$\lim_{q\nearrow 1}\hat{\hat{Z}}(\zeta,q)=(3.3.8)+(3.3.9)=(3.3.10)+(3.3.11)$$

Adding the first summand of (3.3.10) to the first summand of (3.3.11) yields

$$\left[4-\frac{8p}{2pj}\right]\Re(\zeta). \tag{3.3.12}$$

Adding the second summand of (3.3.10) to the second summand of (3.3.11) and re-indexing gives

$$\left[\frac{8p-4pj}{2pj}\right]\Re(\zeta)+\sum_{k=3}^{j-1}\left[\frac{4pk-4p}{2pj}-1\right]\Re(\zeta^{k-1})+\sum_{k=1}^{j-3}\left[\frac{-4pk-4p}{2pj}+1\right]\Re(\zeta^{k+1})+\left[\frac{-4pj}{2pj}\right] \tag{3.3.13}$$

where the $k=1$ and $k=2$ terms have been pulled out of the second summand of (3.3.10), and the $k=j-1$ and $k=j-2$ terms have been pulled out of the second summand of (3.3.11). One can re-index and cancel the remaining sums of (3.3.13) so we are left with

$$(3.3.13)=-2+\left[-2+\frac{8p}{4pj}\right]\Re(\zeta).$$

Finally we get that

$$\lim_{q\nearrow 1}\hat{\hat{Z}}(\zeta,q)=(3.3.12)+(3.3.13)=2\Re(\zeta)-2=(\zeta^{\frac{1}{2}}-\zeta^{-\frac{1}{2}})^2.$$

Now we revisit the Poincaré homology sphere. To expand

$$\sum_{i=1}^{2pj}(\frac{n}{2pj}-\frac{1}{2})\varphi(n;\zeta),$$

we begin as before except line (3.3.4) should be substituted with

$$-\sum_{k=1}^{j}\left(\frac{\alpha_1+2pk}{2pj}-\frac{1}{2}\right)\Re(\zeta^{k-1})+\sum_{k=-1}^{j-2}\left(\frac{2pk+2p-\alpha_1}{2pj}-\frac{1}{2}\right)\Re(\zeta^{k+2}).$$

This has the same effect as adding

$$\left(\frac{\alpha_1}{2pj}-\frac{1}{2}\right)\Re(\zeta^{-1})-\left(\frac{\alpha_1+2pj}{2pj}-\frac{1}{2}\right)\Re(\zeta^{j-1})-\left(\frac{2pj-\alpha_1}{2pj}-\frac{1}{2}\right)\Re(\zeta^{j+1})+\left(\frac{-\alpha_1}{2pj}-\frac{1}{2}\right)\Re(\zeta)$$
$$=\left(\frac{-\alpha_1-2pj+\alpha_1-2pj}{2pj}\right)\Re(\zeta)=-2\Re(\zeta)$$

to the overall sum we calculated in the case where $(b_1,b_2,b_3)\neq(2,3,5)$. In other words, we are

1. Subtracting the $k=0$ term from the first sum in (3.3.4)

2. Adding in the $k=j$ term to the first sum in (3.3.4)

3. Subtracting the $k=j-1$ term from the second sum in (3.3.4)

4. Adding in a $k=-1$ term to the second sum in (3.3.4).

However this cancels out with $D=2\Re(\zeta)$ so the final result is the same and the limit is equal to $\zeta+\zeta^{-1}-2$. □

3.4 Quantum modularity for Brieskorn spheres

In this section we prove Theorem 3.1.2, which states that for a Brieskorn sphere Σ and root of unity ζ, the associated invariant series $\widehat{\widehat{Z}}_\Sigma(\zeta, q)$ is, up to normalization, a quantum modular form. Specifically,

$$\widehat{\widehat{Z}}_\Sigma(\zeta, q) = q^\Delta \left(C - A_\zeta(\tau)\right),$$

where

$$A_\zeta(\tau) = \sum_{n \geq 0} \varphi(n; \zeta) q^{\frac{n^2}{4p}}$$

is a quantum modular form.

In light of the work summarized in Section 2.4, it suffices to show that

$$\sum_{n \geq 0} n\varphi(n; \zeta) q^{\frac{n^2}{4pj}} \tag{3.4.1}$$

is a cusp form for $\Gamma(4pj)$. Then the results of Section 2.4.1 used in conjunction with Lemma 2.4.3 will imply

$$\sum_{n \geq 0} \varphi(n; \zeta) q^{\frac{n^2}{4p}}$$

is a quantum modular form. We begin with an elementary lemma which will be useful for simplifying our expressions later.

Lemma 3.4.1. *Let $0 \leq n < 2pj$ be such that $n \equiv \pm\alpha_k \pmod{2p}$ for some k. Then we have $n^2 \equiv w + 4pi \pmod{4pj}$ for some $0 \leq i < j$, where w is the common congruence class modulo $4p$ of the α_k^2's coming from Lemma 3.2.2.*

Proof. We may write $n = 2pm \pm \alpha_i$ for some m and $\alpha_i^2 = 4pd + w$ for some $d \in \mathbb{Z}$. Then

$$n^2 = 4p(pm^2 \pm m\alpha_i + d) + w,$$

and i is equal to the congruence class of

$$(pm^2 \pm m\alpha_i + d) \pmod{j}.$$

□

We are now ready to show that (3.4.1) is indeed a cusp form. We will do this by decomposing it into a sum of theta functions. Since $\varphi(n;\zeta)$ is $2pj$-periodic, we have

$$\sum_{n\geq 0} n\varphi(n;\zeta)q^{\frac{n^2}{4pj}} = \sum_{0\leq\alpha<2pj} \varphi(\alpha;\zeta)\sum_{n\geq 0}(2pjn+\alpha)q^{\frac{(2pjn+\alpha)^2}{4pj}}.$$

Every α for which $\varphi(\alpha;\zeta)$ is nonzero satisfies $\alpha \equiv \pm\alpha_k \pmod{2p}$ for some k. Thus, we can write this sum as

$$\sum_{\substack{0\leq\alpha<2pj \\ \alpha\equiv\alpha_k(2p)}} \varphi(\alpha,\zeta)\sum_{n\geq 0}(2pjn+\alpha)q^{\frac{(2pjn+\alpha)^2}{4pj}} \tag{3.4.2}$$

$$+ \sum_{\substack{0<\alpha\leq 2pj \\ \alpha\equiv\alpha_k(2p)}} \varphi(2pj-\alpha,\zeta)\sum_{n\geq 0}(2pjn+(2pj-\alpha))q^{\frac{(2pjn+(2pj-\alpha))^2}{4pj}}. \tag{3.4.3}$$

Using the fact that $\varphi(n;\zeta)$ is odd and $2pj$-periodic, (3.4.3) can be rewritten as

$$\sum_{\substack{0<\alpha\leq 2pj \\ \alpha\equiv\alpha_k(2p)}} -\varphi(\alpha,\zeta)\sum_{n\geq 0}(2pj(n+1)-\alpha)q^{\frac{(2pj(n+1)-\alpha))^2}{4pj}}.$$

We may re-index the inner sum by $n+1 \mapsto n$ to get

$$\sum_{\substack{0<\alpha\leq 2pj \\ \alpha\equiv\alpha_k(2p)}} -\varphi(\alpha,\zeta)\sum_{n\geq 1}(2pjn-\alpha)q^{\frac{(2pjn-\alpha)^2}{4pj}},$$

and then re-index by $n \mapsto -n$ to get

$$\sum_{\substack{0<\alpha\leq 2pj \\ \alpha\equiv\alpha_k(2p)}} -\varphi(\alpha,\zeta)\sum_{n\leq -1}(-2pn-\alpha)q^{\frac{(-2pn-\alpha)^2}{4pj}} = \sum_{\substack{0<\alpha\leq 2pj \\ \alpha\equiv\alpha_k(2p)}} \varphi(\alpha,\zeta)\sum_{n\leq -1}(2pn+\alpha)q^{\frac{(2pn+\alpha)^2}{4pj}}.$$

Combining this back with (3.4.2) we obtain

$$\sum_{n\geq 0} n\varphi(n;\zeta)q^{\frac{n^2}{4pj}} = \sum_{\substack{0\leq\alpha<2pj \\ \alpha\equiv\alpha_k(2p)}} \varphi(\alpha;\zeta)\sum_{\substack{n\in\mathbb{Z} \\ n\equiv\alpha(2pj)}} nq^{\frac{n^2}{4pj}}. \tag{3.4.4}$$

The inner sum of the above equation is a theta function which is modular of weight $3/2$.

More generally define

$$\Theta(\tau;k,M) := \sum_{\substack{n\in\mathbb{Z} \\ n\equiv k(M)}} nq^{\frac{n^2}{2M}}.$$

The inner sum of (3.4.4) is $\Theta(\tau;\alpha,2pj)$.

By Proposition 2.1 of [65], we have that for $\gamma \in \Gamma_1(2M)$ that

$$\Theta(\gamma\tau;k,M) = e^{\frac{\pi iabk^2}{M}}\varepsilon_d^{-3}\left(\frac{2Mc}{d}\right)(c\tau+d)^{3/2}\Theta(\tau;ak,M),$$

and since $k \equiv ak \pmod{M}$, we have

$$\Theta(z;ak,M) = \Theta(z;k,M),$$

and the transformation law for modularity is satisfied.

Note that if $n_1^2 \equiv n_2^2 \pmod{4pj}$ then $\Theta(\tau; n_1, 2pj)$ will have the same multiplier as $\Theta(\tau; n_2, 2pj)$. This is because, by Lemma 6.1, every n for which the coefficient of $q^{\frac{n^2}{4pj}}$ in (3.4.4) is nonzero satisfies $n^2 \equiv w + 4pi \pmod{4pj}$ for some $0 \leq i < j$ and

$$e^{\frac{\pi i a b n^2}{2pj}} = e^{\frac{\pi i a b (w+4pi)}{2pj}}.$$

One may then group the n's based on the corresponding i to get j functions $f_i(\tau)$ which for $\gamma = \left(\begin{smallmatrix} a & b \\ c & d \end{smallmatrix}\right) \in \Gamma_1(4pj)$ satisfy

$$f_i(\gamma\tau) = e^{\frac{\pi i a b (w+4pi)}{2pj}} \varepsilon_d^{-3} \left(\frac{4pjc}{d}\right) (c\tau + d)^{3/2} f_i(\tau).$$

Note the dependence of this transformation law on i. If one restricts to $\gamma \in \Gamma(4pj) \subset \Gamma_1(4pj)$, the multipliers for each f_i become identical as $b \equiv 0 \pmod{4pj}$. Thus the sum of the f_i's transform together as a cusp form on $\Gamma(4pj)$. $\square$

3.5 The (t, q)-series invariants of Seifert manifolds

This section contains proofs of the results pertaining to (t, q)-series of Seifert manifolds, specifically Theorems 3.1.3 through 3.1.7. At the end of the chapter we present additional calculations of the (t, q)-series for other families of manifolds, which we hope will lend themselves to further analysis for modularity properties. From now on, we adopt the following convention when ordering vertices of a Seifert manifold's plumbing graph: v_0 will be the node, v_1 through v_k will be the k leaves, the remaining vertices v_{k+1} through v_{s-1} will be the joints. Throughout the section we will need the following lemma:

Lemma 3.5.1. *Let M be a negative definite plumbed 3-manifold with $b_1 = 0$. Define m, s, and u as before. Then we may write*

$$P^{\infty}_{W,0}(M)(t^2, q) = q^{-\frac{3s+m\cdot u}{4}} \sum_{\ell \in \delta + 2\mathbb{Z}^s} (\prod_i W_{\delta_i}(\ell_i)) q^{\frac{\ell^t M^{-1} \ell}{4}} t^{\ell \cdot u}.$$

Proof. From the definition in [7] and a simple calculation in [51, Section 3] we know that for a spin^c structure $[k]$ we have

$$P^{\infty}_{W,[k]}(t^2, q) = q^{-\frac{3s+m\cdot u}{4}} \sum_{x \in \mathbb{Z}^s} W_{\Gamma,k}(x) q^{\frac{\ell^t M^{-1} \ell}{4}} t^{2(\Theta_k + \langle x, u \rangle)},$$

where $W_{\Gamma,k}(x)$ is given by the admissible family of functions, $\ell = k - Mu + 2Mx$, and $\Theta_k = \frac{k\cdot u - \langle u,u \rangle}{2}$.

A straightforward calculation shows that

$$2(\Theta_k + \langle x, u \rangle) = \ell \cdot u.$$

Moreover, $W_{\Gamma,k}(x) = \prod_i W_{\delta_i}(k - Mu + 2Mx)_i$. Therefore we may re-index our sum as

$$P^{\infty}_{W,[k]}(t^2, q) = q^{-\frac{3s+m\cdot u}{4}} \sum_{\ell \in k - Mu + 2M\mathbb{Z}^s} \prod_i (W_{\delta_i}(\ell_i)) q^{-\frac{\ell^t M^{-1} \ell}{4}} t^{\ell \cdot u}.$$

Now summing over all $[k] \in \frac{m + 2\mathbb{Z}^s}{2M\mathbb{Z}^s}$, we may write

$$
\begin{aligned}
P^{\infty}_{W,0}(t^2,q) &= \sum_{[k]\in \text{spin}^c(M)} P^{\infty}_{W,[k]}(M) \\
&= \sum_{[k]\in \frac{m+2\mathbb{Z}^s}{2M\mathbb{Z}^s}} q^{-\frac{3s+m\cdot u}{4}} \sum_{\ell\in k-Mu+2M\mathbb{Z}^s} \prod_i (W_{\delta_i}(\ell_i)) q^{-\frac{\ell^t M^{-1}\ell}{4}} t^{\ell\cdot u} \\
&= q^{-\frac{3s+m\cdot u}{4}} \sum_{\delta+2\mathbb{Z}^s} \prod_i (W_{\delta_i}(\ell_i)) q^{-\frac{\ell^t M^{-1}\ell}{4}} t^{\ell\cdot u}.
\end{aligned}
$$

The previous equality is true because, for each $[k] \in \frac{m+2\mathbb{Z}^s}{2M\mathbb{Z}^s}$, we are summing over all possible representatives of its image under the isomorphism

$$
\begin{aligned}
\frac{m+2\mathbb{Z}^s}{2M\mathbb{Z}^s} &\to \frac{\delta+2\mathbb{Z}^s}{2M\mathbb{Z}^s} \\
[k] &\mapsto [k-Mu],
\end{aligned}
$$

and therefore we are taking the sum, over each congruence class of $\frac{\delta+2\mathbb{Z}^s}{2M\mathbb{Z}^s}$, of all of its representatives in $\delta+2\mathbb{Z}^s$. This is equivalent to taking the sum over all $\delta+2\mathbb{Z}^s$.

□

Remark. *$P^{\infty}_{W,[k]}$ may be further simplified by only summing over those ℓ_i such that*

$$\ell_i = 0 \Leftarrow \delta_i = 2$$

and

$$\ell_i = \pm 1 \Leftarrow \delta_i = 1.$$

These restrictions follow from Definition 2.6.1 of admissible families.

3.5.1 The $\widehat{Z}$ series of Seifert Manifolds

The purpose of this section is to state and prove Theorem 3.1.3, which presents a precise formula for the $\widehat{\widehat{Z}}_0(t,q)$ series invariant of Seifert manifolds depending only on Seifert data. We begin with some necessary lemmas about symmetric expansions.

Lemma 3.5.2. *Let $M = M(b;(a_1,b_1),\dots(a_k,b_k))$. For all $\ell \in \delta + 2\mathbb{Z}^s$, let $C(\ell)$ denote the coefficient of $\vec{z}^{\ell}$ in*

$$s.e.(\prod_v (z_v - z_v^{-1})^{2-\delta_v}.$$

Then

$$C(\ell) = C(-\ell).$$

Proof. Sending $\ell \mapsto -\ell$ multiplies the coefficient by $(-1)^k(-1)^{k-2} = 1$. The factor of $(-1)^k$ comes from sending $\ell_i \mapsto -\ell_i$ for $1 \le i \le k$, and the factor of $(-1)^{k-2}$ comes from sending $\ell_0 \mapsto -\ell_0$. □

Lemma 3.5.3. *Suppose $M(b;(a_1,b_1),\dots(a_k,b_k))$ is a Seifert manifold. Let $A := \prod_i a_i$ and $\overline{a_i} := \frac{A}{a_i}$. Define*

$$f_0(z,t) := \frac{(z^{\overline{a_1}}t^{-1} - z^{-\overline{a_1}}t)\dots((z^{\overline{a_k}}t^{-1} - z^{-\overline{a_k}}t)}{(z^A t^{-1} - z^{-A}t)^{k-2}}$$

and let $C'(\ell)$ denote the coefficient of $z^{\ell_0 A + \sum_{i\ge 1}\overline{a_i}\ell_i}t^{-\ell\cdot u}$ in

$$s.e.(f_0(z,t)).$$

Then

$$C(\ell) = C'(\ell)$$

Proof. This follows from the fact that $f_0(z,t)$ can be obtained from

$$\prod_v (z_v - z_v^{-1})^{2-\delta_v}$$

via the substitution

$$z_0 \mapsto z^A t^{-1}$$
$$z_i \mapsto z^{\overline{a_i}} t^{-1}.$$

□

Corollary 3.5.4. $C'(\ell) = C'(-\ell))$.

Theorem 3.5.5. *Let $M(b; (a_1, b_1), \ldots, (a_k, b_k))$ be a Seifert manifold with plumbing matrix M. Then:*

$$\hat{\hat{Z}}(M)(t^2, q^{|H|}) = q^{\Lambda} \mathcal{L}_A(s.e.(f_0(t,z)))$$

where $\Lambda = \Lambda(Y)$ is the prefactor as in the proof of [28, Theorem 4.2], $|H| = |H_1(M;\mathbb{Z})|$, and $\mathcal{L}_A$ is the Laplace transform sending $z^n t^m \mapsto q^{\frac{n^2}{4A}} t^m$.

Proof. Applying Lemma 3.5.1, we have

$$\hat{\hat{Z}}_0(M)(t^2, q) = q^{-\frac{3s+\mathrm{Tr}(M)}{4}} \sum_{\ell \in \delta + 2\mathbb{Z}^s} (\prod_i \widehat{W}_{\delta_i}(\ell_i))) q^{\frac{\ell^t M^{-1} \ell}{4}} t^{\ell \cdot u}$$

Note that $(\prod_i \widehat{W}_{\delta_i}(\ell_i)))$ identifies the coefficient on $\vec{z}^{-\vec{\ell}}$ in the symmetric expansion of $\prod_v (z_v - z_v^{-1})^{2-\delta_v}$. As in the proof of [28, Theorem 4.2] we may compute $\hat{\hat{Z}}_0(t^2, q^{|H|})$ by replacing terms of the form

$$q^{-\frac{\ell^t M^{-1} \ell}{4}} t^{u \cdot \ell}$$

with terms of the form

$$q^{-\frac{\ell^t(-1)^s \text{adj}M\ell}{4}} t^{u\cdot\ell},$$

where adj$M$ denotes the adjugate matrix [2]. For notational convenience, we will let

$$M' := (-1)^s \text{adj}M.$$

Exactly as in the proof of [28, Theorem 4.2], we evaluate $\frac{\ell^t M'\ell}{4}$ for each ℓ. Let $\overline{a_{ij}} := \frac{A}{a_i a_j}$. The exponent on q (multiplied by 4 for notational convenience) becomes

$$4\ell^t M'\ell = \ell_0^2 A + 2\sum_{i\neq 0} \ell_0\ell_i\overline{a_i} + \sum_{i\neq j} \ell_i\ell_j\overline{a_{ij}} + \sum_{i\neq 0} \ell_i^2 \text{adj}M_{ii}. \tag{3.5.1}$$

The calculation above is a consequence of the relationship between the adjugate matrix and the *splice diagram* associated to the plumbing graph Γ; for more details see [28, Theorems 3.3 and 4.1]. Applying Corollary 3.5.4, we get that all terms are of the form

$$C(\ell) q^{\frac{\ell^t M'\ell}{4}} [t^{\ell\cdot u} + t^{-\ell\cdot u}].$$

On the other hand, we calculate the symmetric expansion of $f_0(z,t)$. We start with

$$\text{s.e.}(f_0(t,z)) = \left[\prod_{1\leq i\leq k} (z_{v_i}^{\overline{a_i}} t^{-1} - z_{v_i}^{-\overline{a_i}} t)\right] \text{s.e.}\left[z_{v_0}^A t^{-1} - (z_{v_0}^A t^{-1})^{-1})^{2-k}\right].$$

We treat $(z^A t^{-1})$ as one variable y and expand as we would $(y - y^{-1})^{2-k}$. Therefore in the

[2] The authors of [28] make the replacement of M with adj(M), but this only works when M has positive determinant. When M has negative determinant (and this occurs exactly when s is odd), adj(M) is no longer negative definite, and the powers of q become negative. Specifically, one would get a series in $q^{-|H|}$. Replacing adj$M$ with $(-1)^s$adj(M) fixes this minor issue.

symmetric expansion of $f_0(z,t)$ all terms will be of the form

$$C(\ell)z^{A\ell_0+\sum_{i\geq 1}\overline{a_i}\ell_i}t^{-\ell\cdot u}$$

Note that for $1\leq i\leq k, \ell_i=\pm 1$.

After the Laplace transform, the power on q corresponding to each $\pm\ell$, again multiplied by 4, becomes

$$(A\ell_0+\sum_{i\neq 0}\ell_i\overline{a_i})^2/A=\ell_0^2A+2\sum_{i\neq 0}\ell_0\ell_i\overline{a_i}+\sum_{i\neq j,i,j\geq 1}\ell_i\ell_j\overline{a_{ij}}+\sum_{i\neq 0}\ell_i^2\overline{a_{ii}}, \tag{3.5.2}$$

which we will shorten to $n(\pm\ell)$. Each term of the symmetric expansion is of the form

$$C(\ell)q^{\frac{n(\pm\ell)}{4}}[t^{\ell\cdot u}+t^{-\ell\cdot u}].$$

The only difference between the powers of q in equation (3.5.1) and the powers of q in equation (3.5.2) is the coefficient on ℓ_i^2 for $i\neq 0$. However, for all ℓ that appear as exponents in the symmetric expansion, $\ell_i^2=1$ when $1\leq i\leq k$. Therefore the above discrepancy can be corrected in the prefactor by following the same process from the proof of [28, Theorem 4.2]. □

3.5.2 Quantum modularity properties of $\widehat{Z}$ for 3 singular fibers

This section discusses the proof of Theorem 3.1.4, which mirrors that of Theorem 3.1.2 and therefore will not be repeated in full. However, we will establish necessary prerequisites in order for the argument of Section 3.4 to be applied. Specifically we will prove the following.

Proposition 3.5.6. *Let $M=M(b;(a_1,b_1),(a_2,b_2),(a_3,b_3))$ and define $A,\overline{a_i}$ as before. Let*

ω be a $2j$th root of unity. Then there exists a polynomial $p(q)$ such that

$$\mathcal{L}_A(s.e.(f_0(\omega, z))) = \sum_{n\geq 0} \mathcal{C}(n;\omega) q^{\frac{n^2}{4A}} + p(q),$$

where $\mathcal{C}(n;\omega)$ is odd and periodic in n.

From here one can follow the process in [51, Section 6.1] to show that

$$\sum_{n\geq 0} \mathcal{C}(n;\omega) q^{\frac{n^2}{4A}}$$

is a quantum modular form of weight $\frac{1}{2}$ with respect to $\Gamma(4Aj^2)$ by decomposing it into a sum of theta functions.

We now prove Proposition 3.5.6.

Proof. Let $\varepsilon_i = \pm 1$, and let $m \in \mathbb{Z}$. Define

$$C(\varepsilon_1, \varepsilon_2, \varepsilon_3, m) = \begin{cases} -\frac{1}{2}\varepsilon_1\varepsilon_2\varepsilon_3[t^{\sum_i \varepsilon_i + m} + t^{-(\sum_i \varepsilon_i + m)}] & m \text{ odd} \\ 0 & m \text{ even.} \end{cases}$$

The function C has the following symmetry:

$$C(\varepsilon_1, \varepsilon_2, \varepsilon_3, m) = -C(-\varepsilon_1, -\varepsilon_2, -\varepsilon_3, -m).$$

If t is a $2j$th root of unity ω, we also have that

$$C(\varepsilon_1, \varepsilon_2, \varepsilon_3, m) = C(\varepsilon_1, \varepsilon_2, \varepsilon_3, m + 2j).$$

Let

$$Y := \{(\varepsilon_1, \varepsilon_2, \varepsilon_3, m) | \varepsilon_i = \pm 1, m > 0, m \text{ odd}\};$$

$$X = \{(\varepsilon_1, \varepsilon_2, \varepsilon_3, m) | \varepsilon_i = \pm 1, m \in \mathbb{Z}, m \text{ odd}, \sum_i \varepsilon_i \overline{a_i} + mA > 0\}.$$

Observe that both $Y - X$ and $X - Y$ are finite sets (which may be empty). Given $(\varepsilon_1, \varepsilon_2, \varepsilon_3, m)$, let $n := \sum_i \varepsilon_i \overline{a_i} + mA$. We may now rewrite

$$\mathcal{L}_A(\text{s.e.}(f_0(t,z))) = \sum_Y C(\varepsilon_1, \varepsilon_2, \varepsilon_3, m) q^{\frac{n^2}{4A}}.$$

On the other hand, we may re-index and rewrite

$$\sum_X C(\varepsilon_1, \varepsilon_2, \varepsilon_3, m) q^{\frac{n^2}{4A}} = \sum_{n \geq 0} \mathcal{C}(n; \omega) q^{\frac{n^2}{4A}},$$

where $\mathcal{C}(n;\omega)q^{\frac{n^2}{4A}}$ is $2Aj$-periodic and odd in n. Putting everything together we have

$$\sum_Y C(\varepsilon_1, \varepsilon_2, \varepsilon_3, m) q^{\frac{n^2}{4A}} = \sum_X C(\varepsilon_1, \varepsilon_2, \varepsilon_3, m) q^{\frac{n^2}{4A}} + \sum_{Y-X} C(\varepsilon_1, \varepsilon_2, \varepsilon_3, m) q^{\frac{n^2}{4A}} - \sum_{X-Y} C(\varepsilon_1, \varepsilon_2, \varepsilon_3, m) q^{\frac{n^2}{4A}}.$$

As both $X - Y$ and $Y - X$ are finite sets, we may write

$$\mathcal{L}_A(\text{s.e.}(f_0(t,z))) = \sum_{n \geq 0} \mathcal{C}(n; \omega) q^{\frac{n^2}{4A}} + p(q),$$

where $p(q)$ is a polynomial in q. □

Remark. *Because $\mathcal{C}(n;\omega)$ is periodic with mean value zero, one may take radial limits toward roots of unity as in 3.3. Note that $\omega^2 := \zeta$ is a jth root of unity, and for any root of unity ξ, $\lim_{t \searrow 0} \widehat{\widehat{Z}}(\zeta, \xi e^{-t})$ exists and can be expressed as a finite sum in terms of $\mathcal{C}(n;\omega)$. These limits can be thought of as ζ-deformations of Witten-Reshetikhin-Turaev invariants,*

extending the result of [51, Theorem 1.1*].*

3.5.3 The (t,q)-series for 3 singular fibers

Below we prove Theorem 3.1.6, which states that for Seifert manifolds with three exceptional fibers, their (t,q)-series can be written as an asymmetric expansion of the rational function $f_0(t,z)$, specifically

$$P^{\infty}_{W,[0]}(t^2,q^{|H|}) = q^{\Lambda}(\mathcal{L}_A(\text{a.e.}_{W_3(1)}(f_0(t,z))).$$

Proof. We begin with the asymmetric expansion of $(z^At^{-1}-(z^At^{-1})^{-1})$, which is the denominator of $f_0(t,z)$. For $|z^At^{-1}|<1$ we have

$$-\sum_{i\geq 0}(z^At^{-1})^{2i+1}$$

and for $|z^At^{-1}|>1$ we have

$$\sum_{i\geq 0}(z^At^{-1})^{-(2i+1)}.$$

Therefore, the expansions of $f_0(t,z)$ on $|z^At^{-1}|<1$ and $|z^At^{-1}|>1$ can be written as

$$-\prod_{j=1}^{3}(z^{\overline{a_i}}t^{-1}-z^{-\overline{a_i}}t)\sum_{i\geq 0}(z^At^{-1})^{2i+1} = -\sum_{\varepsilon_j=\pm 1,i\geq 0}(\varepsilon_1\varepsilon_2\varepsilon_3)z^{\sum_{j=1}^{k}\varepsilon_j\overline{a}_j+(2i+1)A}t^{-\sum_{j=1}^{k}\varepsilon_j-(2i+1)}$$

and

$$\prod_{j=1}^{3}(z^{\overline{a_i}}t^{-1}-z^{-\overline{a_i}}t))\sum_{i\geq 0}(z^At^{-1})^{-(2i+1)} = \sum_{\varepsilon_j=\pm 1,i\geq 0}(\varepsilon_1\varepsilon_2\varepsilon_3)z^{\sum_{j=1}^{k}\varepsilon_j\overline{a}_j-(2i+1)A}t^{\sum_{j=1}^{k}\varepsilon_j+(2i+1)},$$

respectively. Applying the Laplace transform, the powers of q corresponding to $(\varepsilon_1,\varepsilon_2,\varepsilon_3,2i+$

1) in the expansion on $|z^A t^{-1}| < 1$ are equal to those corresponding to $(-\varepsilon_1, -\varepsilon_2, -\varepsilon_3, 2i+1)$ in the expansion on $|z^A(t)| > 1$, so we may combine the two to write

$$\mathcal{L}_A(\text{a.e.}_{W_3(1)}(t,q) = \sum_{\varepsilon_j, i \geq 0} -\varepsilon_1\varepsilon_2\varepsilon_3 q^{\frac{(\sum_j \epsilon_j \overline{a}_j + (2i+1)A)^2}{4A}} \left[W_3(1)t^{\ell\cdot u} + (1 - W_3(1)t^{-\ell\cdot u}\right] \tag{3.5.3}$$

where $\ell := (\varepsilon_1, \varepsilon_2, \varepsilon_3, 2i+1)$.

On the other hand, working with the formula from Lemma 3.5.1, we may write

$$P^{\infty}_{W,0}(M)(t^2,q) = q^{-\frac{3s+m\cdot u}{4}} \sum_{\ell \in \delta + 2\mathbb{Z}^s} (\prod_i W_{\delta_i}(\ell_i)))q^{\frac{\ell^t M^{-1}\ell}{4}} t^{\sum_i \ell_i}.$$

From the axioms of admissible families, we know that the only ℓ for which $\prod_i W_{\delta_i}(\ell_i)$ is nonzero are those for which $\ell = (m, \pm 1, \pm 1, \pm 1, 0, \dots)$ and $W_3(m) \neq 0$. It also follows from these axioms that

$$W_3(m) = \begin{cases} W_3(1) & m \text{ odd}, m \geq 1 \\ W_3(1) - 1 & m \text{ odd}, m \leq -1 \\ 0 & \text{otherwise.} \end{cases}$$

To calculate $P^{\infty}_{W,[k]}(t^2, q^{|H|})$ we make the same replacement of powers of q as in the proof of Theorem 3.5.5:

$$P^{\infty}_{W,0}(t^2, q^{|H|}) = q^{-|H|\frac{3s+m\cdot u}{4}} \sum_{m \geq 0, \varepsilon_i = \pm 1} -W_3(1)\varepsilon_1\varepsilon_2\varepsilon_3 q^{-\frac{\ell^t M'\ell}{4}} t^{\ell\cdot u} + \varepsilon_1\varepsilon_2\varepsilon_3(W_3(1)-1)q^{-\frac{\ell^t M'\ell}{4}} t^{-\ell\cdot u}. \tag{3.5.4}$$

The only difference between Equations 3.5.3 and 3.5.4 is the powers of q and the prefactor, which can be corrected using the exact same trick as in the proof of Theorem 3.5.5. $\square$

Corollary 3.5.7. *For a Seifert manifold* $M(b;((a_1,b_1),(a_2,b_2),(a_3,b_3))$ *and any admissible family* W, $P^{\infty}_{W,0}(1,q) = \widehat{Z}(q)$.

3.5.4 Mixed modularity properties for 3 singular fibers

This section proves Theorem 3.1.7, establishing $\mathcal{L}_A(\text{a.e.}_{W_3(1)}(f_0(\omega,z)))$ as a sum of quantum modular and modular forms when $M = M(b;(a_1,b_1),(a_2,b_2),(a_3,b_3))$ and ω is a $2j$th root of unity. To accomplish this we decompose $\mathcal{L}_A(\text{a.e.}_{W_3(1)}(f_0(\omega,z)))$ into a linear sum of q-series, one whose coefficients are given by $\mathcal{C}(n;\omega)$, a function that is $2Aj$-periodic and odd in n, and the other whose coefficients are given by $\mathcal{D}(n;\omega)$, which is $2Aj$-periodic and even in n. The fact that the sum involving $\mathcal{C}(n;\omega)$ is a quantum modular form follows from the argument given in Section 3.5.2. The fact that the sum involving $\mathcal{D}(n;\omega)$ is a modular form will follow from applying a result of Goswami and Osburn [24, Lemma 2.1].

Definition 3.5.8. *Consider a function* f *with Laurent expansions of* $\sum_k a_k z^k$ *centered at* $z = 0$ *and* $\sum_k b_k z^{-k}$ *centered at* $z = \infty$. *Let the series difference, denoted s.d., be the formal power series given by*

$$s.d.(f) = \sum_k a_k z^k - \sum_k b_k z^{-k}.$$

Observe that

$$\text{a.e.}_y(f) = \text{s.e.}(f) + (\frac{1}{2} - y)\text{s.d.}(f)$$

so we may write

$$\mathcal{L}_A(\text{a.e.}_{W_3(1)}(f_0(\omega,z)))) = \mathcal{L}_A(\text{s.e.}(f_0)(\omega,z)) + (\frac{1}{2} - W_3(1))\mathcal{L}_A(\text{s.d.}(f_0(\omega,z)).$$

From Section 3.5.2 we know that

$$\mathcal{L}_A(\text{s.e.}(f_0(t,z))) = p_1(q) + \sum_{n\geq 0} \mathcal{C}(n;t) q^{\frac{n^2}{4A}},$$

where $\mathcal{C}(n;t)$ is odd and periodic in n and $p_1(q)$ is a polynomial. In the language of Theorem 3.1.7, $\mathcal{L}_A(\text{s.e.}(f_0(t,z)))$ is θ_f.

Proposition 3.5.9. *For $M = M(b;(a_1,b_1),\dots(a_3,b_3))$ and ω a $2j$th root of unity,*

$$\mathcal{L}_A(s.d.(f_0(\omega,z))) = p_2(q) + \sum_{n\geq 0} \mathcal{D}(n;\omega) q^{\frac{n^2}{4A}},$$

where $\mathcal{D}(n;\omega)$ is even and $2Aj$-periodic in n and $p_2(q)$ is a polynomial.

Remark. *In the language of Theorem 3.1.7,*

$$\sum_{n\geq 0} \mathcal{D}(n;\omega) q^{\frac{n^2}{4A}} = \Theta_f,$$

and $p_1(q) + p_2(q) = p(q)$.

Proof. The expansions of $f_0(t,z)$ on $|z^A t^{-1}| < 1$, and $|z^A t^{-1}| > 1$, respectively, are

$$-\sum_{\varepsilon_i=\pm 1, i\geq 0} \varepsilon_1\varepsilon_2\varepsilon_3 z^{(\sum_j \varepsilon_j \overline{a_j} + (2i+1)A)} t^{-\sum_j \varepsilon_j - (2i+1)} \text{ and } \sum_{\varepsilon_i=\pm 1, i\geq 0} \varepsilon_1\varepsilon_2\varepsilon_3 z^{\sum_j \varepsilon_j \overline{a_j} - (2i+1)A} t^{-\sum_j \varepsilon_j + (2i+1)}.$$

Therefore we may write

$$\mathcal{L}_A(\text{s.d.}(f_0(t,z)) = \sum_{\varepsilon_i=\pm 1, m>0, m \text{ odd}} D(\varepsilon_1,\varepsilon_2,\varepsilon_3,m) q^{\frac{n^2}{4A}},$$

where $n := \sum_i \varepsilon_i \overline{a_i} + mA$ and

$$D(\varepsilon_1, \varepsilon_2\varepsilon_3, m) = \begin{cases} \varepsilon_1\varepsilon_2\varepsilon_3[t^{\sum_i \varepsilon_i + m} - t^{-(\sum_i \varepsilon_i + m)}] & m \text{ odd} \\ 0 & m \text{ even.} \end{cases}$$

Observe that $D(-\varepsilon_1, -\varepsilon_2, -\varepsilon_3, -m) = D(\varepsilon_1, \varepsilon_2, \varepsilon_3, m)$, and for ω a $2j$th root of unity, $D(\varepsilon_1, \varepsilon_2, \varepsilon_3, m) = D(\varepsilon_1, \varepsilon_2, \varepsilon_3, m + 2j)$.

Let X and Y refer to the same sets as in the proof of Proposition 3.5.6. Observe that

$$\sum_X D(\varepsilon_1, \varepsilon_2, \varepsilon_3, m) q^{\frac{n^2}{4A}} = \sum_{n \geq 0} \mathcal{D}(n; \omega) q^{\frac{n^2}{4a}} \tag{3.5.5}$$

where $\mathcal{D}(n; \omega)$ is $2Aj$ periodic and even in n, and

$$\sum_Y D(\varepsilon_1, \varepsilon_2, \varepsilon_3, m) q^{\frac{n^2}{4A}} = \mathcal{L}_A(\text{s.d.}(f_0(\omega, z))).$$

Then we may write

$$\mathcal{L}_A(\text{s.d.}(f_0(\omega, z)) = \sum_{n \geq 0} \mathcal{D}(n; \omega) q^{\frac{n^2}{4A}} + \sum_{Y - X} D(\varepsilon_1, \varepsilon_2, \varepsilon_3, m) q^{\frac{n^2}{4A}} - \sum_{X - Y} D(\varepsilon_1, \varepsilon_2, \varepsilon_3, m) q^{\frac{n^2}{4A}},$$

and since $X - Y$ and $Y - X$ are finite sets, the two corresponding sums form a polynomial $p_2(q)$ we arrive at the desired decomposition. □

The modularity result will follow from applying [24, Lemma 2.1] and Lemma 2.4.3 to (3.5.5). We describe this process below.

Lemma 3.5.10. *There exists some k such that for all n with $\mathcal{D}(n; t) \neq 0$,*

$$n^2 \equiv k \pmod{4A}.$$

Proof. Let n_1, n_2 be such that $\mathcal{D}(n_i; t) \neq 0$. Then there exists some $(\varepsilon_1, \varepsilon_2, \varepsilon_3, m_1)$, m_1 odd, such that $n_1 = \sum_i \varepsilon_i \overline{a_i} + m_1 A$, and some $(\varepsilon_1', \varepsilon_2', \varepsilon_3', m_2)$, m_2 odd, such that $n_2 = \sum_i \varepsilon_i' \overline{a_i} + m_2 A$. A straightforward calculation verifies that

$$n_1^2 - n_2^2 \equiv 0 \pmod{4A.}$$

□

Lemma 3.5.11. *Let $k_i := 4A(i) + k$, for $0 \leq i \leq (j-1)$. If n is such that $\mathcal{D}(n; t) \neq 0$, then*

$$n^2 \equiv k_i \pmod{4Aj}$$

for some $0 \leq i \leq (j-1)$.

Definition 3.5.12 (Section 1 of [24])**.** *Let $1 \leq k_i \leq 4Aj$. Define*

$$S_i := \{1 \leq k \leq 2Aj | k^2 \equiv k_i \pmod{4Aj}\}$$

and

$$\mathcal{S}_i := S_i \cup \{4Aj - k | k \in S_i\}.$$

Lemma 3.5.13. *For a fixed manifold M, $\mathcal{D}(n; \omega)$ is supported on $\bigcup_i \mathcal{S}_i$.*

Definition 3.5.14. *Let $\mathcal{D}_i(n; \omega)$ be the restriction of $\mathcal{D}$ to $\mathcal{S}_i$.*

Note that

$$\sum_{n \geq 0} \mathcal{D}(n; \omega) q^{\frac{n^2}{4A}} = \sum_{1 \leq i \leq (j-1)} \sum_{n \geq 0} \mathcal{D}_i(n; \omega) q^{\frac{n^2}{4A}}.$$

Decomposing $\mathcal{D}$ into j summands will allow us to realize each associated q-series as a modular form. Then we will show that these modular forms transform together with respect

to $\Gamma(4Aj)$. The following result of [24], rewritten in terms of our notation, may be applied to each $\mathcal{D}_i(n;\omega)$:

Lemma 3.5.15 ([24], Lemma 2.1)**.** *Let $\mathcal{D}_i(n;\omega)$ be an even, $2Aj$-periodic function supported on $\mathcal{S}_i$. Then*

$$\theta_{\mathcal{D}} := \sum_{n\geq 0} \mathcal{D}(n;\omega) q^{\frac{n^2}{4Aj}} \tag{3.5.6}$$

is a modular form of weight $\frac{1}{2}$ with respect to $\Gamma_1(4Aj)$ and

$$\theta_{\mathcal{D}}(\gamma\tau) = e^{\frac{\pi i a b k_i}{2Aj}} \left(\frac{4cAj}{d}\right) \varepsilon_d^{-1} (cz+d)^{\frac{1}{2}} \theta_{\mathcal{D}}(\tau).$$

Here the multiplier depends on k_i. However, if we further restrict to the subgroup $\Gamma(4Aj)$, $b \equiv 0 \pmod{4Aj}$ and this dependence is eliminated. Therefore, the j summands transform as one under the action of $\Gamma(4Aj) \leq \Gamma_1(4Aj)$. Finally, we apply Lemma 2.4.3 to conclude Theorem 3.1.4.

3.5.5 The role of admissible families: selected calculations

Theorem 3.1.6 from Section 3.5.3 illuminates a possible interpretation of the role of W in $P^{\infty}_{W,[k]}(t,q)$. In the case of Seifert manifolds with three exceptional fibers, the $\widehat{\widehat{Z}}$ series is the unique series resulting from a symmetric expansion. The following calculations further motivate an understanding of the $P^{\infty}_{W,0}$ as an asymmetric deformation of the $\widehat{\widehat{Z}}$ series.

H-shaped graphs

Example 3.5.16 ([49], Example 5.5)**.** *Let M be a manifold with an H-shaped graph, i.e. a graph with two nodes of degree 3 and four leaves. We will refer to the two nodes as v_0 and*

v_1, and the four leaves as v_2 through v_5. Starting with the formula given by Lemma 3.5.1 and further restricting $\ell_i = \pm 1$ for $2 \leq i \leq 5$, we have

$$P^{\infty}_{W,0}(M)(t^2,q) = q^{-\frac{3s+m\cdot u}{4}} \sum_{m,n,\ odd,\ \varepsilon_i=\pm 1} W_3(m)W_3(n)(-\varepsilon_1)(-\varepsilon_2)(-\varepsilon_3)(-\varepsilon_4) q^{\frac{\ell^t M^{-1}\ell}{4}} t^{\ell\cdot u},$$

where $\ell_i = (m, n, \varepsilon_1, \ldots, \varepsilon_4, 0, \ldots, 0)$.

Because $W_3(m)$ and $W_3(n)$ depend only on the sign of m and n, we can split the sum into four cases. These four sums coincide with the four possible regions of $\mathbb{C}^s$ on which one can expand

$$\prod_i (z_i - z_i^{-1})^{2-\delta_v} :$$

Region of Laurent expansion	*Signs of* (m,n)	*Coefficient on corresponding sum*
$\lvert z_0\rvert < 1, \lvert z_1\rvert < 1$	$(+,+)$	$(W_3(1)-1)^2$
$\lvert z_0\rvert < 1, \lvert z_1\rvert > 1$	$(+,-)$	$(W_3(1))(W_3(1)-1)$
$\lvert z_0\rvert > 1, \lvert z_1\rvert < 1$	$(-,+)$	$(W_3(1))(W_3(1)-1)$
$\lvert z_0\rvert > 1, \lvert z_1\rvert > 1$	$(-,-)$	$(W_3(1))^2$.

Note that the coefficients on each of the four sums are equal if and only if $W_3(1) = \frac{1}{2}$, i.e. $W = \widehat{W}$, and the $\widehat{\widehat{Z}}$ invariant is recovered. In this case the coefficient on each sum is $\frac{1}{4}$. In this sense the $P^{\infty}_{W,[k]}$ invariant associated to this family of manifolds can also be interpreted as an asymmetric deformation of the $\widehat{\widehat{Z}}$ invariant.

From here we may use symmetries associated with $\ell \mapsto -\ell$ to combine the $(+,+)$ sum with the $(-,-)$ sum and the $(+,-)$ sum with the $(-,+)$ sum. After doing so we arrive at the following:

$$P^{\infty}_{W,0}(M)(t^2,q) = q^{-\frac{3s+m\cdot u}{4}} \sum_{\varepsilon_i=\pm 1, m,n>0, m,n \text{ odd}} \varepsilon_1\varepsilon_2\varepsilon_3\varepsilon_4 q^{\frac{\ell^t M^{-1}\ell}{4}}[(W_3(1))^2 t^{\ell\cdot u} + (W_3(1)-1)^2 t^{-\ell\cdot u}]$$
$$+ q^{-\frac{3s+m\cdot u}{4}}(W_3(1))(W_3(1)-1) \sum_{\varepsilon_i=\pm 1, m>0, n<0, m,n \text{ odd}} \varepsilon_1\varepsilon_2\varepsilon_3\varepsilon_4 q^{\frac{\ell^t M^{-1}\ell}{4}}[t^{\ell\cdot u} + t^{-\ell\cdot u}].$$

4-leg star graphs

Example 3.5.17 ([49], Example 5.6)**.** *Let M be manifold whose plumbing graph has one 4-valent node, 4 leaves, and any amount of joints. It was observed by Peter Johnson, who gave a general formula for $W_n(r)$ in terms of $\{W_n(0), W_n(1)\}_{n\in\mathbb{N}}$, that*

$$W_4(m) = \begin{cases} W_4(0) + (W_3(1)-1)\frac{n}{2} & m \text{ even, } m \leq 0 \\ W_4(0) + W_3(1)\frac{n}{2} & m \text{ even, } m > 0 \\ 0 & \text{otherwise.} \end{cases}$$

When $W = \widehat{W}$, we have

$$\widehat{W}_4(n) = \begin{cases} \frac{|n|}{4} & n \text{ even} \\ 0 & \text{otherwise.} \end{cases}$$

Using Lemma 3.5.1 and further restricting to $\ell_i = \pm 1$ for $1 \leq i \leq 4$ we may write:

$$P^{\infty}_{W,0}(M)(t^2,q) = q^{-\frac{3s+m\cdot u}{4}} \sum_{\varepsilon_i=\pm 1, n \text{ even}, n<0} \varepsilon_1\varepsilon_2\varepsilon_3\varepsilon_4 q^{\frac{-\ell^t M'\ell}{4}}(W_4(0) + (W_3(1)-1)\frac{n}{2})t^{\ell\cdot u}$$
$$+ q^{-\frac{3s+m\cdot u}{4}} \sum_{\varepsilon_i=\pm 1, n \text{ even}, n>0} \varepsilon_1\varepsilon_2\varepsilon_3\varepsilon_4 q^{-\frac{\ell^t M'\ell}{4}}(W_4(0) + W_3(1)\frac{n}{2})t^{\ell\cdot u}$$
$$+ q^{-\frac{3s+m\cdot u}{4}} W_4(0) \sum_{\varepsilon_i=\pm 1} \varepsilon_1\varepsilon_2\varepsilon_3\varepsilon_4 q^{-\frac{\ell^t M'\ell}{4}} t^{\sum_i \varepsilon_i},$$

where the third sum corresponds to the $n = 0$ *case. Combining all terms with a coefficient of* $W_4(0)$*, we get*

$$\begin{aligned} P^{\infty}_{W,0}(M)(t^2,q) = (1-W_3(1))q^{-\frac{3s+m\cdot u}{4}} \sum_{\varepsilon_i=\pm 1, n \text{ even, } n<0} \varepsilon_1\varepsilon_2\varepsilon_3\varepsilon_4 q^{-\frac{\ell^t M'\ell}{4}} \frac{|n|}{2} t^{\ell\cdot u} \\ + W_3(1)q^{-\frac{3s+m\cdot u}{4}} \sum_{\varepsilon_i=\pm 1, n \text{ even, } n>0} \varepsilon_1\varepsilon_2\varepsilon_3\varepsilon_4 q^{-\frac{\ell^t M'\ell}{4}} \frac{|n|}{2} t^{\ell\cdot u} \\ + W_4(0)q^{-\frac{3s+m\cdot u}{4}} \sum_{\varepsilon_i=\pm 1, n \text{ even}} \varepsilon_1\varepsilon_2\varepsilon_3\varepsilon_4 q^{\frac{\ell^t M'\ell}{4}} t^{\ell\cdot u}. \end{aligned}$$

The first sum above is the Laplace transform ($\vec{z}^{\vec{\ell}} \mapsto q^{\frac{-\ell^t M^{-1}\ell}{4}}$) of the expansion of

$$\prod_v (z_v - z_v^{-1})^{2-\delta_v} \tag{3.5.7}$$

on $|z_0| < 1$ and the second sum is the Laplace transform of the expansion of (3.5.7) on $|z_0| > 1$. The meaning of the third sum is unclear to the author, however when $W = \widehat{W}$, the sum disappears as $\widehat{W}_4(0) = 0$. In this sense Example 3.5.17 can also be seen as an asymmetric deformation of the $\widehat{\widehat{Z}}$ invariant. If $W = \widehat{W}$, then $W_3(1) = \frac{1}{2}$ and the symmetric expansion is recovered.

Chapter 4

Annular Links from Thompson's Group T

4.1 Overview of results

This chapter provides a method for building links in the thickened annulus $\mathbb{A} \times I$ from Thompson's group T. Relevant background information is discussed in Sections 2.7 and 2.8.

Given an edge-signed graph $\Gamma \hookrightarrow \mathbb{A}$, one can construct a diagram of an annular link $L_{\mathbb{A}}(g)$ in analogy with Tait's construction of links from planar graphs; see Figure 4.1, which previously appeared as Figure 2.22 in Section 2.7.3. Jones proved that given any Tait graph $\Gamma \in \mathbb{R}^2$, there is some $g \in F$ which produces the same link as Γ. The following theorem states that the same is true for annular links and T:

Theorem 4.1.1. *Let $\Gamma \hookrightarrow \mathbb{A}$ be an edge-signed embedded graph. Then there exists some $g \in T$ such that $\mathcal{L}_{\mathbb{A}}(g)$ is isotopic in $\mathbb{A} \times I$ to $L_{\mathbb{A}}(\Gamma)$.*

As discussed in Section 2.7.2 elements of T can be specified by triples $(R, S; k)$, where R and S are trees and k is an integer. When R, S and k are relevant, we will use $\mathcal{L}_{\mathbb{A}}(R, S; k)$ to refer to the link resulting from the unique element $g \in T$ determined by the triple. Using this notation, we can establish the Jones polynomial of annular links as a function of positive

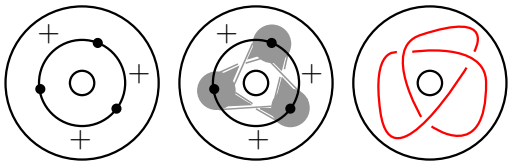

Figure 4.1: An annular link built from an edge-signed graph embedded in $\mathbb{A}$.

type on $\vec{T}$, the oriented subgroup of T which was introduced in [36] and is discussed in Section 4.2.

Corollary 4.1.2 ([50], Corollary 1.2)**.** *For $g = (R, S; k) \in \vec{T}$, let n be the number of leaves in R, and let $V^{\mathbb{A}}_{\mathcal{L}}(t)$ denote the Jones polynomial of an annular link $\mathcal{L}$, where unknotted curves wrapping once around $\mathbb{A}$ are equal to $(-t^{-\frac{1}{2}} - t^{\frac{1}{2}})$. Define $V^{\mathbb{A}}_g(t) : \vec{T} \to \mathbb{C}$ analogously to* [5]*, that is,*

$$V^{\mathbb{A}}_g(t) := V^{\mathbb{A}}_{\mathcal{L}_{\mathbb{A}}(R,S;k)}(t)(-t^{\frac{-1}{2}} - t^{\frac{1}{2}})^{-n+1}.$$

Then, for $t \in \{1, i, e^{\pm\frac{\pi i}{3}}\}$, $V^{\mathbb{A}}_g(t)$ is a function of positive type on $\vec{T}$, and consequently the Jones polynomial of $\mathcal{L}_{\mathbb{A}}(g)$, evaluated at $t \in \{1, i, e^{\pm\frac{\pi i}{3}}\}$, arises from a unitary representation of $\vec{T}$.

4.2 Constructing links from group elements

To construct annular links from T, this section introduces two equivalent methods analogous to those introduced by Jones for F.

The first method is pictured in Figure 4.2. Given $g = (R, S; k)$, consider the associated cylindrical strand diagram D_g. Following the method for building links from F, add edges to R and S to make them ternary trees, and consider these new edges numbered from left

to right. The edge above each root is considered to be numbered 0. Next, stack "empty" cylinders above and below D_g and connect numbered edges with non-crossing arcs according to the following rule: when the nth edge of R is connected to the mth edge of S and $n > m$, the arc connecting them must wrap around the annulus. Otherwise, the arc does not wrap around the annulus. Note that this rule guarantees that the arc connecting the top root to another edge will never wrap around the cylinder, and the arc connecting the bottom root to another edge will always wrap around the cylinder, unless a single arc connects the two roots (in which case $g \in F$). Finally, all 4-valent vertices become crossings as in Jones' construction.

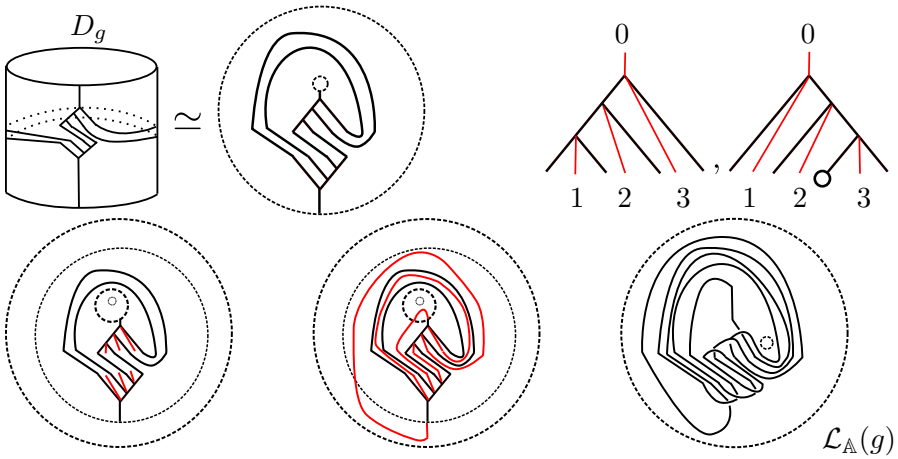

Figure 4.2: Building the annular link $\mathcal{L}_{\mathbb{A}}(g)$ from $g \in T$ via the strand diagram D_g.

The second method for building annular links from T, pictured in Figure 4.3, involves building an edge-signed graph $\Gamma_{\mathbb{A}}(g) \hookrightarrow \mathbb{A}$ and defining $\mathcal{L}_{\mathbb{A}}(g) := L_{\mathbb{A}}(\Gamma_{\mathbb{A}}(g))$. The graph $\Gamma_{\mathbb{A}}(g)$ is built from $\Gamma(R)$ and $\Gamma(S)$, which are created as in Jones' construction (see Section 2.8.) However, the first vertex of $\Gamma(R)$ is now identified with the kth vertex of $\Gamma(S)$, and edges of R attaching to edges to their left in S must wrap counterclockwise around $\mathbb{A}$; see Figure 4.3. This second construction will be used in Section 4.3 to prove Theorem 4.1.1.

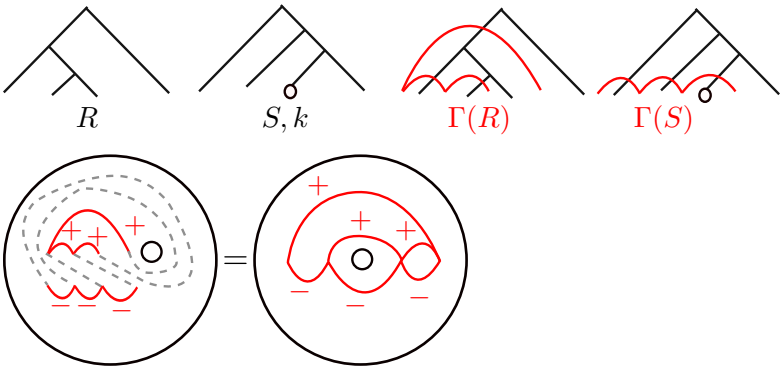

Figure 4.3: Building the graph $\Gamma_{\mathbb{A}}(g)$ from $g = (R, S; k)$. Dotted lines denote identification of vertices; they are not edges.

Annular links created from T are closely related to Jones' *planar* links built from T; see [36, Section 4.2]. By construction, $\Gamma(g)$ is the image of $\Gamma_{\mathbb{A}}(g)$ under the inclusion $\mathbb{A} \hookrightarrow \mathbb{R}^2$. Consequently, the diagram $\mathcal{L}(g)$ is the image of the diagram $\mathcal{L}_{\mathbb{A}}(g)$ under the same inclusion. From this we can relate the Kauffman bracket of $\mathcal{L}_{\mathbb{A}}(g)$ to that of $\mathcal{L}(g)$:

Proposition 4.2.1 ([50], Proposition 3.1)**.** *Let $g \in T$ be given by $(R, S; k)$. Consider $\mathcal{L}_{\mathbb{A}}(g)$ as an element of $\mathbb{C}[x]$, the Skein module $\mathcal{S}(\mathbb{A})$ of the thickened annulus. Evaluating at $x = (-t^{\frac{-1}{2}} - t^{\frac{1}{2}})$ returns the Kauffman Bracket of $\mathcal{L}(g) \in S^3$.*

To discuss the analogous result for the Jones polynomial, we first recall the oriented subgroup $\vec{T}$, whose associated annular links admit a natural orientation. The Jones polynomial of an oriented annular link $\mathcal{L}$, denoted $V^{\mathbb{A}}_{\mathcal{L}}(t, h) \in \mathbb{Z}[t^{\pm\frac{1}{2}}, h]$, can be evaluated by first using the usual skein relation to remove all crossings, and then setting unknotted circles bounding disks equal to $(-t^{\frac{1}{2}} - t^{-\frac{1}{2}})$, and unknotted circles wrapping once around the annulus equal to h.

The following proposition relates the Jones polynomial of $\mathcal{L}(g)$ to that of $\mathcal{L}_{\mathbb{A}}(g)$.

Proposition 4.2.2 ([50], Proposition 3.2)**.** *Let $g \in \vec{T}$. Setting $h := (-t^{\frac{1}{2}} - t^{-\frac{1}{2}})$, the Jones polynomial of $\mathcal{L}_{\mathbb{A}}(g)$ is equal to that of $\mathcal{L}(g)$.*

Propositions 4.2.1 and 4.2.2, together with Aiello and Conti's proofs of [5, Theorems 6.2 and 7.4], imply Corollary 4.1.2.

4.2.1 Annular Thompson badness

Toward a proof of Theorem 4.1.1, we now establish the annular analogue for Jones' Thompson Badness. In this section and Section 4.3, we think of $\mathbb{A}$ as $\mathbb{D}^1 \setminus \{(0,0)\}$.

Definition 4.2.3. *Let $\Gamma \hookrightarrow \mathbb{A}$ be an edge-signed graph. We say Γ is ATB-**friendly** if:*

- *Γ has no loops.*
- *all vertices lie on the x axis.*
- *all edges have interiors either entirely above, or entirely below the x axis.*

Now suppose a graph $\Gamma \hookrightarrow \mathbb{A}$ is ATB-friendly. Define $e_v^{in}, e^{up}, e^{down}, e_-^{up}, e_+^{down}$ as before. Let v_L describe the leftmost vertex and let v_1 describe the vertex immediately to the right of the origin. Label the N vertices by $\{1, \ldots, N\}$ such that v_1 is labeled 1, the vertex immediately to its right is labeled 2, and so on, until the rightmost vertex is labeled $k-1$. Then label the leftmost vertex k and continue increasing left to right until the vertex immediately to the left of the origin is labeled N. For example,

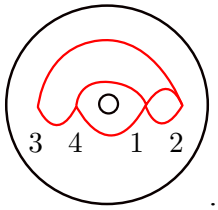

Let $l(v)$ refer to the label of v. By construction $(v_L) = k$. Define

$$e_v^< := \{e \in e(\Gamma) : e \text{ connects } v \text{ to some } w \text{ such that } l(w) < l(v)\}.$$

Now define Annular Thompson Badness, or ATB, as follows:

$$ATB(\Gamma) := \sum_{v \in V(\Gamma)\setminus v_L} |1 - |e_v^{in} \cap e^{down}|| + \sum_{v \in V(\Gamma)\setminus v_1} |1 - |e_v^< \cap e^{up}|| + |e_-^{up}| + |e_+^{down}|.$$

The following proposition motivates this definition as the correct analogue for Thompson Badness.

Proposition 4.2.4 ([50], Proposition 3.3)**.** *Let $\Gamma \hookrightarrow \mathbb{A}$ be an ATB-friendly graph. Then $ATB(\Gamma) = 0$ if and only if $\Gamma = \Gamma_{\mathbb{A}}(g)$ for some $g \in T$.*

Proof. Suppose $\Gamma = \Gamma_{\mathbb{A}}(g)$, where $g = (R, S; k)$. By construction, $|e_-^{up}| = |e_+^{down}| = 0$.

It remains to show $\sum_{v \in V(\Gamma)\setminus v_\ell} |1 - |e_v^{in} \cap e^{down}|| = \sum_{v \in V(\Gamma)\setminus v_1} |1 - |e_v^< \cap e^{up}|| = 0$. Beginning with the first quantity, let Γ_- denote the subgraph of Γ whose edges have interiors in the lower half plane. Since $\Gamma_- = \Gamma(S)$ and $\Gamma(R, S)$ has Thompson Badness equal to zero, $\sum_{v \in V(\Gamma)\setminus v_L} |1 - |e_v^{in} \cap e^{down}|| = 0$.

It remains to show that

$$\sum_{v \in V(\Gamma)\setminus v_1} |1 - |e_v^< \cap e^{up}|| = 0.$$

Define Γ_+ analogously to Γ_-. Because of the edges wrapping around the annulus, $\Gamma_+ \neq \Gamma(R)$, but we can recover $\Gamma(R)$ from Γ_+. This is accomplished by embedding Γ_+ in $\mathbb{R}^2$ so that labels of the edges increase from left to right. Call this embedding Γ'_+ and observe that $\Gamma'_+ = \Gamma(R)$.

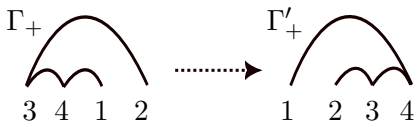

Letting v'_L refer to the leftmost vertex of Γ'_+, we have

$$\sum_{v \in V(\Gamma'_+) \setminus \{v'_L\}} |1 - |e^{up} \cap e_v^{in}|| = \sum_{v \in V(\Gamma) \setminus v_1} |1 - |e^{up} \cap e_v^{<}||.$$

Since $\Gamma(R, S)$ has Thompson badness zero, the left hand side must be zero. Therefore, $ATB(\Gamma_{\mathbb{A}}(g)) = 0$.

Conversely, let Γ be a graph with $ATB(\Gamma) = 0$. Let (R, S) be the unique pair of trees corresponding to (Γ'_+, Γ_-). Then $\Gamma = \Gamma_{\mathbb{A}}(g)$ where $g = (R, S; l(v_L))$. □

4.3 The proof of Theorem 4.1.1

This section uses Annular Thompson Badness to prove 4.1.1. Given a general graph Γ, we wish to find a graph Γ' and $L_{\mathbb{A}}(\Gamma) \simeq L_{\mathbb{A}}(\Gamma')$, with $ATB(\Gamma') < ATB(\Gamma)$. For this we use Jones' definition of 2-equivalence [36].

Recall that two edge-signed planar graphs are defined to be 2-equivalent if they are related by a finite sequence of three moves, which Jones calls 2-moves [36]. These moves were introduced in Section 2.7.3 of this thesis. Jones uses 2-moves to show that every link has a diagram whose Tait graph has Thompson Badness zero, and thus can be built from an element of the Thompson group. The proof of Theorem 4.1.1 will use an analogous strategy to reduce Annular Thompson Badness of a given edge-signed graph $\Gamma \hookrightarrow \mathbb{A}$. To accomplish this we wish to calculate ATB of any graph Γ, but so far the definition of $ATB(\Gamma)$ requires that Γ is ATB-friendly. The following lemma takes care of this.

Lemma 4.3.1 ([50], Lemma 4.1)**.** *Let* $\Gamma \hookrightarrow \mathbb{A}$ *be an edge-signed graph. Then* Γ *is* 2*-equivalent to an* ATB*-friendly graph.*

Proof. Begin by arranging all vertices on the x-axis, which is always possible. At this point, if Γ is ATB-friendly we are done. Otherwise, both loops and edges whose interiors are in both the upper and lower half-plane can be corrected with moves of Type IIa. Both cases are shown in Figure 4.4. □

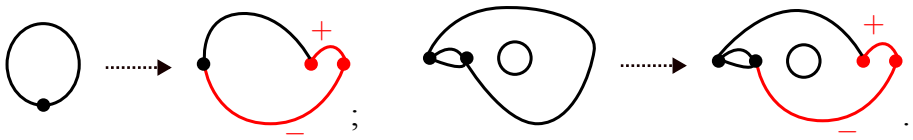

Figure 4.4: Using moves of Type IIa to correct for a loop (left) and an edge whose interior is in both the upper and lower-half plane (right).

Therefore, for any graph $\Gamma \hookrightarrow \mathbb{A}$, we define $ATB(\Gamma) := ATB(\Gamma')$ where Γ' is obtained from Γ as in the proof of Lemma 4.3.1.

Remark. *The following, when applied inductively, proves Theorem 4.1.1.*

Theorem 4.3.2 ([50], Theorem 4.2)**.** *Let* $\Gamma \hookrightarrow \mathbb{A}$ *be an edge-signed graph. If* $ATB(\Gamma) \neq 0$*, there exists* Γ' *such that* Γ' *is 2-equivalent to* Γ*, and* $ATB(\Gamma') < ATB(\Gamma)$*.*

This proof can be thought of as an extension of Jones' proof of [36, Lemma 5.3.13] to the annular case.

Proof. To begin, we split into three cases, based on what is causing $ATB(\Gamma) > 0$:

1. $\sum_{v \in v(\Gamma) \setminus v_L} |1 - |e_v^{in} \cap e^{down}|| + \sum_{v \in v(\Gamma) \setminus v_1} |1 - |e_v^{<} \cap e^{up}|| > 0$.
2. The above quantity is zero but $|e_-^{up}| > 0$.

3. The above quantities are zero but $|e_+^{down}| > 0$.

Case 1: The following four-step process will reduce

$$\sum_{v \in v(\Gamma) \setminus v_L} |1 - |e_v^{in} \cap e^{down}|| + \sum_{v \in v(\Gamma) \setminus v_1} |1 - |e_v^{<} \cap e^{up}||$$

to zero while preserving 2-equivalence.

Case 1, Step 1: For each $v \in v(\Gamma) \setminus v_L$ such that $|e_v^{in} \cap e^{down}| = 0$, let the vertex immediately to the left of v be called w and proceed as in [36] regardless of whether $v = v_1$:

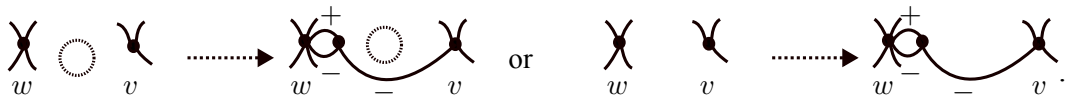

The new vertex does not impact ATB, and the vertex v now has $|e_v^{in} \cap e^{down}| = 1$. Each time this step is applied to a relevant vertex, $\sum_{v \in v(\Gamma) \setminus v_L} |1 - |e_v^{in} \cap e^{down}||$ decreases by 1, and all other quantities remain unchanged, so ATB decreases by 1.

Case 1, Step 2: For each $v \in v(\Gamma) \setminus v_L$ such that $|e_v^{in} \cap e_v^{down}| > 1$, proceed as in [36]:

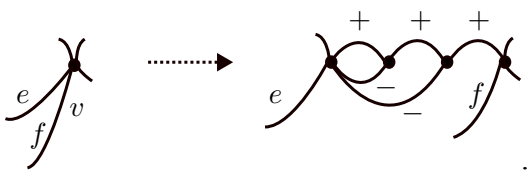

Step 2 ensures that $\sum_{v \in v(\Gamma') \setminus v_L} |1 - |e_v^{in} \cap e^{down}|| = 0$ for all relevant vertices, however it may increase the quantity $\sum_{v \in v(\Gamma') \setminus v_1} |1 - |e_v^{<} \cap e^{up}||$. Take, for example, a vertex v with an outgoing edge stretching over the origin:

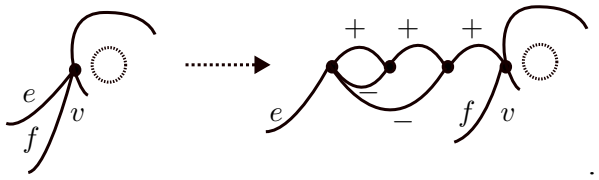

In this example, Step 2 increases $|e_v^< \cap e^{up}|$ from 1 to 2. This will be addressed momentarily in Step 4, but at this point steps 1 and 2 have reduced $\sum_{v \in v(\Gamma) \setminus v_L} |1 - |e_v^{in} \cap e^{down}||$ to 0. If we also have that $\sum_{v \in v(\Gamma) \setminus v_1} |1 - |e_v^< \cap e^{up}|| = 0$, we are done. Otherwise proceed to step 3.

Case 1, Step 3: We wish to deal with vertices $v \in V(\Gamma) \setminus v_1$ for which $|e_v^< \cap e_v^{up}| = 0$. If $v \neq v_L$, let w refer to the vertex immediately to the left of v and proceed as in [36]:

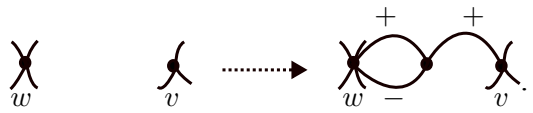

If $v = v_L$, modify the graph as follows:

In both cases, $\sum_{v \in v(\Gamma) \setminus v_1} |1 - |e_v^< \cap e^{up}||$ decreases by 1 and all other quantities remain unchanged. Therefore each time this step is applied to a relevant vertex, ATB decreases by 1.

Case 1, Step 4: We wish to deal with vertices $v \in v(\Gamma) \setminus v_1$ for which $|e_v^< \cap e^{up}| > 1$. This can happen one of four ways. In any case, proceed as in [36], see Figure 4.5. In each of the four cases, $\sum_{v \in v(\Gamma) \setminus v_1} |1 - |e_v^< \cap e^{up}||$ decreases by 1 and all other quantities remain unchanged. Therefore each time this step is applied to a relevant vertex, ATB decreases

by 1. After these four steps, we have

$$\sum_{v \in v(\Gamma) \setminus v_L} |1 - |e_v^{in} \cap e^{down}|| + \sum_{v \in v(\Gamma) \setminus v_1} |1 - |e_v^{<} \cap e^{up}|| = 0,$$

and $|e_-^{up}| + |e_+^{down}|$ remains unchanged. Therefore ATB has been reduced, and this concludes Case 1.

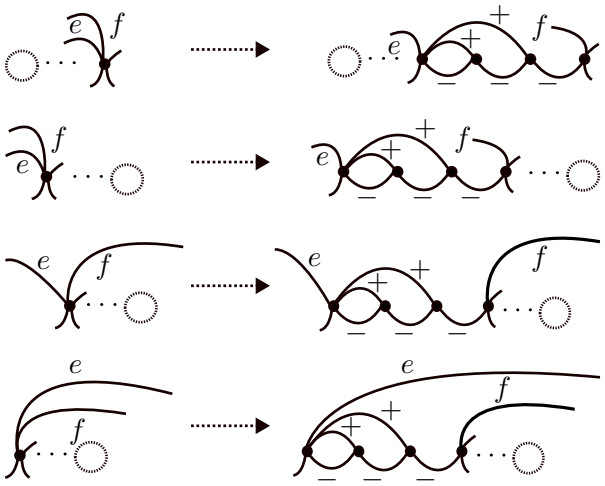

Figure 4.5: Reducing Annular Thompson Badness as in Case 1, Step 4. Four possible modifications are shown, corresponding to four different ways a vertex v can have $|e_v^{<} \cap e^{up}| > 1$.

Case 2: We have $\sum_{v \in v(\Gamma) \setminus v_L} |1 - |e_v^{in} \cap e^{down}|| + \sum_{v \in v(\Gamma) \setminus v_1} |1 - |e_v^{<} \cap e^{up}|| = 0$ and $|e_+^{down}| > 0$. From now on, only edges in $|e_-^{up}| \cup |e_+^{down}|$ will be pictured with a sign; the rest are understood to be in $|e_-^{down}| \cup |e_+^{up}|$. Fix an edge in $e' \in e_+^{down}$ and call its terminal vertex v. We further split into two cases, depending on whether $v = v_1$. Let w refer to the vertex immediately to the left of v. If $v \neq v_1$, proceed as in [36] (see Figure 4.6).

If $v = v_1$, proceed as in Figure 4.7.

Note that m denotes the number of edges coming into v from the other side of the annulus.

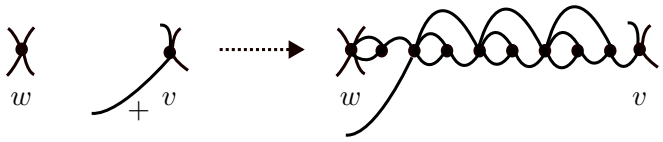

Figure 4.6: Reducing Annular Thompson Badness as in Case 2, when $v \neq v_1$.

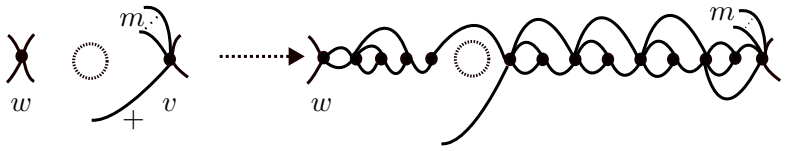

Figure 4.7: Reducing Annular Thompson Badness as in Case 2, when $v = v_1$.

Distinguishing these edges in the picture is necessary because, by virtue of stretching over the origin, they are not in $e_v^<$ and will not affect ATB.

One may wonder why we treat $v = v_1$ differently from $v \neq v_1$ in Figures 4.6 and 4.7. Figure 4.8 depicts what would have happened if we did not. The vertex v_k now has $|e_{v_k}^< \cap e^{\text{up}}| = 2$ which increases ATB by 1 and necessitates a correction as in Case 1, step 4, bringing us back to Figure 4.7.

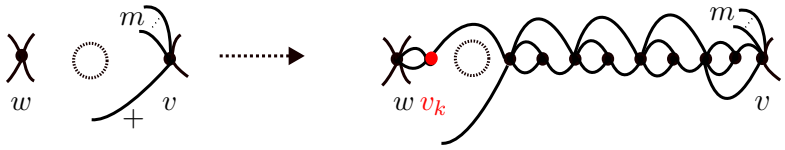

Figure 4.8: An illustration of why Case 2 must be treated differently when $v = v_1$.

To see how Figure 4.6 preserves 2-equivalence use Type IIb moves to remove canceling 2-cycles with opposite signs, then use Type I moves to eliminate 1-valent vertices, and finally use Type IIa moves to collapse canceling edges, pictured in red, so that the original edge, pictured in blue, remains. A similar sequence of moves demonstrates the 2-equivalence for Figure 4.7.

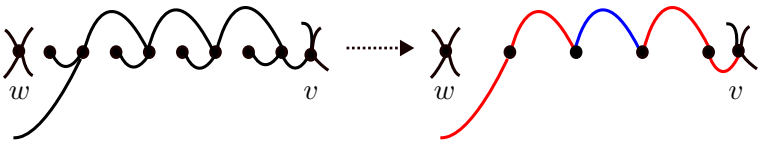

The modifications in Figures 4.6 and 4.7 decrease $|e_+^{down}|$ by 1 and do not impact the quantity $\sum_{v\in v(\Gamma)\setminus v_L} |1 - |e_v^{in} \cap e^{down}|| + \sum_{v\in v(\Gamma)\setminus v_1} |1 - |e_v^{<} \cap e^{up}||$ or $|e_-^{up}|$. Therefore each time this modification is applied to an edge in e_+^{down}, ATB decreases by 1 and any edge in e_+^{down} can be corrected.

Case 3: All other quantities relevant to $ATB(\Gamma)$ are zero, but $|e_-^{up}| > 0$. Once again we further split into cases, depending on which side of $\mathbb{A}$ contains the terminal vertex v of a problematic edge e'.

If v is on the left side of $\mathbb{A}$, let w refer to the vertex immediately to the left of v and proceed as in [36]:

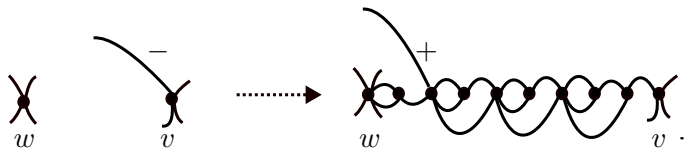

A key fact that makes the above work is that as long as v is on the left side of $\mathbb{A}$, we have $|e_v^{in} \cap e^{up}| = 1$, which was assumed in [36]. When this is not true, a different correction will be required; specifically, if instead e' terminates at some v on the right side of $\mathbb{A}$, we may have that $|e_v^{in} \cap e^{up}| > 1$, due to any number of edges entering v from above which stretch over the origin. We must further divide into two cases, based on whether e' itself stretches over the origin.

If not, perform the following combination of moves of Type I, IIa, and IIb, finitely many times until $|e_v^{in} \cap e^{up}| = 1$:

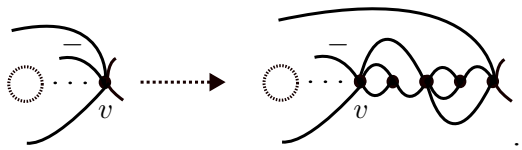

Then, we may proceed as in the previous case. If, on the other hand, e' does stretch over the origin, apply the above modification to isolate e' from all other edges in $|e_v^{in} \cap e^{up}|$ stretching over the origin. Once the problematic edge is isolated, one may modify the graph as follows:

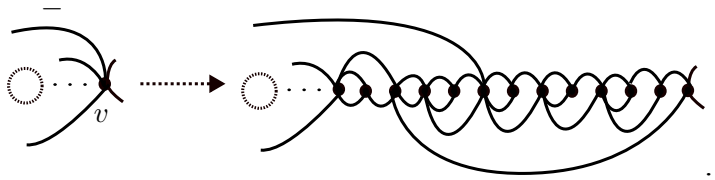

To see 2-equivalence, use Type IIb moves to remove canceling 2-cycles, then use Type I moves to remove 1-valent vertices. Lastly apply Type IIa moves to collapse the three pairs of canceling edges pictured below in red, blue, and green.

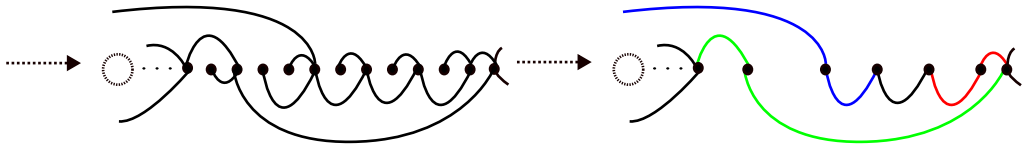

The modifications in this step reduce $|e_-^{up}|$ by 1 and do not affect any other quantities relevant to ATB. This concludes Case 3. These three cases demonstrate that any edge-signed graph embedded in $\mathbb{A}$ with nonzero ATB is 2-equivalent to a graph with lower ATB. □

4.3.1 Example: a positive trefoil embedded in $\mathbb{A} \times I$

Let $\Gamma \hookrightarrow \mathbb{A}$ be the graph pictured below, which corresponds to the positive trefoil embedded as in Figure 4.1. The graph $\Gamma \hookrightarrow \mathbb{A}$ has $|e_+^{down}| = 1$, $|e_-^{up}| = 0$, $|e_{v_3}^{in} \cap e^{down}| = 0$, $|e_{v_1}^{in} \cap e^{down}| = 1$, $|e_{v_2}^{<} \cap e^{up}| = 0$, $|e_{v_3}^{<} \cap e^{up}| = 2$. Following the process outlined in Theo-

rem 4.1.1 leads to the element $g = (R, S; k) \in T$ pictured below, and $\mathcal{L}_{\mathbb{A}}(g) = L_{\mathbb{A}}(\Gamma)$.

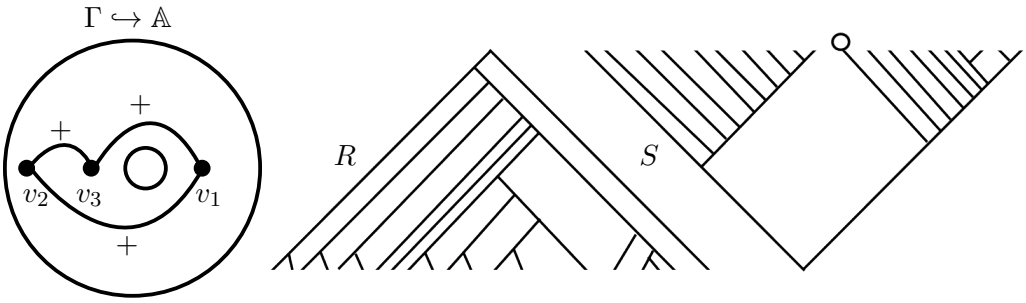

Figure 4.9: The triple $(R, S; k)$ such that $\mathcal{L}_{\mathbb{A}}(R, S; k) = L_{\mathbb{A}}(\Gamma)$.

Let us go into more detail about how the triple $(R, S; k)$ was obtained. Starting with Γ, observe that v_3 has $|e_v^{in} \cap e^{down}| = 0$, so we modify the graph to correct this, see Figure 4.10. New vertices and edges are pictured in red. From here, observe that v_2, the leftmost vertex, has $|e_v^{<} \cap e^{up}| = 0$, so we correct for this as pictured in Figure 4.11. We then correct the vertex immediately to the left to the origin, which has $|e_v^{<} \cap e^{up}| = 2$, see Figure 4.12. Finally we correct the sign of the single edge in $|e_+^{down}|$ as in Figure 4.13. We have arrived at a graph $\overline{\Gamma}$ which is 2-equivalent to Γ, but whose annular Thompson badness is equal to zero. From $\overline{\Gamma}$ we may extract $\overline{\Gamma}_+$, $\overline{\Gamma}_-$, $\overline{\Gamma}'_+$, and k as in the proof of Proposition 4.2.4. From here, R and S are built from $\overline{\Gamma}'_+$ and $\overline{\Gamma}_-$ respectively.

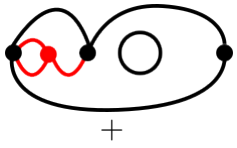

Figure 4.10

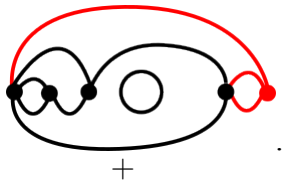

Figure 4.11

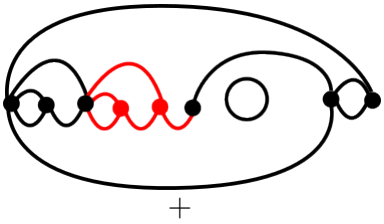

Figure 4.12

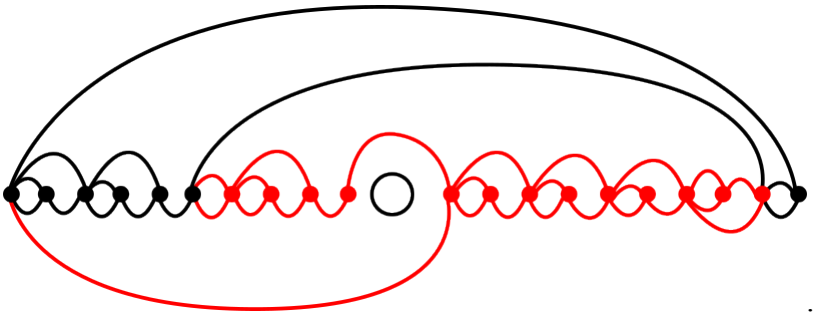

Figure 4.13

Chapter 5

Khovanov Homology and Tangles from F

This chapter presents the lax group action of Thompson's group $\vec{F}$ on a category of Khovanov chain complexes, based on joint work with Slava Krushkal and Yangxiao Luo [44]. This begins with an asymptotically faithful construction of (n, n)-tangles from F, via Belk's notion of strand diagrams. For background information about strand diagrams, see Section 2.7.1.

5.1 Building tangles from F

The aim of this section is to introduce the method by which we construct $(2^{k+1}, 2^{k+1})$-tangles from elements $g \in F$, and to prove that this construction is asymptotically faithful. To build tangles out of Thompson group elements, we will first use isomorphisms

$$\Theta_k : F \to \mathcal{R}_{2^k}^{2^k}$$

to obtain reduced $(2^k, 2^k)$ strand diagrams associated to each group element. Then we will define a functor T sending each $(2^k, 2^k)$-strand diagram to an unoriented $(2^{k+1}, 2^{k+1})$ tangle $T(\Theta_k(g))$. The functor T is a generalization of Jones' functor from forests to tangles

introduced in [36]. A forest is a strand diagram with only splits, see Figure 5.2 for an example. We follow the convention of Jones in [36] that forests grow downward, see Figure 5.2. Forests growing upward will be referred to as *inverse forests*.

The map Θ_k will involve *symmetric* trees $S_k \in \mathcal{R}^1_{2^k}$ (see Figure 5.1).

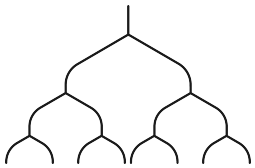

Figure 5.1: A symmetric tree S_3, with 8 leaves

Definition 5.1.1. *Let S_k be the symmetric tree with 2^k leaves and let $\delta : F \to \mathcal{R}^1_1$ be the isomorphism from Section 2.7.1 Define*

$$\Theta_k(g) := S_k * \delta(g) * S_k^*,$$

i.e. conjugation by S_k.

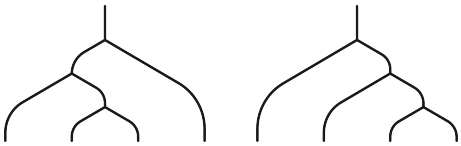

Figure 5.2: An example of a forest $D \in \mathcal{D}^2_8$.

Toward a definition of the functor T, we define two categories of strand diagrams and tangles, respectively.

Definition 5.1.2. *Let $\mathfrak{D}$ be the category whose objects are positive integers, and the morphisms from m to n are (m, n)-strand diagrams. Compositions are concatenations of strand diagrams.*

Similarly, let $\mathfrak{T}$ be the category whose objects are positive integers, and the morphisms from m to n are unoriented $(2m, 2n)$-tangles. Compositions are concatenations of tangles.

Now we define a functor $T\colon \mathfrak{D} \to \mathfrak{T}$. First, T acts by the identity on objects. Given an (m, n)-strand diagram Γ embedded in $[0, 1] \times [0, 1]$, we construct a $(2m, 2n)$-tangle $T(\Gamma)$ as follows.

Observe that the complement of Γ is a disjoint union of some polygons $P_1, P_2, ..., P_N$. Assume P_i is neither the leftmost region nor the rightmost region, then the boundary of P_i consists of:

1. only some edges of Γ, or
2. some edges of Γ and an interval on the lower side, or
3. some edges of Γ and an interval on the upper side, or
4. some edges of Γ, an interval on the lower side, and an interval on the upper side

See Figure 5.5 where the regions are labeled $1 - 4$, according to the definition above.

Proposition 5.1.3. *If P_i has boundary of type (1), then P_i has a unique maximum point at a split, and a unique minimum point at a merge. If P_i has boundary of type (2), then P_i has a unique maximum point at a split. If P_i has boundary of type (3), then P_i has a unique minimum point at a merge.*

Proof. We give a proof for the regions of type (1); the argument for the other two cases is directly analogous. The given polygonal region P_i is topologically a disk. A priori, there are two types of minima and maxima of the *boundary* ∂D of a planar region D. This first type is where the minimum of the boundary is also a minimum of the region D, and

similarly a maximum of ∂D is also a maximum of D. The second type is where a minimum, respectively maximum of ∂D is a maximum, respectively minimum of D. Since the edges of a strand diagram have non-zero slopes (see Definition 2.7.1), the boundary of P_i does not have extrema of the second type. The extrema of the first kind take place precisely at merges and splits, as shown in Figure 5.3. Suppose P_i has more than one local minimum. It

Figure 5.3: A maximum and a minimum of P_i.

follows from ambient Morse theory (or in this case, also from planar topology) that, looking at sublevel sets of the height function, the minima of the first kind give rise to 0-handles of P_i. Since P_i is connected, these 0-handles eventually must be connected by 1-handles. Attaching a 1-handle to P_i corresponds to a maximum of ∂P_i of the second type. Since this is impossible in a strand diagram, P_i has a unique minimum. The same argument shows that there is also a unique maximum. □

Consider each polygon P_i which is not leftmost or rightmost. If P_i has boundary of type (1), we introduce an edge connecting the unique maximum point and the unique minimum point of P_i. If P_i has boundary of type (2), we add an edge connecting the unique maximum point of P_i to a point in the interior of the interval in ∂P_i on the bottom of the square. The definition for type (3) is analogous. If P_i has boundary of type (4), we connect a point in the interior of the top interval to a point in the interior on the bottom. Let Γ' denote the resulting graph. The new edges are drawn red in Figure 5.4.

Note that Γ' is a graph with $(2m-1)$ univalent vertices on the top side of the square, $(2n-1)$ univalent vertices on the bottom side, and all other vertices are 4-valent, containing either

a split or a merge of the original strand diagram. We replace each 4-valent vertex by a crossing as in Figure 5.4. Finally, we add a trivial strand on the leftmost side to get an unoriented $(2m, 2n)$-tangle $T(\Gamma)$. See Figure 5.5 for an example.

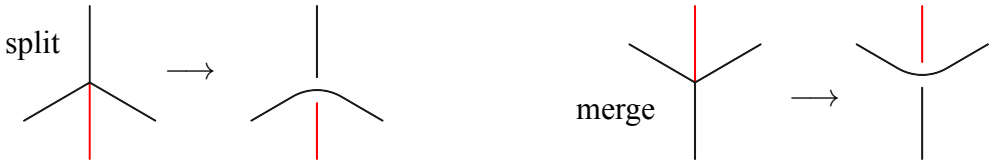

Figure 5.4: The local replacement at 4-valent vertices of Γ', with added edges in Γ' marked in red.

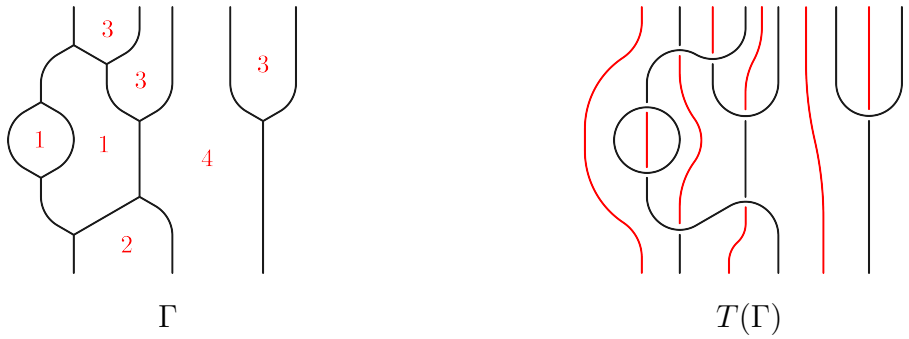

Figure 5.5: A $(5, 3)$-strand diagram Γ and its associated $(10, 6)$-tangle $T(\Gamma)$. Each polygon P in the complement of Γ (except the leftmost one and the rightmost one) is marked by a number k, meaning that P has boundary of type (k).

If E is a forest, then the complement of E does not contain any polygons with boundary of type (1) and (3). In the definition of $T(E)$ above, we just need to connect each split with the interval on the bottom of the square, and we add a strand connecting the top and bottom intervals of each type (4) polygon except the rightmost one. Each split in E gives rise to an arc connecting two points on the bottom edge of the square in $T(E)$, and we refer to these arcs as *turnbacks*. Jones also constructed tangles from forests in [36]; comparing $T(E)$ with Jones' functor, the only difference is that in our construction, $T(E)$ has an extra trivial strand on the left. For an example, see Figure 5.6.

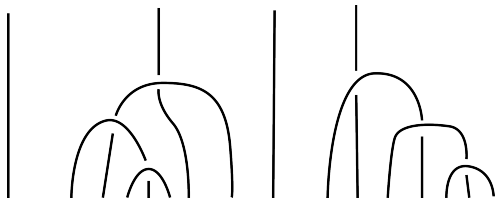

Figure 5.6: The tangle $T(D)$, with D as in Figure 5.2.

Definition 5.1.4. *A strand diagram* Γ *is called a* biforest *if* $\Gamma = F_1 \circ F_2^*$ *for some forests* F_1 *and* F_2.

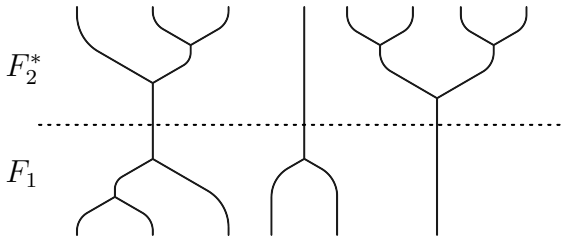

Figure 5.7: A biforest in $\mathcal{D}_6^8$.

Proposition 5.1.5. *Given two biforests* Γ *and* Γ' *with the same number of endpoints,* $\Gamma \neq \Gamma'$ *implies that* $T(\Gamma) \ncong T(\Gamma')$.

Here tangles are considered equivalent, i.e. $T(\Gamma) \cong T(\Gamma')$, if they are related by an isotopy fixing the endpoints.

Proof. Let $\Gamma = F_1 \circ F_2^*, \Gamma' = G_1 \circ G_2^*$. Since $\Gamma \neq \Gamma'$, $F_i \neq G_i$ for some $i \in \{1,2\} i = 1,2$. Without loss of generality, suppose $F_1 \neq G_1$. Then $T(\Gamma)$ and $T(\Gamma')$ differ by at least one turnback near $[0,1] \times \{0\}$. □

Remark. *Proposition 5.1.5 does not hold for arbitrary strand diagrams. For example, an infinite family of* $(1,1)$*-strand diagrams, coming from an infinite family of distinct Thompson group elements given by the ordered pairs of partitions*

$$(\{[0,\frac{1}{2}],[\frac{1}{2},\frac{3}{4}],[\frac{3}{4},\frac{7}{8}],\dots\},\{\dots,[\frac{1}{8},\frac{1}{4}],[\frac{1}{4},\frac{1}{2}],[\frac{1}{2},1]\})$$

produce the trivial tangle with two vertical strands. Similarly, it is known that Jones' construction in [36] produces the unlink from many distinct elements of F.

5.1.1 The statement and proof of faithfulness

In this section we prove asymptotic faithfulness of the construction of tangles from F. More precisely, we show that given any $g \neq h \in F$, there exists some K such that for $k \geq K$, $T(\Theta_k(g)) \ncong T(\Theta_k(h))$. This statement highlights a key difference between the creation of tangles from F in this paper, and that of links in [36]. In general, the construction of links from F is not faithful.

In this section we refer to the *maximum height* of a tree S to be the maximum distance from a leaf in S to the root. For example, the maximum height of S_k is k.

Lemma 5.1.6. *Let $\Gamma \in \mathcal{R}_n^1$, i.e. Γ is a binary tree with n leaves. If d is the maximum height of Γ and $k \geq d$, then $\Gamma * S_k^* \in \mathcal{R}_n^{2^k}$ contains only merges.*

Imprecisely, the resulting strand diagram $\Gamma * S_k^* \in \mathcal{R}_n^{2^k}$ may be thought of as encoding the "difference" between S_k and Γ.

Proof. It follows from the fact that Γ is a sub-tree of S_k that S_k contains every split of Γ (and sometimes more). In the concatenated but unreduced picture $\Gamma \circ S_k^*$, every split in T and its corresponding merge in S_k^* can be eliminated by a reduction of Type II. The resulting reduced diagram only has merges, given by merges in S_k^* that do not correspond to splits in T. □

The following result is a more detailed version of Theorem G in the Introduction. To relate the notation in the two statements, $n = 2^k$ and $T_n = T \circ \Theta_k$.

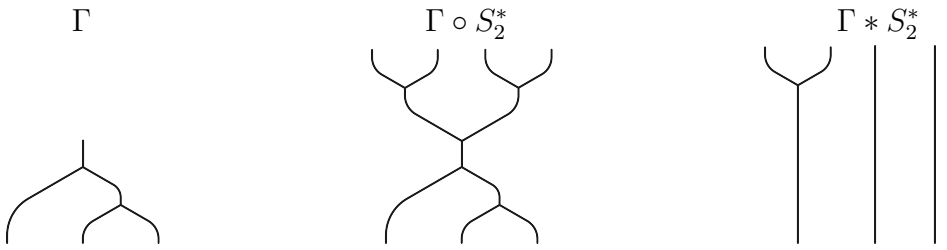

Figure 5.8: The tree S_2 has one more split than the tree Γ. When $\Gamma \circ S_2^*$ is reduced to $\Gamma * S_2^*$, the single merge remaining corresponds to this split.

Theorem 5.1.7. *Suppose* $g, h \in F, g \neq h$. *Let* $m = \max(\textit{height}(g), \textit{height}(h))$. *For* k *such that* $2^k \geq m$, *we have* $T(\Theta_k(g)) \ncong T(\Theta_k(h))$.

Proof. Let $\delta(g) = T_2^* * T_1$, and $\delta(h) = U_2^* * U_1$, where (T_1, T_2) and (U_1, U_2) both are reduced as pairs of trees. Note that

$$\Theta_k(g) = S_k * T_2^* * T_1 * S_k^* = (S_k * T_2^*) * (S_k * T_1^*)^*$$

By Lemma 5.1.6 we know that $S_k * T_2^*$ and $S_k * T_1^*$ both are forests, so the unreduced concatenation $(S_k * T_2^*) \circ (S_k * T_1^*)^*$ is a biforest. However, reducing a biforest results in another biforest, so $\Theta_k(g)$ and $\Theta_k(h)$ are biforests.

Because Θ_k is an isomorphism, $g \neq h$ implies $\Theta_k(g) \neq \Theta_k(h)$. Proposition 5.1.5 implies $T(\Theta_k(g)) \ncong T(\Theta_k(h))$. □

5.2 Orientability

The Khovanov chain complexes considered in Section 5.3 are defined for oriented tangles. To this end, we will now consider the analogues of the above constructions and results in the oriented case.

Recall the oriented strand diagrams and isomorphisms

$$\vec{\delta} : \vec{F} \to \mathcal{R}_+^+$$

from Section 2.8.2.

For any oriented tree $\vec{s}$, we have an isomorphism $\vec{\Phi}_s : \mathcal{R}_+^+ \to \mathcal{R}_{\sigma_s}^{\sigma_s}$ sending $\vec{\Gamma}$ to its conjugate $\vec{s} * \vec{\Gamma} * (\vec{s})^*$. The maps $\vec{\Phi}_s$ are analogous to the isomorphisms $\mathcal{R}_1^1 \to \mathcal{R}_n^n$, considered in the unoriented case in the paragraph preceding Definition 5.1.1. The inverse $(\vec{\Phi}_s)^{-1}$ uses conjugation with $(\vec{s})^*$ instead.

As in the unoriented case, we will always take s to be the symmetric tree S_k for some positive integer k. It turns out that the 2^k-sign induced by S_k has a special form.

Recall definition 2.8.3 of an n-sign. Given an n-sign ν, we can construct a $2n$-sign, which we call 2ν, by replacing each $+$ with $(+,-)$ and each $-$ with $(-,+)$. Repeating this k-times results in a $2^k n$-sign $2^k\nu$.

Proposition 5.2.1. *Given a positive integer k, the 2^k-sign σ_{S_k} induced by symmetric tree S_k is 2^k+, where $+$ is considered as a 1-sign.*

Proof. We give a proof by induction. When $k = 1$, S_1 has a single split. After we put a $+$-sign in the leftmost region, this split becomes a positive split. By Figure 2.27a, a positive split induces $(+,-)$, so the 2-sign induced by S_1 is $(+,-) = 2+$.

Assume S_k induces the 2^k-sign $\sigma_{S_k} = 2^k+$. Then notice that to get S_{k+1}, we just need to add a split at each leaf of S_k. The split at the i^{th} leaf of S_k is a positive (resp. negative) split if the i^{th} sign in σ_{S_k} is $+$ (resp. $-$), because this sign is in the upper left region of the split. By Figure 2.27a and Figure 2.27b, a positive split induces $(...,+,-,...)$, a negative split induces $(...,-,+,...)$. Thus, to obtain $\sigma_{S_{k+1}}$, we just need to replace each $(...,+,...)$ in σ_{S_k}

by $(..., +, -, ...)$, each $(..., -, ...)$ in σ_{S_k} by $(..., -, +, ...)$. It follows that $\sigma_{S_{k+1}} = 2\sigma_{S_k} = 2(2^k+) = 2^{k+1}+$. □

Thus for any positive integer k, we have $\vec{F} \cong \mathcal{R}^{2^k+}_{2^k+}$, with an explicit isomorphism given by $\vec{\Theta}_k := \vec{\Phi}_{S_k} \circ \vec{\delta}$.

5.2.1 Building oriented tangles from $\vec{F}$

First we introduce $\vec{\mathfrak{D}}$ and $\vec{\mathfrak{T}}$, oriented analogues of the categories $\mathfrak{D}$ and $\mathfrak{T}$. Let S be an oriented (p, q)-tangle in the square (with p points on the top side and q points on the bottom side), and consider the induced upward or downward orientations at its endpoints. On both the top and the bottom, we indicate the downward orientation of an endpoint with a $+$, and the upward orientation with a $-$ sign. Note that the signs are positioned at the endpoints of the tangle; this is different from the case of strand diagrams where signs denote orientations of the subintervals on the top and the bottom of the square, separated by the endpoints. If S induces a p-sign ζ on the top, and a q-sign η on the bottom side, we say that S is an oriented tangle from ζ to η.

Definition 5.2.2. *Let $\vec{\mathfrak{D}}$ be the category with objects n-signs for arbitrary positive integers n. The morphisms from μ to ν are oriented strand diagrams from μ to ν. Compositions are concatenations of strand diagrams and signed regions.*

Similarly, let $\vec{\mathfrak{T}}$ be the category with objects n-signs for arbitrary positive integers n. The morphisms from μ to ν are oriented tangles from 2μ to 2ν. Compositions are concatenations of tangles.

Similarly to the functor $T\colon \mathfrak{D} \to \mathfrak{T}$, we construct a functor $\vec{T}\colon \vec{\mathfrak{D}} \to \vec{\mathfrak{T}}$ sending oriented strand diagrams to oriented tangles. $\vec{T}$ acts by the identity on objects. Given an oriented

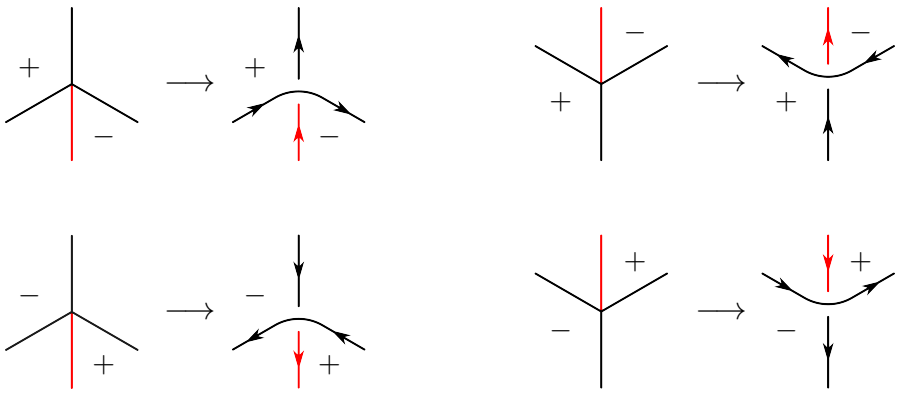

Figure 5.9: Around each crossing of $\vec{T}(\vec{\Gamma})$, its orientation can be equivalently obtained by replacing 4-valent vertices of Γ' by oriented crossings.

strand diagram $\vec{\Gamma}$ from an m-sign μ to an n-sign ν, we will construct $\vec{T}(\vec{\Gamma})$ by assigning an orientation to the unoriented tangle $T(\Gamma)$, where Γ is the unoriented strand diagram underlying $\vec{\Gamma}$.

Suppose $P_1, P_2, ..., P_N$ are signed polygons in the complement of $\vec{\Gamma}$, excluding the rightmost one. Recall that to construct $T(\Gamma)$, we add an edge in each polygon P_i to get a graph Γ', then replace each 4-valent vertex by a crossing as in Figure 5.9. Notice that each time we add an edge, some signed polygon P_i is split into two regions. To obtain an orientation on $T(\Gamma)$, we move the sign of each P_i to the region to the right of the added edge. Now consider the induced orientation of the boundary arcs of each signed region.

The orientation of $\vec{T}(\vec{\Gamma})$ around each crossing can also be obtained by a local replacement at 4-valent vertices of Γ' as in Figure 5.9.

Note that each $+$-signed region induces the downward $(+)$ orientation on its left boundary arc, and the upward $(-)$ orientation on its right boundary arcs. The induced orientations are reversed for a $-$ signed region (see Figure 5.10).

Similarly to the asymptotic faithfulness of the construction of unoriented tangles from F, we have an oriented counterpart as follows.

Figure 5.10: An oriented strand diagram $\vec{\Gamma}$ from $(+,-,-)$ to $(+,-)$ and its associated oriented tangle $\vec{T}(\vec{\Gamma})$ from $(+,-,-,+,-,+)$ to $(+,-,-,+)$.

Theorem 5.2.3. *Suppose* $g, h \in \vec{F}, g \neq h$. *Let* $n = \max(\text{height}(g), \text{height}(h))$. *For* k *such that* $2^k \geq n$, *we have* $\vec{T}(\vec{\Theta}_k(g)) \ncong \vec{T}(\vec{\Theta}_k(h))$.

The proof is immediate, since $T(\Theta_k(g)) \neq T(\Theta_k(h))$, where $\Theta_k(g), \Theta_k(h)$ denote the unoriented strand diagrams underlying $\vec{\Theta}_k(g), \vec{\Theta}_k(h)$.

5.3 A lax group action on Khovanov's chain complexes

We now introduce a category on which $\vec{F}$ admits a lax group action.

5.3.1 The categories $\mathcal{K}_n^m$ and $\overline{\mathcal{K}_n^m}$

Here we define the category $\overline{\mathcal{K}_n^m}$ on which $\vec{F}$ admits the structure of a lax group action. Our category is a generalization of the category $\mathcal{K}_n^m$ constructed in [40].

Recall that Section 2.9 introduced Khovanov's chain complexes of (H^m, H^n)-bimodules associated to tangles. Khovanov defines a general (H^m, H^n)-bimodule to be *geometric* if it is isomorphic to a finite direct sum of bimodules $\mathcal{F}(a)$, for $a \in \hat{B}_n^m$ [40, Section 2.8].

We use the notation of [40, Section 2.8] and let $\mathcal{K}_n^m$ refer to the category of bounded chain complexes of geometric (H^m, H^n)-bimodules, up to chain homotopy. We will consider the homotopy category $\overline{\mathcal{K}}_n^m$ of (not necessarily bounded) chain complexes of (H^m, H^n)-bimodules which are countable direct sums of bimodules $\mathcal{F}(a)$.

Remark. *We note that some of the usual features of the category $\mathcal{K}_n^m$ are not available for $\overline{\mathcal{K}}_n^m$; for example its Grothendieck group is undefined. This triangulated category will be the setting of the action of the Thompson group constructed below. In fact, the chain complexes associated with strand diagrams in Definition 5.3.5 are just a mild generalization of Khovanov's invariant of tangles, see Remark 5.3.3.*

In [41], Khovanov defined a 2-category $\mathcal{C}$ to be a combinatorial realization of the 2-category of tangle cobordisms. $\mathcal{C}$ has the same objects and 1-morphisms as $\vec{\mathfrak{T}}$. The 2-morphisms of $\mathcal{C}$ are "movies" of tangle diagrams describing tangle cobordisms, up to Carter and Saito's movie moves. Khovanov also defined a 2-category of geometric bimodule complexes $\widehat{\mathbb{K}}$, with objects nonnegative integers, 1-morphisms $Mor(m, n) = \mathcal{K}_n^m$ and 2-morphisms defined to be all (not necessarily grading preserving) morphisms of complexes of bimodules up to chain homotopy and up to a sign. A well-defined 2-functor $\mathcal{F} : \mathcal{C} \to \widehat{\mathbb{K}}$ is constructed in [41, Section 4].

5.3.2 The definition of a lax group action

We now introduce two bicategories involved in the definition of a lax group action. Relevant background material is discussed in Section 2.9.3 of this thesis, and more details can be found in [34, Ch. 2].

Definition 5.3.1. *Let G be a group. Define $*_G$ to be the bicategory with the single object $\{*\}$ and $Mor(*, *) = G$, where composition of morphisms $g \circ h$ is given by the group*

operation gh for all $g, h \in G$. We define the 2-morphisms to be trivial, and the associator and unitors to be identity natural transformations.

Definition 5.3.2. *Consider the 2-category $\mathcal{C}at$, whose objects are small categories, morphisms are functors, and 2-morphisms are natural transformations between functors.*

Definition 5.3.3 ([44], Definition 5.1)**.** *Given a group G and a small category $\mathcal{C}$, a lax group action of G on $\mathcal{C}$ is defined to be a lax functor $P\colon *_G \to \mathcal{C}at$ such that $P(*) = \mathcal{C}$.*

We refer the reader to [34, Definition 4.1.2] for the definition of a lax functor. It follows from this definition and the properties of $\mathcal{C}at$ and $*_G$ that a lax group action is determined by the following data:

(a) a family of functors $\{P_g\colon \mathcal{C} \to \mathcal{C} \mid g \in G\}$,

(b) a natural transformation $\lambda\colon Id \to P_e$, where Id is the identity endofunctor of $\mathcal{C}$ and $e \in G$ is the identity element,

(c) a family of natural transformations $\{t_{h,g}\colon P_h \circ P_g \to P_{hg} \mid g, h \in G\}$,

satisfying

1. For any $g \in G$, any $A \in \mathcal{C}$, we have $t_{e,g}(A) \circ \lambda_{P_g(A)} = \mathrm{Id}_{P_g(A)}$ and $t_{g,e}(A) \circ P_g(\lambda_A) = \mathrm{Id}_{P_g(A)}$,

2. For any $g, h, k \in G$, any $A \in \mathcal{C}$, the following diagram commutes

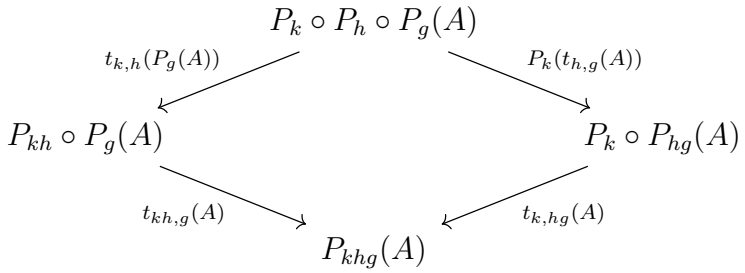

Remark. *A genuine group action of G on $\mathcal{C}$ is a pseudo functor (cf. [34, Definition 4.1.2]) $Q\colon *_G \to \mathcal{C}at$ such that $Q(*) = \mathcal{C}$, and $Q_g \in \mathcal{M}or(\mathcal{C},\mathcal{C})$ is an autoequivalence for any $g \in G$. In other words, a lax group action P is a genuine group action if P further satisfies*

(3) $P_g\colon \mathcal{C} \to \mathcal{C}$ is an autoequivalence for any g.

(4) $\lambda\colon Id \to P_e$ is a natural isomorphism.

(5) $t_{h,g}\colon P_h \circ P_g \to P_{hg}$ is a natural isomorphism for any $g, h \in G$.

In item (3), autoequivalence means that there exists another functor F such that $P_g \circ F$ and $F \circ P_g$ are both naturally isomorphic to the identity functor $Id_{\mathcal{C}}$.

5.3.3 The construction of the lax group action

We begin by introducing, for each reduced (m,n)-strand diagram D, a chain complex $C^*(D) \in \mathrm{Ob}(\overline{\mathcal{K}}_n^m)$. Observe that every reduced oriented strand diagram is equal to $F_1^* \circ F_2$ for some pair of oriented forests F_1, F_2. In this section we assume that all strand diagrams and tangles are oriented, and for brevity of notation we will omit arrows on symbols denoting oriented tangles and strand diagrams.

Definition 5.3.4. *Let $D = F_1^* \circ F_2$ be a reduced oriented (m,n)-strand diagram, and let $\ell \in \mathbb{N}$ be the number of leaves in F_1 and F_2. If L is some forest with ℓ roots whose orientation is compatible with that of F_1 and F_2, we can create a new (not necessarily reduced) strand diagram $D(L)$ given by*

$$D(L) := F_1^* \circ L^* \circ L \circ F_2.$$

Definition 5.3.5. *Let $D = F_1^* \circ F_2 \in \vec{\mathcal{R}}_\nu^\mu$ be a reduced oriented strand diagram, where μ is an m-sign and ν is an n-sign, and let ℓ be as above. We use $F(\ell)$ to refer to the set of*

all oriented forests with ℓ roots and orientations compatible with that of F_1, F_2. Then we define

$$C^*(D) := \bigoplus_{L \in F(\ell)} \mathcal{F}(\vec{T}(D(L))) \in \overline{\mathcal{K}}_n^m,$$

where $\vec{T}$ is the functor defined in Section 5.2 and $\mathcal{F}(\vec{T}(D(L)))$ is the Khovanov chain complex.

Remark. *The strand diagram $D(L)$ is equivalent to D; in fact $L^* \circ L$ may be reduced to the identity strand diagram using type I moves. Thus the chain complex $C^*(D)$ is assembled of Khovanov complexes of tangles corresponding to all ways of stabilizing D using the type I move. The reason for this definition will be clear in the construction of the lax group action below; specifically, Proposition 5.3.10 shows that the chain map corresponding to a composition of type II reductions is well-defined but this is not necessarily the case for a composition of both type I and type II reductions. Also note that the effect on the tangle $\vec{T}(D)$ of a stabilization by $L^* \circ L$ is an introduction of unknots which may be isotoped off of the tangle diagram for $\vec{T}(D)$ using Reidemeister II moves. Therefore up to chain homotopy, each summand $\mathcal{F}(\vec{T}(D(L)))$ is a direct sum of several copies of $\mathcal{F}(\vec{T}(D))$ with q-degree shifts.*

We now introduce the first bit of data required to determine a lax group action, that is, a family of functors $\{P_g \colon \overline{\mathcal{K}}_n^{2^k} \to \overline{\mathcal{K}}_n^{2^k} \mid g \in \vec{F}\}$.

Definition 5.3.6. *Fix $k \geq 0, n \geq 0$. Let A^*, B^* be chain complexes in $\overline{\mathcal{K}}_n^{2^k}$ $\overline{\mathcal{K}}_{2^k}^{2^k}$, and let $f \colon A^* \to B^*$ be a chain map. For each $g \in \vec{F}$ define an endofunctor P_g of $\overline{\mathcal{K}}_n^{2^k}$ by*

$$P_g(A^*) := C^*(\Theta_k(g)) \otimes_{H^{2^k}} A^*,$$

and

$$P_g(f) := \mathrm{Id} \otimes f \colon C^*(\Theta_k(g)) \otimes_{H^{2^k}} A^* \to C^*(\Theta_k(g)) \otimes_{H^{2^k}} B^*.$$

Next we introduce the natural transformation λ from the identity endofunctor of $\overline{\mathcal{K}}_n^{2^k}$ to P_e, the functor associated to the identity element $e \in \vec{F}$ as above. This consists of, for each $A^* \in \overline{\mathcal{K}}_n^{2^k}$, a chain map $\lambda_{A^*} \colon A^* \to C^*(\Theta_k(e)) \otimes_{H^{2^k}} A^*$.

By definition, $C^*(\Theta_k(e)) = \bigoplus_{L \in F(2^k)} \mathcal{F}(\vec{T}(\Theta_k(e)(L)))$. Consider the direct summand given by letting L be Id_{2^k}, the identity $(2^k+, 2^k+)$-strand diagram. It is also true that $\Theta_k(e) = \mathrm{Id}_{2^k}$. The functor $\vec{T}$ sends $\Theta_k(e)$ to the identity $(2^{k+1}+, 2^{k+1}+)$-tangle $\mathrm{Vert}_{2^{k+1}}$, by introducing an extra strand to the left of each component. Therefore

$$\mathcal{F}(\vec{T}(\Theta_k(e)(\mathrm{Id}_{2^k}))) = \mathcal{F}(\vec{T}(\Theta_k(e))) = \mathcal{F}(\mathrm{Vert}_{2^{k+1}})$$

is a chain complex with a single homological grading. Note that $\mathcal{F}(\mathrm{Vert}_{2^{k+1}}) = H^{2^k}$ as H^{2^k}-bimodules [40]. We denote the unit in H^{2^k} by 1_{2^k}.

Definition 5.3.7. *For each $A^* \in \overline{\mathcal{K}}_n^{2^k}$ the natural transformation*

$$\lambda_{A^*} \colon A^* \to C^*(\Theta_k(e)) \otimes_{H^{2^k}} A^*$$

from the identity endofunctor to P_e is given by tensoring with 1_{2^k}, i.e. taking A^* by the identity map to the direct summand $1_{2^k} \otimes A^*$.

In order to give a family of natural transformations $\{t_{h,g} \colon P_h \circ P_g \to P_{hg} \mid g, h \in \vec{F}\}$, we introduce some preliminary definitions and lemmas.

Definition 5.3.8. *Let the 2-category $\mathcal{D}$ have the same objects and 1-morphisms as $\vec{\mathfrak{D}}$. Define the 2-morphisms in $\mathcal{D}$ to be sequences of Type II moves (see Definition 2.8.4).*

Recall Khovanov's 2-category $\mathcal{C}$, mentioned at the end of Section 5.3.1. We extend the 1-functor $\vec{T}\colon \vec{\mathfrak{D}} \to \vec{\mathfrak{T}}$ to a 2-functor $\mathbb{T} : \mathcal{D} \to \mathcal{C}$, by keeping its action on objects and on 1-morphisms, and defining its action on 2-morphisms of $\mathcal{D}$ as follows. We let $\mathbb{T}$ send a positive Type II move to the movie shown in Figure 5.11a, which is a saddle cobordism followed by a Reidemeister II move. Reversing orientations, we obtain the movie of a negative Type II move, see Figure 5.11b.

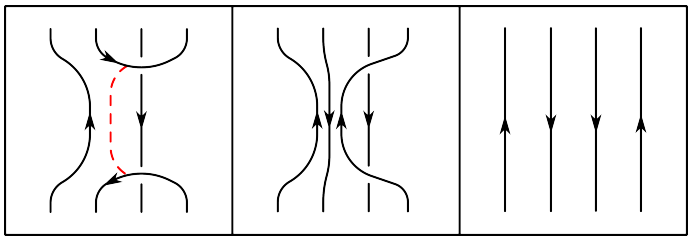

(a)

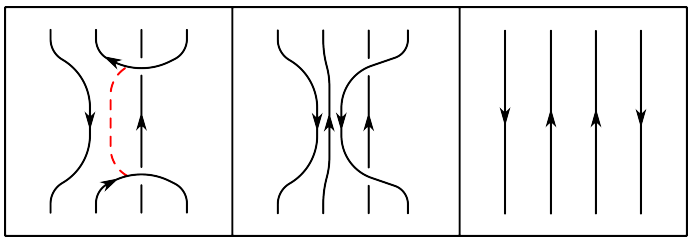

(b)

Figure 5.11: Movies of (a) positive Type II move. (b) negative Type II move.

Definition 5.3.9. *An oriented strand diagram is said to be* Type II-reduced *if it is not subject to any Type II moves.*

Given a (μ, ν)-strand diagram Γ, let r denote a sequence of Type II moves taking Γ to Γ', where Γ' is Type II-reduced. By an argument similar to the proof of [55, Proposition 2.1.1], Γ' is unique. However the choice of a sequence r from Γ to Γ' is not unique in general. Note that each Type II move in r corresponds to a pair of vertices, the endpoints of the edge which is removed.

Proposition 5.3.10 ([44], Proposition 5.15)**.** $\mathbb{T}(r)$ *is independent of a choice of* r.

Proof. To prove the statement, we will characterize pairs of vertices in Γ encoding the Type II moves in a sequence reducing Γ to Γ'. To this end, consider paths (geodesics) in Γ which are monotonic with respect to the height function, parametrized so that the height is a decreasing function of the parameter. It is convenient to consider paths which start and end at mid-points of edges of the strand diagram. Any such path γ follows a sequence of merges and splits. In more detail, consider a sequence of labels corresponding to each path γ: label it with l (respectively r) whenever it enters a merge from the left (respectively from the right), and similarly label it with l^{-1}, r^{-1} whenever it exits a split on the left or on the right. For example, the path shown in Figure 5.12 is labeled $lll^{-1}rr^{-1}l^{-1}$. Consider the free group $F_{l,r}$ generated by l, r; then the sequence of labels may be thought of as a word w_γ in the generators.

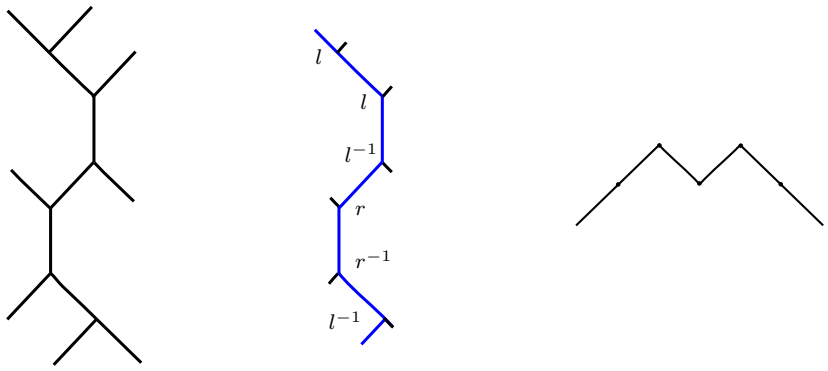

Figure 5.12: Left: a part of a strand diagram. Center: an admissible path γ, colored blue, with $w_\gamma = lll^{-1}rr^{-1}l^{-1}$. Right: the weight function corresponding to γ.

Now define integer weights labeling γ as it passes mid-points of edges of the strand diagram. The beginning point of γ is assigned weight 0. The weight function is given by the augmentation of the word w_γ, that is the sum of exponents of the letters along the path, from the start to the given point. The weights may also be characterized by requiring that passing

a merge adds 1, passing a split split subtracts 1. Type II moves in a sequence r reducing Γ to Γ' are in bijection with pairs of vertices in Γ corresponding to *admissible* paths γ satisfying the following properties:

1. The exponent of the first letter in w_γ is $+1$,
2. The word w_γ represents the trivial element of the free group $F_{l,r}$,
3. The endpoint of γ has weight 0,
4. The weights between the beginning and the end of γ are strictly positive.

An example of an admissible path is shown in Figure 5.12. The pair of vertices (specifying a type II move) corresponding to γ are the first and the last vertices of Γ it passes through, which are a merge and a split respectively, by properties (1), (3) and (4). Condition (2) corresponds to the fact that the "vertical" center interval (as shown in Figure 2.13) of each type II move in a sequence reducing Γ to Γ' is a result of previous type II moves in the sequence.

It follows from conditions (3), (4) that two admissible paths γ_1, γ_2 cannot be interlaced, meaning that $\gamma_1 \cap \gamma_2$ contains precisely one endpoint of both γ_1 and γ_2. In other words, any two admissible paths are either (a) disjoint, (b) nested, say γ_1 is in the interior of γ_2, or (c) they overlap, meaning that the intersection $\gamma_1 \cap \gamma_2$ is an interval contained in the interior of γ_1 and in the interior of γ_2. The saddle maps on Khovanov chain complexes arising from Type II moves along disjoint paths commute. The case (b) corresponds to the γ_1 move being done before the γ_2 move. In the case (c), a preceding move along $\gamma_1 \cap \gamma_2$ makes γ_1 and γ_2 disjoint. In any of these case, either the order of moves is well-defined, or they commute, showing that the map on Khovanov chain complexes is independent of a choice of r. $\square$

Remark. *The piece-wise linear graphs of admissible weight functions along admissible paths are precisely* Dyck paths *studied in combinatorics and statistical mechanics.*

Suppose Γ is a Type II-reduced (σ, μ)-strand diagram and Λ is a Type II-reduced (μ, ρ)-strand diagram. Let $\Lambda \cdot \Gamma$ denote the Type II-reduced (σ, ρ)-strand diagram corresponding to $\Lambda \circ \Gamma$. Note that only type II moves are used here, and in general $\Lambda \cdot \Gamma$ is different from the reduced strand diagram $\Lambda * \Gamma$ defined in Section 2.7.1, where both types I and II moves are used. Let r be a sequence of type II moves reducing $\Lambda \circ \Gamma$ to $\Lambda \cdot \Gamma$. Khovanov's functor $\mathcal{F}$ gives a chain map

$$\mathcal{F}(\mathbb{T}(r)) \colon \mathcal{F}(\mathbb{T}(\Lambda \circ \Gamma)) \to \mathcal{F}(\mathbb{T}(\Lambda \cdot \Gamma)).$$

By [41, Proposition 13], there is an isomorphism

$$\psi : \mathcal{F}(\mathbb{T}(\Lambda)) \otimes_{H^m} \mathcal{F}(\mathbb{T}(\Gamma)) \to \mathcal{F}(\mathbb{T}(\Lambda) \circ \mathbb{T}(\Gamma)) = \mathcal{F}(\mathbb{T}(\Lambda \circ \Gamma)).$$

Definition 5.3.11. *Let Γ, Λ be as above. Define the map*

$$\phi(\Gamma, \Lambda) := \mathcal{F}(\mathbb{T}(r)) \circ \psi : \mathcal{F}(\mathbb{T}(\Lambda)) \otimes_{H^m} \mathcal{F}(\mathbb{T}(\Gamma)) \to \mathcal{F}(\mathbb{T}(\Lambda \cdot \Gamma)) \tag{5.3.1}$$

By Proposition 5.3.10, $\mathbb{T}(r)$ is independent of a choice of r, so $\phi(\Gamma, \Lambda)$ is well defined.

Let g, h be any two elements in $\vec{F}$. Considering $\Theta_k(g)$, $\Theta_k(h)$ and $\Theta_k(hg)$ as pairs of forests, let u, v and w denote their respective numbers of leaves.

Lemma 5.3.12 ([44], Lemma 5.18)**.** *For any $U \in F(u)$ and $V \in F(v)$, there exists $W \in$*

$F(w)$ *such that*

$$\Theta_k(h)(V) \cdot \Theta_k(g)(U) = \Theta_k(hg)(W).$$

Proof. Letting $\sim$ denote the equivalence of strand diagrams, notice that

$$\Theta_k(h)(V)\cdot\Theta_k(g)(U) \sim \Theta_k(h)(V)\circ\Theta_k(g)(U) \sim \Theta_k(h)\circ\Theta_k(g) \sim \Theta_k(h)*\Theta_k(g) = \Theta_k(hg).$$

Therefore $\Theta_k(h)(V) \cdot \Theta_k(g)(U)$ is a Type II-reduced strand diagram equivalent to the reduced strand diagram $\Theta_k(hg)$. Next, observe that the type II-reduced strand diagram $\Theta_k(h)(V) \cdot \Theta_k(g)(U)$ can be fully reduced by Type I moves. Said differently, $\Theta_k(h)(V) \cdot \Theta_k(g)(U)$ can be obtained by a sequence of reversed Type I moves (inserting carets) from $\Theta_k(hg)$.

Moreover, as we explain next, these carets can only be put on certain edges. We know from the fact that $\Theta_k(hg)$ is reduced that $\Theta_k(hg) = E_2^* * E_1$ for some forests E_1 and E_2. We say an edge in $\Theta_k(hg)$ is a *bridge* if a concatenation point between E_2^* and E_1 is on this edge. If a Type II-reduced graph differs from $E_2^* * E_1$ by carets, it can only be obtained from $E_2^* * E_1$ by inserting carets on *bridges*, or on new bridges created by other previously inserted carets. Putting carets elsewhere creates a diagram that is not Type II-reduced, as such carets can always be cancelled in a Type II move.

The process of putting carets on bridges is equivalent to the process of inserting $W^* \circ W$ between E_2^* and E_1, for some forest W. Therefore,

$$\Theta_k(h)(V) \cdot \Theta_k(g)(U) = E_2^* \circ W^* \circ W \circ E_1 = \Theta_k(hg)(W).$$

. □

Definition 5.3.13. *Given $g, h \in \vec{F}$, define*

$$\phi(h, g) = \bigoplus_{U \in F(u), V \in F(v)} \phi(\Theta_k(h)(V), \Theta_k(g)(U)), \tag{5.3.2}$$

a chain map from

$$C^*(\Theta_k(h)) \otimes_{H^{2^k}} C^*(\Theta_k(g)) = \bigoplus_{U \in F(u), V \in F(v)} \mathcal{F}(\mathbb{T}(\Theta_k(h)(V))) \otimes_{H^{2^k}} \mathcal{F}(\mathbb{T}(\Theta_k(g)(U)))$$

to

$$C^*(\Theta_k(hg)) = \bigoplus_{W \in F(w)} \mathcal{F}(\mathbb{T}(\Theta_k(hg)(W))).$$

Then for any $A^* \in \overline{\mathcal{K}}_n^{2^k}$, define the natural transformation

$$t_{h,g}(A^*) = \phi(h, g) \otimes id \tag{5.3.3}$$

from

$$P_h \circ P_g(A^*) = C^*(\Theta_k(h)) \otimes_{H^{2^k}} C^*(\Theta_k(g)) \otimes_{H^{2^k}} A^*$$

to

$$P_{hg}(A^*) = C^*(\Theta_k(hg)) \otimes_{H^{2^k}} A^*.$$

Theorem 5.3.14 ([44], Theorem 5.20)**.** *The data $(\{P_g\}_{g \in \vec{F}}, \lambda, \{t_{h,g}\}_{g,h \in \vec{F}})$ determines a lax action of $\vec{F}$ on $\overline{\mathcal{K}}_n^{2^k}$.*

Next, we verify that the collection of functors $\{P_g\}_{g \in \vec{F}}$, the natural transformation λ, and the collection of natural transformations $\{t_{h,g}\}_{g,h \in \vec{F}}$, satisfy the necessary properties outlined after Definition 5.3.3.

5.3.4 Verifying the axioms

To check the first axiom of a lax group action, we need the following lemma.

Lemma 5.3.15. *For any $g \in \vec{F}$ and any chain u in $C^*(\Theta_k(g))$, we have $(\phi(g,e))(u\otimes 1^{2^k}) = u$ and $(\phi(e,g))(1^{2^k} \otimes u) = u$.*

Proof. We will prove the first equation; a similar argument proves the second equation.

By definition, $C^*(\Theta_k(g)) = \bigoplus_{L\in F(l)} \mathcal{F}(\mathbb{T}(\Theta_k(g)(L)))$, so we can assume $u \in \mathcal{F}(\mathbb{T}(\Theta_k(g)(L)))$ for some $L \in F(l)$ and check that $\phi(\Theta_k(g)(L), \Theta_k(e))(u \otimes 1^{2^k}) = u$.

Notice that $\Theta_k(e)$ is a trivial strand diagram, so $\Theta_k(g)(L) \circ \Theta_k(e) = \Theta_k(g)(L)$ is Type II-reduced, i.e. the Type II move sequence r from $\Theta_k(g)(L) \circ \Theta_k(e)$ to $\Theta_k(g)(L) \cdot \Theta_k(e)$ is empty. Thus $\mathcal{F}(\mathbb{T}(r))$ is identity map and

$$\phi(\Theta_k(g)(L), \Theta_k(e)) = \mathcal{F}(\mathbb{T}(r)) \circ \psi = \psi$$

Here ψ is the isomorphism

$$\psi : \mathcal{F}(\mathbb{T}(\Theta_k(g)(L))) \otimes_{H^{2^k}} \mathcal{F}(\mathbb{T}(\Theta_k(e)) \to \mathcal{F}(\mathbb{T}(\Theta_k(g)(L) \circ \Theta_k(e))) = \mathcal{F}(\mathbb{T}(\Theta_k(g)(L))).$$

To see $\psi(u \otimes 1^{2^k}) = u$, we just need to observe that ψ is equivalent to the right H^{2^k}-action on chain modules of $\mathcal{F}(\mathbb{T}(\Theta_k(g)(L)))$. So the unit 1^{2^k} acts trivially. □

Using the above Lemma we may verify the first axiom. For any $u \otimes a \in P_g(A^*)$, we have

$$(t_{e,g}(A^*) \circ \lambda_{P_g(A^*)})(u \otimes a) = t_{e,g}(A^*)(1^{2^k} \otimes u \otimes a) = \phi(e,g)(1^{2^k} \otimes u) \otimes a = u \otimes a,$$
$$(t_{g,e}(A^*) \circ P_g(\lambda_{A^*}))(u \otimes a) = t_{g,e}(A^*)(u \otimes 1^{2^k} \otimes a) = \phi(g,e)(u \otimes 1^{2^k}) \otimes a = u \otimes a,$$

So $t_{e,g}(A^*) \circ \lambda_{P_g(A^*)} = \mathrm{Id}_{P_g(A^*)}$ and $t_{g,e}(A^*) \circ P_g(\lambda_{A^*}) = \mathrm{Id}_{P_g(A^*)}$.

For the associativity axiom, we need to check that the following diagram commutes for any $f, g, h \in \vec{F}$.

$$\begin{array}{ccc} C^*(\Theta_k(h)) \otimes_{H^{2^k}} C^*(\Theta_k(g)) \otimes_{H^{2^k}} C^*(\Theta_k(f)) & \xrightarrow{id \otimes \phi(g,f)} & C^*(\Theta_k(h)) \otimes_{H^{2^k}} C^*(\Theta_k(gf)) \\ \downarrow{\scriptstyle \phi(h,g)\otimes id} & & \downarrow{\scriptstyle \phi(h,gf)} \\ C^*(\Theta_k(hg)) \otimes_{H^{2^k}} C^*(\Theta_k(f)) & \xrightarrow[\phi(hg,f)]{} & C^*(\Theta_k(hgf)) \end{array}$$

Recall that $C^*(\Theta_k(g))$ is defined to be a direct sum of $\mathcal{F}(\mathbb{T}(\Theta_k(g)(L)))$ over forests L, where $\Theta_k(g)(L)$ is obtained by inserting $L^* \circ L$ in the middle of $\Theta_k(g)$. The commutativity of the above diagram is therefore equivalent to the commutativity of the following diagram for any Γ, Λ, Π obtained by inserting forests in the middle of $\Theta_k(f), \Theta_k(g), \Theta_k(h)$ respectively.

$$\begin{array}{ccc} \mathcal{F}(\mathbb{T}(\Pi)) \otimes_{H^{2^k}} \mathcal{F}(\mathbb{T}(\Lambda)) \otimes_{H^{2^k}} \mathcal{F}(\mathbb{T}(\Gamma)) & \xrightarrow{id \otimes \phi(\Lambda,\Gamma)} & \mathcal{F}(\mathbb{T}(\Pi)) \otimes_{H^{2^k}} \mathcal{F}(\mathbb{T}(\Lambda \cdot \Gamma)) \\ \downarrow{\scriptstyle \phi(\Pi,\Lambda)\otimes id} & & \downarrow{\scriptstyle \phi(\Pi,\Lambda\cdot\Gamma)} \\ \mathcal{F}(\mathbb{T}(\Pi \cdot \Lambda)) \otimes_{H^{2^k}} \mathcal{F}(\mathbb{T}(\Gamma)) & \xrightarrow[\phi(\Pi\cdot\Lambda,\Gamma)]{} & \mathcal{F}(\mathbb{T}(\Pi \cdot \Lambda \cdot \Gamma)) \end{array}$$

In the above diagram, we choose a Type II move sequence p from $\Pi \circ \Lambda$ to $\Pi \cdot \Lambda$, a sequence q from $(\Pi \cdot \Lambda) \circ \Gamma$ to $\Pi \cdot \Lambda \cdot \Gamma$, a sequence r from $\Lambda \circ \Gamma$ to $\Lambda \cdot \Gamma$, a sequence s from $\Pi \circ (\Lambda \cdot \Gamma)$ to $\Pi \cdot \Lambda \cdot \Gamma$, then let $\phi(\Pi, \Lambda) = \mathcal{F}(\mathbb{T}(p))$, $\phi(\Pi \cdot \Lambda, \Gamma) = \mathcal{F}(\mathbb{T}(q))$, $\phi(\Lambda, \Gamma) = \mathcal{F}(\mathbb{T}(r))$, $\phi(\Pi, \Lambda \cdot \Gamma) = \mathcal{F}(\mathbb{T}(s))$.

If we regard p as a sequence of Type II moves from $\Pi \circ \Lambda \circ \Gamma$ to $(\Pi \cdot \Lambda) \circ \Gamma$ and r as a sequence of Type II moves from $\Pi \circ \Lambda \circ \Gamma$ to $\Pi \circ (\Lambda \cdot \Gamma)$, then we can rewrite the diagram

as

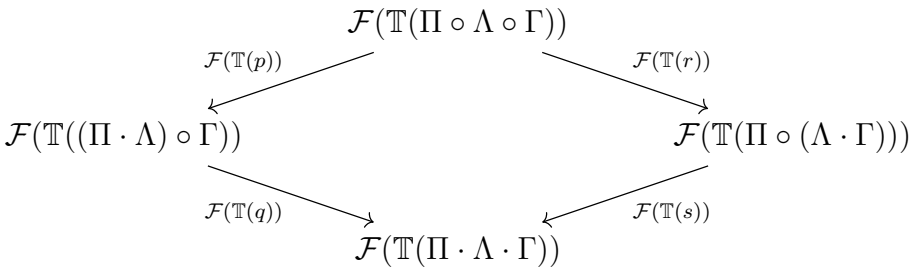

Note that qp and sr are two sequences of Type II moves from $\Pi \circ \Lambda \circ \Gamma$ to $\Pi \cdot \Lambda \cdot \Gamma$, so $\mathbb{T}(qp) = \mathbb{T}(sr)$ by Proposition 5.3.10. Then we have $\mathcal{F}(\mathbb{T}(q)) \circ \mathcal{F}(\mathbb{T}(p)) = \mathcal{F}(\mathbb{T}(qp)) = \mathcal{F}(\mathbb{T}(sr)) = \mathcal{F}(\mathbb{T}(s)) \circ \mathcal{F}(\mathbb{T}(r))$.

This concludes the proof of the associativity axiom and of Theorem 5.3.14.

Bibliography

[1] Valeriano Aiello. “On the Alexander Theorem for the oriented Thompson group F”. *Algebraic & Geometric Topology* 20.1 (2020), pp. 429–438.

[2] Valeriano Aiello and Sebastian Baader. “Positive oriented Thompson links”. *Preprint, arXiv:2101.04534* (2021).

[3] Valeriano Aiello and Sebastian Baader. “Arborescence of positive Thompson links”. *Pacific Journal of Mathematics* 316 (2022), pp. 237–248.

[4] Valeriano Aiello and Roberto Conti. “Graph polynomials and link invariants as positive type functions on Thompson’s group F”. *Journal of Knot Theory and Its Ramifications* 28.02 (Feb. 2019).

[5] Valeriano Aiello and Roberto Conti. “The Jones Polynomial and Functions of Positive Type on the Oriented Jones–Thompson Groups $\vec{F}$ and $\vec{T}$”. *Complex Analysis and Operator Theory* 13 (2019), pp. 3127–3149.

[6] Valeriano Aiello, Roberto Conti, and Vaughan Jones. “The HOMFLYPT polynomial and the oriented Thompson group”. *Quantum Topology* 9.3 (July 2018), pp. 461–472.

[7] Rostislav Akhmechet, Peter K. Johnson, and Vyacheslav Krushkal. “Lattice cohomology and q-series invariants of 3-manifolds”. *Journal für die reine und angewandte Mathematik (Crelles Journal)* 2023.796 (2023), pp. 269–299.

[8] Marta M. Asaeda, Jozef H. Przytycki, and Adam S. Sikora. “Categorification of the Kauffman bracket skein module of I–bundles over surfaces”. *Algebraic & Geometric Topology* 4.2 (Dec. 2004), pp. 1177–1210.

[9] Dror Bar-Natan. “Khovanov’s homology for tangles and cobordisms”. *Geometry & Topology* 9.3 (2005), pp. 1443–1499.

[10] Anna Beliakova, Krzysztof K. Putyra, and Stephan M. Wehrli. “Quantum link homology via trace functor I”. *Inventiones Mathematicae* 215 (2019), pp. 383–492.

[11] James Belk. “Thompson’s Group $\vec{F}$”. PhD thesis. Cornell University, 2004.

[12] James Belk and Francesco Matucci. “Conjugacy and dynamics in Thompson’s groups”. *Geometriae Dedicata* 169 (2014), pp. 239–261.

[13] Kathrin Bringmann, Amanda Folsom, Ken Ono, and Larry Rolen. *Harmonic Maass forms and mock modular forms: theory and applications*. Vol. 64. American Mathematical Society, 2017.

[14] Kathrin Bringmann, Karl Mahlburg, and Antun Milas. “Higher depth quantum modular forms and plumbed 3-manifolds”. *Letters in Mathematical Physics* 110.10 (2020), pp. 2675–2702.

[15] Kathrin Bringmann, Karl Mahlburg, and Antun Milas. “Quantum modular forms and plumbing graphs of 3-manifolds”. *Journal of Combinatorial Theory, Series A* 170 (2020), p. 105145.

[16] Kathrin Bringmann and Larry Rolen. “Half-integral weight Eichler integrals and quantum modular forms”. *Journal of Number Theory* 161 (2016), pp. 240–254.

[17] James W. Cannon, William R. Floyd, and Walter R. Parry. “Introductory notes on Richard Thompson’s groups”. *L’Enseigement Mathématique* 42.2 (1996).

[18] Miranda C. N. Cheng, Sungbon. Chun, Francesca Ferrari, Sergei Gukov, and Sarah M Harrison. “3d modularity”. *Journal of High Energy Physics* 2019.10 (2019), pp. 1–95.

[19] Miranda C. N. Cheng, Sungbong Chun, Boris Feigin, Francesca Ferrari, Sergei Gukov, Sarah M. Harrison, and Davide Passaro. "3-manifolds and VOA characters". *Communications in Mathematical Physics* 405.2 (2024), p. 44.

[20] Miranda C. N. Cheng, Ioana Coman, Piotr Kucharski, Davide Passaro, and Gabriele Sgroi. "3d Modularity Revisited". *Preprint, arXiv:2403.14920* (2024).

[21] Amanda Folsom, Ken Ono, and Robert C. Rhoades. "Mock theta functions and quantum modular forms". *Forum of Mathematics, Pi*. Vol. 1. Cambridge University Press. 2013.

[22] Stavros Garoufalidis and Thang T. Q. Lê. "Nahm sums, stability and the colored Jones polynomial". *Research in the Mathematical Sciences* 2 (2015), pp. 1–55.

[23] Gili Golan and Mark Sapir. "On Jones' subgroup of R. Thompson group F". *Journal of Algebra* 470 (2017), pp. 122–159.

[24] Ankush Goswami and Robert Osburn. "Quantum modularity of partial theta series with periodic coefficients". *Forum Mathematicum* 33.2 (2021), pp. 451–463.

[25] Lothar Göttsche. "Modular forms and Donaldson invariants for 4-manifolds with $b+ = 1$". *Journal of the American Mathematical Society* (1996), pp. 827–843.

[26] Ariana Grymski and Emily Peters. "Conway rational tangles and the Thompson group". *Preprint, arXiv:2212.00100* (2022).

[27] Victor Guba and Mark Sapir. *Diagram Groups*. Vol. 620. American Mathematical Society, 1997.

[28] Sergei Gukov, Ludmil Katzarkov, and Josef Svoboda. "$\hat{Z}_b$ for plumbed manifolds and splice diagrams". *Preprint, arXiv:2304.00699* (2024).

[29] Sergei Gukov and Ciprian Manolescu. "A two-variable series for knot complements". *Quantum Topology* 12.1 (2021), pp. 1–109.

[30] Sergei Gukov, Du Pei, Pavel Putrov, and Cumrun Vafa. “BPS spectra and 3-manifold invariants”. *J. Knot Theory Ramifications* 29.2 (2020).

[31] Sergei Gukov, Pavel Putrov, and Cumrun Vafa. “Fivebranes and 3-manifold homology”. *Journal of High Energy Physics* 2017.7 (2017), pp. 1–82.

[32] Kyle Hayden and Isaac Sundberg. “Khovanov homology and exotic surfaces in the 4-ball”. *Journal für die reine und angewandte Mathematik (Crelles Journal)* 2024.809 (2024), pp. 217–246.

[33] Kazuhiro Hikami. “On the quantum invariant for the Brieskorn homology spheres”. *International Journal of Mathematics* 16.06 (2005), pp. 661–685.

[34] Niles Johnson and Donald Yau. *2-dimensional categories*. Oxford University Press, Oxford, 2021.

[35] Vaughan F. R. Jones. “A polynomial invariant for knots via Von Neumann Algebras”. *Bulletin of the American Mathematical Society* 12.1 (1985).

[36] Vaughan F. R. Jones. “Some unitary representations of Thompson’s groups F and T”. *Journal of Combinatorial Algebra* 1.1 (2017), pp. 1–44.

[37] Vaughan F. R. Jones. “On the construction of knots and links from Thompson’s groups”. *Knots, Low-Dimensional Topology and Applications: Knots in Hellas, International Olympic Academy, Greece, July 2016* (2019), pp. 43–66.

[38] Louis H. Kauffman. “State models and the Jones polynomial”. *New Developments in the Theory of Knots* 11 (1990), p. 162.

[39] Mikhail Khovanov. “A categorification of the Jones oplynomial”. *Duke Mathematical Journal* 101 (2000), pp. 359–426.

[40] Mikhail Khovanov. “A functor-valued invariant of tangles”. *Algebraic & Geometric Topology* 2 (2002), pp. 665–741.

[41] Mikhail Khovanov. “An invariant of tangle cobordisms”. *Transactions of the American Mathematical Society* 358.1 (2006), pp. 315–327. issn: 0002-9947,1088-6850.

[42] Robion Kirby. “A calculus for framed links in S^3”. *Inventiones Mathematicae* 45.1 (1978), pp. 35–56.

[43] Peter B. Kronheimer and Tomasz S. Mrowka. “Khovanov homology is an unknot-detector”. *Publications Mathématiques de l’IHÉS* 113 (2011), pp. 97–208.

[44] Vyacheslav Kruskhal, Louisa Liles, and Yangxiao Luo. “Thompson’s group F, tangles, and link homology”. *Preprint, arXiv:2403.16838* (2024).

[45] Ruth Lawrence and Don Zagier. “Modular forms and quantum invariants of 3-manifolds”. *Asian Journal of Mathematics* 3.1 (1999), pp. 93–108.

[46] W. B. Raymond Lickorish. “A representation of orientable combinatorial 3-manifolds”. *Annals of Mathematics* 76.3 (1962), pp. 531–540.

[47] W. B. Raymond Lickorish. “Invariants for 3-manifolds from the combinatorics of the Jones polynomial”. *Pacific Journal of Mathematics* 149.2 (1991), pp. 337–347.

[48] W. B. Raymond Lickorish. *An Introduction to Knot Theory*. Springer New York, NY, 1997.

[49] Louisa Liles. “(t, q)-Series invariants of Seifert manifolds”. *Preprint, arXiv:2410.10561* (2024).

[50] Louisa Liles. “Annular links from Thompson’s group T”. *To appear in Algebraic & Geometric Topology* (2024).

[51] Louisa Liles and Eleanor McSpirit. “Infinite Families of Quantum-Modular 3-Manifold Invariants”. *Communications in Number Theory and Physics* 18 (2024), pp. 237–260.

[52] Robert Lipshitz, Peter S. Ozsváth, and Dylan P. Thurston. “Bimodules in bordered Heegaard Floer homology”. *Geometry & Topology* 19.2 (2015), pp. 525–724.

[53] Jeremy Lovejoy. “Quantum q-series identities”. *Hardy-Ramanujan Journal* 44 (2022).

[54] Jeremy Lovejoy and Robert Osburn. “The colored Jones polynomial and Kontsevich–Zagier series for double twist knots”. *Journal of Knot Theory and Its Ramifications* 30.05 (2021), p. 2150031.

[55] Francesco Matucci. “Algorithms and classification in groups of piecewise-linear homeomorphisms”. PhD thesis. Cornell University, 2008.

[56] Allison H. Moore and Nicola Tarasca. “Higher rank series and root puzzles for plumbed 3-manifolds”. *Preprint, arXiv:2405.14972* (2024).

[57] Yuya Murakami. “A proof of a conjecture of Gukov–Pei–Putrov–Vafa”. *Communications in Mathematical Physics* 405.11 (2024), p. 274.

[58] András Némethi. “Lattice cohomology of normal surface singularities”. *Publications of the Research Institute for Mathematical Sciences* 44.2 (2008), pp. 507–543.

[59] Walter D. Neumann. “A calculus for plumbing applied to the topology of complex surface singularities and degenerating complex curves”. *Transactions of the American Mathematical Society* 268.2 (1981), pp. 299–344.

[60] Walter D. Neumann and Frank Raymond. “Seifert manifolds, plumbing, μ-invariant and orientation reversing maps”. *Algebraic and Geometric Topology: Proceedings of a Symposium held at Santa Barbara in honor of Raymond L. Wilder, July 25–29, 1977*. Springer. 2006, pp. 163–196.

[61] Jordan Nikkel and Yunxiang Ren. “On Jones’ subgroup of R. Thompson’s group T”. *International Journal of Algebra and Computation* 28.05 (2018), pp. 877–903.

[62] Ken Ono. *The Web of Modularity: Arithmetic of the Coefficients of Modular Forms and q-series*. 102. American Mathematical Society, 2004.

[63] Sunghyuk Park. “Higher Rank hat $\widehat{Z}$ and F_K”. *SIGMA. Symmetry, Integrability and Geometry: Methods and Applications* 16 (2020), p. 044.

[64] Nicolai Reshetikhin and Vladimir Turaev. “Invariants of 3-manifolds via link polynomials and quantum groups”. *Inventiones Mathematicae* 103.1 (1991), pp. 547–597.

[65] Goro Shimura. “Modular forms of half integral weight”. *Modular Functions of One Variable I: Proceedings International Summer School University of Antwerp, RUCA July 17–August 3, 1972*. Springer. 1973, pp. 57–74.

[66] Andrew H. Wallace. “Modifications and cobounding manifolds”. *Canadian Journal of Mathematics* 12 (1960), pp. 503–528.

[67] Edward Witten. “Quantum field theory and the Jones polynomial”. *Communications in Mathematical Physics* 121.3 (1989), pp. 351–399.

[68] Don Zagier. “Quantum modular forms”. *Quanta of Maths* 11 (2010), pp. 659–675.